The interaction of M13 coat protein with lipid bilayers

a spectroscopic study

promotor : dr. T.J. Schaafsma, hoogleraar in de moleculaire fysica
co-promotor: dr. M.A. Hemminga, universitair hoofddocent

J.C. Sanders

The interaction of M13 coat protein with lipid bilayers

a spectroscopic study

proefschrift

ter verkrijging van de graad van
doctor in de landbouw- en milieuwetenschappen
op gezag van de rector magnificus
dr. H.C. van der Plas
in het openbaar te verdedigen
op dinsdag 21 april 1992
des namiddags te vier uur in de aula
van de Landbouwuniversiteit te Wageningen

Stellingen

De kennis van de secundaire structuur van een membraan eiwit is essentieel voor het begrip van de interacties van het membraaneiwit met zijn lipide omgeving.

Hoofdstuk 4 van dit proefschrift.

Op grond van de resultaten van Spruijt et al. kan de verklaring van Johnson & Hudson dat het multi-exponentieel verval van de enige tryptofaan van het manteleiwit van het M13 bacteriofaag veroorzaakt wordt door de vorming van een heterogeen dimeer, verworpen worden.

Spruijt, R. B., Wolfs, C. J. A. M. en Hemminga, M. A. (1989) Biochemistry 28, 9159-9165.
Johnson, I. D. en Hudson, B. S. (1989) Biochemistry 28, 6392-6400.

De ontwikkeling en toepassing van tijdopgeloste confocale fluorescentie imaging is voornamelijk van de kennis van het fotofysisch gedrag van de fluorescente probes en in mindere mate van de instrumentele ontwikkeling, afhankelijk.

De door Kano et al. aangevoerde dissociatie van porfyrinedimeren als verklaring voor de verschuiving van de NMR resonanties van porfyrines bij toenemende temperatuur is onjuist.

Kano, K., Nukajima, T. en Hashimoto, S. (1987) J. Phys. Chem. 91, 6614-6619

De stelling dat de NMR T_2 relaxatietijd, op grond van een vector analyse, langer kan zijn dan de NMR relaxatietijd T_1, is onjuist.

Traficante (1992) Conc. in Magn. Res. 3, 171-177.

Scanning force microscopy aan hydrofiele molekulen dient, om tot betrouwbare resultaten te komen, in een waterige omgeving en met een hydrofobe tip gedaan te worden.

Bustamante, B. (1992) Biochemistry 31, 22-26.

Het gebruik van de term "rf puls" in verhandelingen over NMR is onzorgvuldig en dient vervangen te worden door de term "magnetische rf puls".

Bij de invoering van tolheffing op autosnelwegen dient deze voor heel Nederland te gelden, om discriminatie op grond van woonplaats uit te sluiten.

Als een oorspronkelijk aan Rembrandt toegeschreven werk op grond van nieuwe inzichten niet aan de meester maar aan een van zijn leerlingen toegeschreven moet worden doet dat geen afbreuk aan de artistieke waarde van het werk.

Stellingen behorende bij het proefschrift:
"The interaction of M13 coat protein with lipid bilayers; A spectroscopic study"
Johan Sanders, januari 1992.

VOORWOORD

In dit proefschrift worden de resultaten besproken van het onderzoek dat is uitgevoerd van 1988 tot 1992 bij de vakgroep moleculaire fysica aan de Landbouw Universiteit te Wageningen. Dit onderzoek was niet mogelijk geweest zonder de hulp van vele mensen, waarvan ik vooral de promotor Prof. dr T. J. Schaafsma, de co-promotor; dr Marcus Hemminga en de analisten Ruud Spruijt en Cor Wolfs wil bedanken.

Daarnaast hebben vele personen uit het binnen en buitenland bijgedragen aan het voor u liggende proefschrift. Ik wil allen bedanken voor hun stimulerende bijdrage. NWO en de EG wil ik bedanken voor hun financiële bijdrage, die dit onderzoek mogelijk maakte.

Johan Sanders
december 1991

CONTENTS

Chapter 1-Introduction

Chapter 2-The secondary structure of M13 coat protein in phospholipids studied by circular dichroism, Raman and Fourier transform infrared spectroscopic measurements
Submitted to Biochem. Biophys. Acta.

Chapter 3-Conformation and aggregation of M13 coat protein studied by molecular dynamics
Biophys. Chem. 41 (1991), 193-202.

Chapter 4-Formation of non-bilayer structures induced by M13 coat protein depends on the conformation of the protein
Submitted to Biochem. Biophys. Acta.

Chapter 5-A NMR investigation on the interactions of the α-oligomeric form of the M13 coat protein with lipids, which mimic the Escherichia coli inner membrane
Biochem. Biophys. Acta. 1006, (1991), 102-108.

Chapter 6-A small protein in model membranes: a time resolved fluorescence and ESR study on the interaction of M13 coat protein with lipid bilayers
Submitted to Europ. Biophys. J.

Chapter 7-Summarizing discussion- Samenvatting

Abbreviations
Curriculum vitae

CHAPTER 1

Introduction

M13 bacteriophage

The filamentous bacteriophage M13 consists of a circular, single stranded DNA of 6407 nucleotides [1], protected by 2700 copies of coat protein molecules [2,3,4].

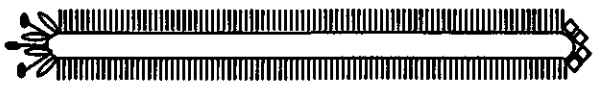

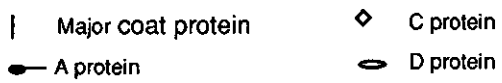

Figure 1. Schematic model of the M13 bacteriophage [5].

98% of the protein coat is formed by the gene 8 product, the major coat protein. Apart from this major coat protein a few copies of other proteins can be found in the bacteriophage: the absorption protein (MW 42.600), C and D protein (MW 3.500 and MW 11.500)(see Fig.1). The major coat protein in the bacteriophage is in an entirely α-helix conformation [6,7]. Upon infection of *E. coli* by the M13 bacteriophage this major coat protein is stored in the cytoplasmatic membrane, while DNA replication takes place in the cytoplasm. The newly synthesized DNA is coated by the bacteriophage gene 5 product [8]. At the same time new major coat protein is synthesized as a water soluble procoat. The procoat has an additional leader sequence at the N-terminus consisting of 23 amino acids [8,9,10]. The procoat is incorporated in the plasma-membrane and the leader sequence is cleaved off by a leader peptidase. During the assembly process new and old major coat protein replace the gene 5 product at the DNA [11]. The newly formed virus leaves the *E. coli* cell without lyses of the host [12].

M13 coat protein

In this thesis a small part of the reproductive cycle of the M13 bacteriophage is studied in more detail, namely the interaction of the major coat protein (MW 5240)(which will be called from now on the M13 coat protein) with lipid bilayers. The M13 coat protein consists

of 50 amino-acids: An acidic domain of 20 amino acids at the N terminus and a basic domain of 10 residues at the C terminus. The remaining 20 amino acids that form the central part of the protein are thought to be the membrane spanning part of the M13 coat protein when the protein is incorporated in the lipid bilayer (Fig. 2).

NH_3^+-Ala-Glu-Gly-Asp-Asp-Pro-Ala-Lys-Ala-Ala-	
Phe-Asn-Ser-Leu-Gln-Ala-Ser-Ala-Thr-Glu-	Acidic domain
Tyr-Ile-Gly-Tyr-Ala-Trp-Ala-Met-Val-Val	
Val-Ile-Val-Gly-Ala-Thr-Ile-Gly-Ile-Lys-	Hydrophobic domain
Leu-Phe-Lys-Lys-Phe-Thr-Ser-Lys-Ala-Ser-COO^-	Basic domain

Figure 2. Primary amino-acid sequence of the M13 coat protein.

The M13 coat protein has been extensively studied after solubilizing in detergents and reconstitution into lipid bilayers. Studies with the M13 coat protein in SDS micelles revealed that M13 coat protein has a high α-helix percentage [13] and that M13 coat protein could be obtained in a dimeric state [14]. This state of the M13 coat protein is called the b-state or the α-oligomeric form [13]. More relevant, because of their greater resemblance to natural lipid bilayers, are the studies performed on the M13 coat protein in model lipid bilayers. These studies revealed that a second form of the M13 coat protein could be obtained, which is dominated by a high percentage of β-sheet conformation. The protein with the β-sheet conformation was shown to be strongly aggregated [14,15,16]. This form of the M13 coat protein was called the c-state or β-polymeric form [13].

In various biophysical studies, described in the literature, it is unclear which form of the M13 coat protein has been studied. In some cases, on the basis of the results reported it can be suggested which form of the coat protein was actually studied. For example, the studies of Kimelman et al., [19], Johnson and Hudson [20] and Wolber and Hudson [21], showed that the M13 coat protein is monomeric or dimeric, suggesting that they were studying the protein in the α-oligomeric form. Other authors found that M13 coat protein was highly aggregated, which suggest that these workers were studying the M13 coat protein in the β-polymeric form [22,23,24,25,26,27].

Van Gorkom and Wolfs carefully checked which form of the M13 coat protein they were studying by checking the aggregation and conformation of the M13 coat protein used [18,28]. Their studies were performed on the M13 coat protein in the β-polymeric form and showed that the M13 coat protein in this form is capable of creating a fraction of lipids, which is influenced by the protein and which can not exchange with the bulk lipids. It was suggested

that these lipids were trapped by the protein aggregate. However a complete explanation for the spectral changes in their ^{2}H-NMR and ^{31}P-NMR spectra was not given [28].

Protein-lipid interactions

Apart from the functioning of M13 coat protein in the reproductive cycle of the M13 bacteriophage the presence of two membrane bound forms of M13 coat protein makes M13 coat protein a good model system to study protein-lipid interactions.

Since the discovering by Jost and Griffiths in 1973 [29] that lipids at the interface of an integral membrane protein have different properties as compared to the bulk lipids, much effort has been expended to study these protein-lipid interactions in more detail. One has to use model systems and simplified models to describe protein-lipid interactions, because of the inherent complexity of these natural protein-lipid systems.

The experimental approach used and questions asked in this thesis involve the study of the molecular details of interactions using spectroscopic techniques. An overview of the current state of the field of protein-lipid interaction, studied using spectroscopical and theoretical studies, can be found in Progress in Protein-Lipid interactions volume I [30] and II [31]. Since the appearance of these two volumes additional new methods have been developed: The modification of the protein structure by genetic methods to study the effect of amino acids on for example, protein translocation [32,33], the study of the tertiary conformation of crystalized membrane proteins by scattering experiments [34] or by using solid state NMR techniques to study the secondary structure of membrane bound proteins [35]. In addition the simulation of experimental data using more and more elaborate models is of growing interest in biophysical research [36,37,38,39,40].

Apart from these new methods magnetic resonance and optical techniques have been and are successfully used to investigate protein-lipid interactions [30,31]. Especially research in which a combination of the different techniques is used, has proved to be successful. Not only does one obtain different information by using a combination of the various techniques, for example, information about the secondary structure of the protein by FTIR and the molecular order and dynamics of the lipid by deuterium NMR, but one also obtains additional information about the molecular motions which occur at the protein-lipid interface due to the sensitivity of the various techniques for different timescales. Using the techniques mentioned above one can study the motional range of correlation times of 10^{-11} s (using time resolved fluorescence spectroscopy) to 10^{-3} s (using deuterium magnetic resonance relaxation studies). In the following paragraphs the spectroscopic techniques are discussed in the light of the experiments presented in this thesis to reveal M13 coat protein-lipid interactions.

Circular dichroism

CD spectra are the result of a difference in absorption of left and right circulary polarized light, which is normally expressed in an ellipticity. CD spectroscopy in the UV region (190-240 nm) can be used to obtain information about the secondary structure of protein molecules in water as well as in lipid membranes. This is because CD spectra of the various secondary structures show very distinct features. This makes it possible to fit a recorded CD spectrum of a protein with unknown secondary structure, to varying contributions of the different secondary structures. The CD spectra of a protein with unknown secondary structure are analyzed using computer programs, which compare the recorded spectra with CD spectra from a reference set of proteins with known secondary structure. The different secondary structures, which can be found from these analyses are α-helix, β-sheet, β-turn and remainder [41].

The accuracy of the determination of the secondary structure depends not only on the signal to noise ratio in the spectra, but also on the type of secondary structure to be found. More accurate results are obtained for proteins with a high α-helix or β-sheet structure [42]. In addition one should realize that the secondary structure determinations obtained from CD spectra can be distorted due to optical artifacts, such as light-scattering, absorption flattening effects [43], contribution of tryptophans in the far UV region [44], and uncertainties in protein concentration, which reduce the accuracy of the result.

Fourier transform infrared spectroscopy

In infrared spectroscopy the absorption bands from vibrational transitions are measured. These transitions generally occur between 5000 cm^{-1} and 200 cm^{-1}. The vibrational absorption bands typically arise from transitions localised in a part of the molecule. For proteins, the interesting vibrations, which give information about the conformation of the proteins are the amide vibrations. These vibrations arise from the backbone and can be assigned to simple groups. The C=O stretch is found in the region 1630-1660 cm^{-1} (amide I) and the N-H deformation at 1520-1550 cm^{-1} (amide II). The amide vibrational energy depends on the secondary structure of the protein. To derive a protein secondary structure a procedure is followed which is comparable to that described for the CD analysis: the amide I region of a protein with unknown secondary structure is compared with a reference set of 20 proteins [45].

Raman spectroscopy

Using Raman spectroscopy, information can be obtained about the vibrational states of molecules. Whereas in FTIR spectroscopy one observes the absorption of light, one looks with Raman spectroscopy at the interaction of incoming light of a known frequency (v) with an oscillating dipole having a characteristic frequency v_1. As a result of the interaction of the dipole with the incoming light, emission is observed at frequencies $v+v_1$ and $v-v_1$. The spectral band at lower energy is called the Stokes band, and is the one normally observed in Raman experiments. The exact frequency with which the amide group vibrates, depends on the conformation of the protein. This makes it possible to assign secondary structures on the basis of the observed amide vibrations of a protein with unknown structure.

As compared with FTIR spectroscopy Raman offers the advantage of no interference from water vibrations. However, in comparison with FTIR spectroscopy, Raman spectroscopists have to deal with both fluorescence backgrounds and limited signal to noise ratios.

Molecular dynamics

The three techniques described above are used to obtain the secondary structures from experimental data. However, it would also be interesting to calculate the secondary structure. For membrane proteins a favourable situation is present, due to restrictions imposed by the lipid. Firstly, the membrane spanning part must be hydrophobic, and secondly these parts must be in an α-helix or β-sheet conformation for the hydrogen bonds to be saturated. This reduced problem might be solved by molecular dynamics (MD) simulations [38,39].

The approach followed in the MD simulations is to develop a continuum approximation for the hydrophobic effect which is based on phenomological energies. The potential energy is described as a sum of interaction terms (Eq. 1);

$$V = V_{angle} + V_{dihedral} + V_{Hbond} + V_{coul} + V_{LJ} + V_{hydrophob} \qquad (1)$$

For the first five terms in Eq. 1 the parameters are taken from Van Gunsteren and Karplus. The last term in Eq. 1 is an additional potential ($V_{hydrophob}$) to account for the lipid/water interface. To describe this potential, a hydrophobicity h_i is attributed to each atom so that the hydrophobicity of each amino acid agrees with the experimental value. The ordering of the water molecules seem to be the dominant source of the hydrophobic effect and because the ordering seems to vary exponentially it is assumed that the hydrophobic potential is also varying exponentially (Eq 2):

$$V_{hydrop} = \begin{cases} \frac{1}{2}\sum_{i=1}^{N} h_i \, e^{-\left(\frac{|Z_i|-Z_0}{\lambda}\right)} & \text{for } |Z_i| > Z_0 \\ \frac{1}{2}\sum_{i=1}^{N} h_i \left[2-e^{-\left(\frac{-|Z_i|-Z_0}{\lambda}\right)}\right] & \text{for } |Z_i| \leq Z_0 \end{cases} \qquad (2)$$

The membrane surfaces are at $+Z_0$ and $-Z_0$. A thickness of 32 Å for a DOPC lipid membrane leeds to Z_0= 16 Å. The decay length over which the potential is active, λ, was taken 2 Å.

Using this potential Molecular Dynamic simulations can be performed on varying starting conformations of membrane proteins and by comparing the energies found for the varying structures after simulation the most likely conformation of a protein can be determined. This has been done previously for two proteins, rhodopsin and glycophorin [38,39]. One would prefer, however, to take the lipid and water molecules explicitly in account. However, MD simulations of lipid membranes are still at the beginning [36,40].

Deuterium nuclear magnetic resonance

In the following paragraphs the three magnetic resonance techniques used in this thesis are outlined. In bilayer systems powder like nuclear magnetic resonance (NMR) spectra are expected (^{2}H-NMR and ^{31}P-NMR), requiring high-power solid state NMR techniques. High resolution NMR is not suitable for these large systems. Spin-label electron spin resonance (ESR) is the third magnetic resonance technique used to study lipid bilayers.

To understand deuterium NMR spectra one has to realize that the deuterium nucleus is a spin I=1 particle. This results in a Hamiltonian (Eq. 3) which is apart from the Zeeman interaction (H_z), dominated by the quadrupolar interaction (H_q).

$$H = H_z + H_q \qquad (3)$$

The quadrupolar interaction (H_q) is the result of the interaction of the nuclear quadrupole moment with the electric field gradient. Solving the Schrödinger equation to the first order gives the energy levels of a deuterium nucleus in a magnetic field. One obtains three energy levels for the three angular momentum values m = 1, 0, -1 (Eqs. 4-6):

$$E_{+1} = -\beta_N g B_0 + \frac{1}{4} eQV^{(2,0)} \quad (4)$$

$$E_0 = -\frac{1}{2} eQV^{(2,0)} \quad (5)$$

$$E_{-1} = \beta_N g B_0 + \frac{1}{4} eQV^{(2,0)} \quad (6)$$

β_N is the nuclear magneton, g the so-called g factor, B_0 the magnetic field strength, Q the nuclear quadrupole moment and $V^{(2,0)}$ the irreducible tensor components of the electric field gradient. Due to the quantum mechanical selection rule, $\Delta m = \pm 1$, two resonances are observed. In a single crystal, where the external magnetic field is parallel to the z principal axis of the quadrupolar interaction tensor $V^{(2,0)} = V_{zz}$, one observes the largest quadrupolar splitting (ΔVq) of these resonances. However in an anisotropic medium the CD bond makes an angle θ with the external applied magnetic field resulting in quadroplar splittings for each angle θ resulting in:

$$\Delta Vq = \frac{3}{2}\frac{eQ}{h} Vzz \frac{3\cos^2\theta - 1}{2} \quad (7)$$

In a liquid crystal there is a rapid fluctuation around the director axis. This results in replacing the angular terms in Eq. 7 by their time averaged value. If B_0 is not parallel to the director axis but makes an angle β with this axis then the observed quadrupolar splitting is:

$$\Delta Vq = \frac{3}{2}\frac{e^2qQ}{h} \overline{\frac{3\cos^2\theta - 1}{2}} \frac{3\cos^2\beta - 1}{2} \quad (8)$$

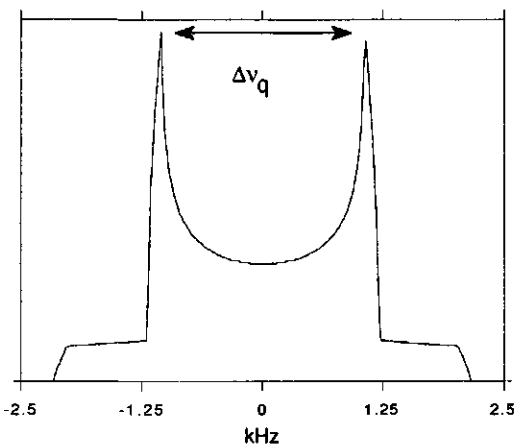

Figure 3. Simulated deuterium NMR spectrum with a quadrupolar splitting (the difference between the two maxima in the spectrum) of 2 kHz.

A typical NMR deuterium spectrum of a liquid crystal, observed as a result of a random distribution of the angles β, is shown in Fig. 3.

Measurements of relaxation times can give information about the dynamics of the lipids in the bilayers. The quadrupolar interaction dominates the relaxation process. The spin lattice relaxation time, T_{1z}, depends on the spectral densities $J(\omega_0)$ and $J(2\omega_0)$, whereas the spin-spin relaxation time T_{2e} depends on the spectral densities $J(0)$, $J(\omega_0)$ and $J(2\omega_0)$. As a result of the dependence of T_{2e} on $J(0)$, this relaxation time is more sensitive to slow motions.

The synthesis of specifically deuterated lipids has allowed the study of protein lipid interactions without perturbations due to the probe molecule, because it is expected that changing a proton for a deuterium nucleus the properties of the lipid molecule are not affected. Studies on protein-lipid interactions using specific deuterated lipids have been performed by various workers [46,47,48,49,50,51,52,53]. Differences in the quadrupolar splitting of ^{2}H-NMR spectra of lipids labelled with deuterium in the headgroup reflect the order of the headgroup segment and the charge distribution at the membrane surface. Phospholipids labelled with deuterium in the chains are used to study the order of the hydrophobic part of the lipid bilayer. Various studies have been performed on chain labelled lipids, which showed their sensitivity to changes in order e.g. the phase transition [54]. Deuterium labels can also be placed on the protein molecule. The fd coat protein, which is closely related to the M13 coat protein, has extensively been studied in bilayers by Opella and coworkers [55,56].

Phosphorus nuclear magnetic resonance

Apart from ^{2}H-NMR one can use ^{31}P-NMR to study changes in the lipid morphology. This lather nucleus is very suitable for NMR experiments due to the fact that the phosphorus is a natural occuring label. The phosphorus NMR lineshape is determined by the chemical shift anisotropy of the phosphorus nucleus and the proton-phosphorus dipolar interactions. The latter term can be removed directly by proton decoupling. The chemical shift anisotropy is described by a tensor, of which in the principal axis system the values for phospholipids are σ_{11}= -80 ppm, σ_{22}= -20 ppm and σ_{33}= +100 ppm. In lipid bilayers the static shielding tensor is averaged to a new effective tensor which is axially symmetric around the director axis. The two components of this averaged tensor $\sigma_{\parallel}$ and $\sigma_{\perp}$ are used to define the chemical shift anisotropy (CSA; $\Delta\sigma$): $\Delta\sigma = \sigma_{\parallel} - \sigma_{\perp}$. Typical CSA values of -50 ppm are

obtained for lipids arranged in a liquid crystalline phase. This results in a ^{31}P-NMR spectrum displayed in Fig. 4.

In hexagonal lipid phases a fast rotation around the cylinder axis as a result of lateral diffusion gives a chemical shift tensor with the components $\frac{\sigma_{\parallel} + \sigma_{\perp}}{2}$ and $\sigma_{\perp}$. This results in a ^{31}P-NMR spectrum displayed in Fig. 5.

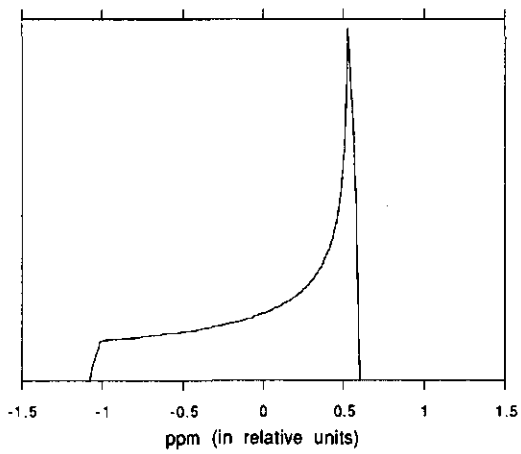

Figure 4. Axially symmetric ^{31}P-NMR powder pattern (the components of the averaged tensor values are $\sigma_{\parallel}$ and $\sigma_{\perp}$).

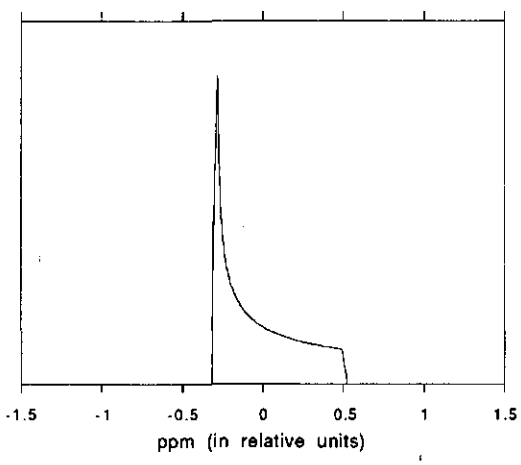

Figure 5. Axially symmetric ^{31}P-NMR powder pattern (the components of the averaged tensor values are $\frac{\sigma_{\parallel} + \sigma_{\perp}}{2}$ and $\sigma_{\perp}$).

Finally in isotropic lipid systems the tensor is completely averaged to one value $\sigma_{iso} = \frac{\sigma_{\parallel} + 2\,\sigma_{\perp}}{3}$ resulting in a ^{31}P-NMR spectrum of an isotropic line at a position given by σ_{iso}. Most lipids are organised in bilayers and integral proteins appear to stabilize the phospholipid bilayer systems. However the lipid structure can be influenced by the presence of membrane proteins and possible role for this lipid polymorphism have been suggested [57].

Electron spin resonance

The last magnetic resonance technique to be mentioned which is used in this thesis for studying protein-lipid interactions is spin label ESR. The spin labelled phospholipids are sensitive to molecular motion on the timescale of 10^{-8} s due to the ^{14}N hyperfine splitting anisotropy of the nitroxide free radical group. ESR is a very useful technique to study protein-lipid interactions due to its inherent high sensitivity as compared to NMR, which allows study of small amounts of protein lipid reconstitutes. In contrast to NMR, where the timescale is slow compared to the exchange rates between bulk and protein associated lipids, one would expect to observe in ESR spectra two component spectra of bilayers containing protein. This was first shown by Jost et al. in 1973 [29]. After incorporation of cytochrome C oxidase they observed a second component, the presence of which depended on the lipid to protein ratio. Other integral membrane proteins showed identical effects [58]. This component could be characterized as being lipids immobilized at the surface of the protein. In addition specificity for various phospholipids, differing only in the headgroup, has been studied using spin-labelled ESR [58].

Recently, various detailed models have been discussed in the literature, which allow the simulation of pure lipid systems, in terms of order parameters and diffusion coefficients [37,59], or in the presence of proteins, in a two site exchange model [60].

Time-resolved fluorescence

Time-resolved fluorescence measurements can provide information about the environment (lifetimes) or the mobility (anisotropy) of the fluorophore studied. The mobilities which can be studied in the range of picoseconds to nanoseconds and therefore allow a study of the dynamics of proteins and lipids. To study the dynamics of the protein one normally uses the intrinsic fluorescent tryptophan, whereas study of the lipids requires specific labelling with for example parinaric acid, or diphenylhexatriene probes.

Time-resolved fluorescence decay provides information about the environment of the probe molecule. The set-up for time resolved fluorescence decay and anisotropy

measurements is depicted in Fig. 6. After a short (polarized) laser light pulse the probe molecules are excited to a higher energy level. The probe molecule emits with its own characteristic lifetime light of a higher wavelength on relaxing to its ground state. Time resolved anisotropy measurements are based on the principle that during the time interval between excitation by polarized light and emission of light (fluorescence), the probe molecule undergoes motions which causes the degree of polarization of the emitted light to decrease. By analysing the polarization decay in terms of models (simple exponential, or more complicated diffusion models) one can describe in detail motions of the protein dynamics (rotation of the whole protein, segmental mobility, amino acid motion) or lipid dynamics (diffusion) and order [62] .

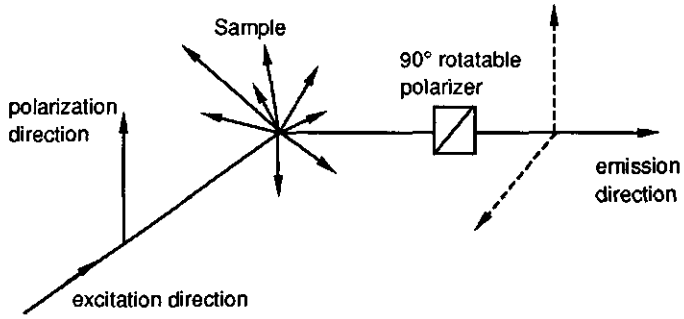

Figure 6. Experimental set-up for a time resolved fluorescence decay and time resolved anisotropy decay measurements. The polarization of the incoming pulse is indicated. As a result of the change in orientation of the probe molecule in the sample during its presence in the exciting state, the polarization is changed. This is followed by detecting the emission light under two detection directions (For an experimental description see O'Connor and Phillips [61]).

Outline of the thesis

In this thesis results are presented of studies on the M13 coat protein in the two different forms, described under "M13 coat protein", reconstituted in various lipid bilayers and studied with spectroscopic techniques.

In the first part of the thesis (chapters 2,3,4) a detailed comparison of the two forms of the M13 coat protein will be presented. In the second chapter of the thesis the secondary structure of the protein is studied using Raman, CD and FTIR. Combining these various techniques allows a more definite statement on the presence of the various secondary structural elements in the M13 coat protein in both the α-oligomeric and β-polymeric form.

In chapter 3 a theoretical study is performed, to try to relate the aggregational and the conformational state of the two different forms of the M13 coat protein as observed in biochemical experiments. This was done by performing molecular dynamics simulation of the M13 coat protein in the two forms, α-oligomeric and β-polymeric, either in a monomeric or dimeric configuration. In chapter 4 the effect of the two different forms of M13 coat protein, the α-oligomeric or β-polymeric forms, on the surrounding lipid matrix is studied using phosphorus and deuterium nuclear magnetic resonance. The results show that the protein in the β-polymeric form distorts the lipid bilayer and induces the presence of non-bilayer structures, whereas the α-oligomeric form of the M13 coat protein does not disturb the bilayer.

The second part of the thesis is a more detailed study on the interaction of the α-oligomeric form of the M13 coat protein with lipid bilayers. In chapter 5 a detailed deuterium magnetic resonance study is described on specific headgroup deuterated phospholipids. It is shown that only slow motions are affected by the M13 coat protein and that the positive charges of the lysines on the protein molecule cause a tilt of the headgroup. In chapter 6 it is shown that the protein in the α-oligomeric form is not capable of inducing a second component in the ESR spectra of spin labelled fatty acids. Using spectral simulations on the ESR spectra and by performing studies on fluorescent lipids it is shown that both the mobility and order of the hydrophobic part of the bilayer is affected by the M13 coat protein.

The concluding part of the thesis, chapter 7 summarises the observed results and the conclusions drawn in this thesis.

References

1 van Wezenbeek, P. M. G. F., Hulsebos, T. J. M. and Schoenmakers, J. G. G. (1980) Gene 11, 129-148.

2 Marvin, D. A. (1985) J. Biosci. 8, 799-813.

3 Ray, D. S. (1969) Mol. Biol. 43, 631-643.

4 Rasched, I. and Oberer, E. (1986) Microbiol. Rev. 50, 401-427.

5 Webster, R. E., Grant, R. A. and Hamilton, L. A. W. (1981) J.Mol.Biol. 152, 357-374.

6 van Asbeck, F., Beyreuther, K., Koehler, H., Von Wettstein. G. and Braunitzer, G. (1969) Hoppe-Seyler's Z. Physiol. Chem. 350, 1047-1066.

7 Day, L. A. (1969) J. Mol. Biol. 39, 265-77.

8 Pratt, D., Tzagoloff, H. and Beadoin, J. (1969) Virology 39, 42-53.

9 Konings, R. N. H., Hulsebos, T. and Van den Hondel, C. A. (1975) J. Virol. 15, 570-84.

10 Sugmoto, K., Sugiski, K. and Takanami, M. (1977) J. Mol. Biol. 110, 487-507.

11 Model, P., McGill, C., Mazur, B. and Fulford, W. D. (1982) Cell 29, 329-35.
12 Hoffman-Berling, H., and Maze, R. (1964) Virology 22, 305-313.
13 Nozaki, Y., Reynolds, J. A. and Tanford, C. (1978) Biochemistry 17, 1239-1246.
14 Datema, K. P. (1987) thesis Agricultural Univerity Wageningen.
15 Fodor S. P. A., Dunker, A. K., Ng, Y. C., Carsten, D. and Williams, R. W. (1981) in: Seventh. biennial Conference on Bacteriophage Assembly. pp 441-455 (Dubow, M.S., ed.) Alan R. Liss Inc., New York.
16 Spruijt, R. B., Wolfs, C. J. A. M. and Hemminga, M. A. (1989) Biochemistry 28, 9159-9165.
17 Spruijt, R. B. and Hemminga, M. A. (1991) submitted to Biochemistry
18 Wolfs, C. J. A. M., Horvàth, L.I., Marsh, D., Watts, A. and Hemminga, M. A. (1989) Biochemistry 28, 9995-10001.
19 Kimelman, D., Tecoma, E. S., Wober, P.K., Hudson, B. S., Wickner, W. T. and Simoni, R. D, (1979) Biochemistry 18, 5874-5880.
20 Johnson, I. D. and Hudson, B. S. (1989) Biochemistry 28, 6392-6400.
21 Wolber, P. K. and Hudson, I. D. (1982) Biophys. J. 37, 253-262
22 Datema, K. P., Wolfs, C. J. A. M., Marsh, D., Watts, A. and Hemminga, M. A. (1987a) Biochemistry 26, 7571-7574
23 Datema, K. P., Visser, A. J. W. G., van Hoek, A., Wolfs, C. J. A. M., Spruijt, R. B. and Hemminga M.A. (1987b) Biochemistry 26, 6145-6152.
24 Datema, K. P., Van Boxtel, B. J. H. and Hemminga, M. A. (1988) J. Mag. Res. 77, 372-376.
25 de Jong, H., Hemminga, M. A. and Marsh, D. (1990) Biochim. Biophys. Acta 1024, 82-88.
26 Peng, K., Visser, A. J. W. G., van Hoek, A., Wolfs, C. J. A. M. and Hemminga, M. A. (1990) Eur. Biophys. J. 18, 277- 283.
27 Peng, K., Visser, A. J. W. G., van Hoek, A., Wolfs, C. J. A. M., Sanders, J. C. and Hemminga, M. A. (1990) Eur. Biophys. J. 18, 285-293.
28 van Gorkom, L. C. M., Horváth, J. I., Hemminga, M. A., Sternberg, B. and Watts, A. (1990) Biochemistry 29, 3828-3834.
29 Jost, P. C., Griffith, O. H., Capaldi, R. A. and Vanderkooi, G. A. (1973) Proc. Natl. Acad. Sci. USA 70, 4756-4763.
30 *Progress in Lipid Protein Interaction* (1985), Watts, A., & De Pont, J. J. H. H. M., Eds., Vol 1, Elseviers Science Publishers, Amsterdam.
31 *Progress in Lipid Protein Interaction* (1987), Watts, A., & De Pont, J. J. H. H. M., Eds., Vol 2, Elseviers Science Publishers, Amsterdam.
32 Jordi, W., Zhou, C., Pilon, M., Demel, K. and de Kruijff, B. (1989) J. Biol. Chem 264, 292-2301.

33 von Heijne, G., Wickner, W. and Dalbey, R. E. (1988) Proc. Natl. Acad. Sci U.S.A. 85, 3363-3366.

34 Deisenhofer, J., Epp, O., Miki, K., Huber, R. and Michel, H. (1985) Nature 318, 618-624.

35 Opella, S. J., Stewart, P. L. and Valentine, K. G. (1987) Q. Rev. Biophys. 19, 7-49.

36 van der Ploeg, P. and Berendsen, H. J. C., (1983) Mol. Phys.49, 233-244.

37 Moser, M., Marsh, D., Meier, P., Wassmer and K-H. and Kothe, G. (1989) Biophys. J. 55, 111-123.

38 Edholm, O. and Johansson, J. (1987) Eur. Biophys. J. 14, 203-209.

39 Edholm, O. and Jähnig, F. (1988) Bioph. Chem. 30, 279-292.

40 Loof, H., Harvey, S. C., Segtest, J. P. and Pastor, R.W. (1991) Biochemistry 30, 2099-2113.

41 Provencher, S. W. and Glöckner, J. (1981) Biochemistry 20, 33-37.

42 Stokkum, I. H. M., Spoelder, H. J. W., Bloemendaal, M., Grondelle, R. and Groen, F. C. A. (1990) Anal. Biochem. 191, 1110-118.

43 Wallace, B. A. and Mao, D. (1984) Anal. Biochemistry 142, 317-328.

44 Khan, Y. M., Villanueva, G. and Newman, S. A. (1989) Jour. Biol. Chem. **, 2139-2142.

45 Lee, D. C., Haris, P. I., Chapman, D. and Mitchell, R. C. (1990), Biochemistry 39, 9185-93.

46 Seelig, J. and Gally, H-U (1976) Biochemistry 15, 5199-5204.

47 Brown, M. F. and Seelig, J. (1978) Biochemistry 17, 381-384.

48 Büldt, G. and Seelig, J. (1980) Biochemistry 16, 6170-6175.

49 Wohlgemuth, R., Waespe-Sarcevic, N. and Seelig, J. (1980) Biochemistry 19,

50 Paddy, M. R., Dahlquist, F. F., Davis, J. H. and Bloom, M. (1981) Biochemistry 20, 3152-3162.

51 Sixl, F. and Watts, A. (1985) Biochemistry 24, 7906-7910.

52 Sixl, F., Brophy, P. J. and Watts, A. (1984) Biochemistry 23, 2032-2039.

53 Scherer P. G. and Seelig J. (1989) Biochemistry 28 , 7720-7728.

54 Bloom, M. and Smith, I. C. P. (1985) in *Progress in Lipid Protein Interaction* (Watts, A., & De Pont, J. J. H. H. M., Eds) Vol 1, pp 61-88, Elseviers Sciencew Publishers, Amsterdam.

55 Opella, S. J., Cross, T. A., DiVerdi, J. A. and Sturm, C. F. (1980) Biophys. J., 32, 531-548.

56 Valentine, K. G., Schneider, D. M., Leo, G. C., Colnago, L. A. and Opella, S. J. (1986) Biophys. J., 49, 36-38.

57 De Kruijff, B., Cullis, P. R., Verkleij, A. J., Van Echteld, C. J. A., Taraschi, T. F., Van Hoogevest, P., Killian, J. A., Rietveld, A. and Van der Steen, A. T. M. (1985) in

Progress in Lipid Protein Interaction (Watts, A., & De Pont, J.J.H.H.M., Eds) Vol 1, pp 89-142, Elseviers Sciencew Publishers, Amsterdam.

58 Marsh, D. (1987) J. Bioenerg. Biomembr., 19, 677-89.

59 Schneider, D. and Freed, J., H. (1989) in *Biological Magnetic Resonance, volume 8: Spin labelling* (Berliner, J., L. and Reuben, J., Eds) 7, pp 1-76, Plenum Press, New York.

60 Horvath, L. I., Brophy, P. J. and Marsh, D. (1988) Biochemistry 27, 46-52.

61 O'Connor, D. V. and Phillips, D. (1984) Time correlated single photon counting, Acad. Press, London.

62 Szabo, A. (1984) J. Chem. Phys 81,150-67.

CHAPTER 2

The secondary structure of M13 coat protein in phospholipids studied by circular dichroism, Raman and Fourier transform infrared spectroscopic measurements

Johan C. Sanders, Parvez I. Haris, Dennis Chapman, Cees Otto and Marcus A. Hemminga

Abstract

M13 bacteriophage is a filamentous phage, which infects *Escherichia coli*. The circular stranded DNA of the phage is surrounded by a protein coat, which predominantly consists of the gene 8 product, the major coat protein. During infection this coat protein is inserted in the host membrane. It has been reported that the membrane-bound M13 coat protein can adopt two different forms, which differ in conformation and aggregation state (Spruijt et al., (1989) Biochemistry 28,9158-9165). Knowledge of the secondary structure of the M13 coat protein in both forms can help to understand how the different forms interact with lipid bilayers. Circular dichroism, Raman and Fourier transform infrared spectroscopy have been applied on M13 coat protein incorporated in lipids under identical experimental conditions. By comparison of the various techniques reliable information about the relative presence of the various secondary structures is obtained. The conformation of the aggregated form is 13% α-helix, 57% β-sheet, 13% turn and 16% remainder, while the conformation of the reversibly aggregated membrane bound form of M13 coat protein is 91% α-helix, 5% β-sheet, 3% turn and 1% remainder. The correspondence of the secondary structure of the lather form and the protein in the virus particle suggests that the membrane bound form with its high α-helical content can bind to the virus particle without large energy implications.

Introduction

M13 bacteriophage is a filamentous phage, which infects *Escherichia coli*. The circular stranded DNA of the phage is surrounded by a protein coat, which predominantly consists of the gene 8 product, the major coat protein. The major coat protein in the phage is completely α-helical as revealed with Raman spectroscopy [1]. During infection this coat protein is inserted in the host membrane. Also newly synthesized coat protein is inserted into the host bilayer, where it is assembled together with old coat protein around DNA to form new M13

bacteriophage particles [2,3]. The major coat protein is composed of three domains: a 19 amino acid long hydrophobic core, the N-terminal (residues 1-20) and the C-terminal (residues 40-50). The hydrophobic core is the membrane spanning part when the protein is in the host bilayer.

It has been reported that M13 coat protein can adopt two different overall conformations when it is inserted in lipid bilayers [4-7]. The presence of either one of these M13 coat protein forms depends on the protein purification, lipid type and salt concentration [7]. These two different forms are referred to as the M13 coat protein in the b and c-state [4,5]. The protein in both the lipid bound forms was shown to be in a less α-helical state as compared to the virus bound protein (a-state). It was therefore suggested that this protein should undergo major conformational changes upon virus formation [4,5], raising several questions concerning the energy implications of this change in conformational state.

In this paper we will carefully study the conformation of these two forms again by application of the different techniques i.e. CD, FTIR and Raman. Quantitative information about the amount of secondary structure arrangements in both different protein forms will enable to understand how these different forms interact with lipid bilayers and the role of the two different forms in the infection process.

Materials and methods

Chemicals: Dioleoyl-phosphatidyl-glycerol (DOPG) and dimiristoyl-phosphatidyl-glycerol (DMPG) are obtained from SIGMA (St. Louis, U. S. A.) and used without further purification.

Protein purification and reconstitution: Bacteriophage M13 is grown and purified as described previously [7]. After removing the chloroform with nitrogen gas the desired amounts of DOPG is lyophilized for at least 12 hours. DMPG and DOPG were solubilized in buffer (buffer A (for the M13 coat protein in the c-state): 8.0 M Urea, 5 mM Tris, 0.1 mM EDTA, 20 mM ammonium sulphate, 140 mM NaCl, pH 8.0; buffer B (for the coat protein in the b-state): 50 mM cholate, 10 mM Tris , 0.2 mM EDTA , 140 mM NaCl, pH 8.0. To buffer A the desired amount of protein, purified by Knippers & Hoffmann-Berling [8] was added to obtain the protein in the c-state and to buffer B the desired amount of protein, purified by Spruijt et al., [7] to obtain the protein in the b-state was added. This was followed by dialysis at room temperature against 100 fold excess buffer. The same buffer (10 mM Tris, 0.2 mM EDTA, 140 mM NaCl, pH 8.0) was used for the protein purified by Knippers & Hoffmann-Berling [8] and Spruijt et al. [7] for a total of 48 hours changing the buffer every 12 hours. Directly after the dialysis procedure the reconstituted lipid-protein complexes were concentrated using an Amicon stirring cell. The samples were devided into

three parts and from each of these parts the secondary structure of the M13 coat protein was determined using either CD, Raman or FTIR. The aggregation state, L/P ratio and the incorporation of the protein was checked as described by Spruijt et al. [7].

CD measurements and analysis: CD measurements were performed at 30 °C on a Jobin-Yvon Dichrograph Mark V in the wavelength range 190-290 nm, using a 0.1 cm path length. The scantime for one scan was 1500 s with a 2 s time constant. The samples for the CD measurements were diluted to an OD_{280} of 0.1. The temperature was under control of a thermo-statted water bath and maintained at 30 °C. Background spectra, consisting of buffer with the same lipid concentration as used in the corresponding sample spectrum, were recorded under the same experimental conditions. Difference spectra were generated by subtracting the background spectra from the corresponding spectra. The difference spectra were transferred to a VAX computer. Spectra (195/200-240 nm) were analysed using a fitting program supplied by Provencher [9]. In the fitting procedure the real ellipticity values were used and no normalization was applied (constrained analyses).

Raman measurements and analyses: Raman spectra were obtained with a Jobin-Yvon HG2S monochromator. A Hamamatsu photomultiplier tube, r942-02, was used in photon counting mode. The tube voltage was 1750 V. The Raman spectra were excited with 514.5 nm light from a Spectra Physics Ar^+-laser (type 2025). The power at the sample was 400 mW. The slitwidths of the spectrometer were adjusted such as to give rise to a resolution of 4 cm^{-1}. The scan interval runs from 400 to 1800 cm^{-1} with a stepwidth of 1 cm^{-1}. The temperature of the sample was under control of a thermo-statted bath (30 °C). Spectra were obtained from lipid/M13 coat protein complexes, pure lipid systems and from the buffer solution. Prior to amide I band analysis the protein spectrum was obtained in the following way:

$$[\text{protein}] = [\text{complex}] - c_1 * [\text{buffer}] - c_2 * [\text{lipid}]$$

where [....] indicates the spectrum of the components. The constants c_1 and c_2 were adjusted in such a way that a flat baseline was obtained between 1500 and 1730 cm^{-1}. The position of the phenylalanine band in the analyzed spectra was at 1002 cm^{-1}. The amide I fit was performed using a singular value decomposition routine. A basis set of 15 reference proteins was obtained from Williams [10].

Infrared measurements and analyses: Infrared spectra were recorded on a Perkin-Elmer 1750 FTIR spectrometer equipped with a fast-recovery TGS detector and a Perkin Elmer data station. Aqueous samples were recorded in a temperature controlled Specac cell

fitted with either a 6 μm tin spacer for studies in H_2O and a 50 μm Teflon spacer for the studies with D_2O. The samples in D_2O were prepared by dialysis of a part of the sample solution against D_2O. The temperature was maintained at 30 °C. The spectrometer was continuously purged with dry air to eliminate water vapour interference. A sample shuttle was used to allow the background spectrum to be signal averaged over the same time period as the sample spectrum. For the H_2O samples 400 scans were coadded, apodized giving a resolution of 4 cm^{-1}. For samples in D_2O 256 scans were coadded and processed as for the samples containing H_2O. Difference spectra were generated by subtracting the appropriate background spectrum containing lipid and buffer. Details about solvent subtraction are described elsewhere [11,12]. Second derivative spectra were generated from the obtained difference spectra using the Perkin-Elmer DERIV routine as described previously [11]. Quantitative analysis in terms of secondary structural elements were performed with the program CIRCOM [12]. This program uses 18 water soluble proteins as a calibration set. The area under the amide I band (i.e. from 1700-1600 cm^{-1}) was made constant and also the set ordinate at 1700 cm^{-1} was set to a constant value. This procedure is applied to adjust for any variation in baseline and absorbance due to variation in path length and concentration [12].

Results

Protein checks: The protein in the c-state is characterized as being highly aggregated as revealed from the HPLC elution profiles, whereas the protein in the b-state shows no aggregation. This is in agreement with the findings of Spruijt et al., [7]. Both samples were checked for the homogeneity and incorporation of the protein by sucrose gradient. Sucrose gradients centrifugation of samples with and without protein show only one band, showing its homogeneity. The band of the samples with protein is at a lower position in the sucrose gradient showing its higher density due to the incorporation of the protein. The L/P ratio was checked after the dialysis procedure and was shown to be 20 for the samples with the M13 coat protein in both states.

CD measurements: The CD spectra of the M13 coat protein either in the c-state or in the b-state both in DOPG and bilayers are given in Fig. 1a and 1b respectively. The secondary structure of the M13 coat protein in the c-state is predominantly β-sheet in both types of lipid systems. However, also smaller amounts of other structures are found (Table I). The α-helix content for the protein in the b-state is 95% and 91% in DOPG and DMPG, respectively. In both lipid types only a small amount of other secondary structural arrangements is observed (Table I). Performing the analyses without taking into account the protein concentration or changing the temperature did not result in a change in the results.

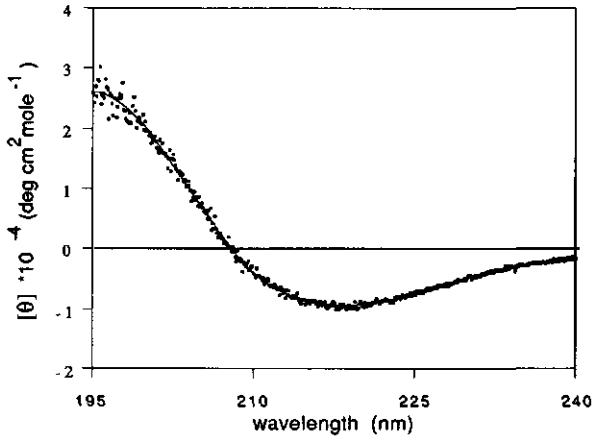

Figure 1A. CD spectrum of the M13 coat protein in the β-polymeric form in DOPG bilayers. The squares represent the data points and the straight line represents the by fitting obtained CD spectrum.

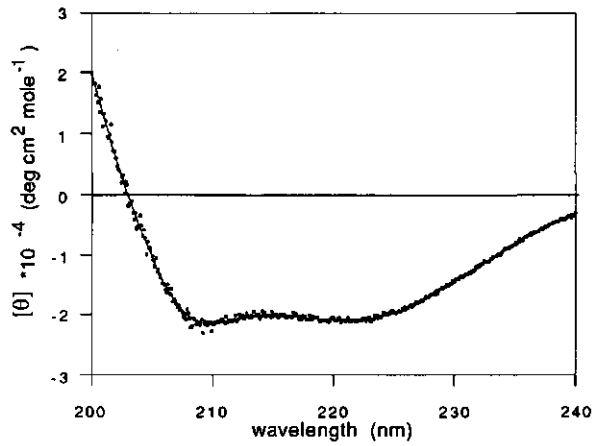

Figure 1B. CD spectrum of the M13 coat protein in the α-oligomeric form in DOPG bilayers. The squares represent the data points and the straight line represents the by fitting obtained CD spectrum.

Raman measurements: The Raman spectra of the amide I region of the protein in the c-state in DMPG bilayers is presented in Fig. 2a and the spectrum of M13 coat protein in the c-state in DOPG bilayers is shown in Fig. 2b. These Raman spectra are obtained after the subtraction procedure as described in materials and methods. The amide I region is of special interest for obtaining information on the secondary structure. In the Raman spectra of the M13 coat protein in the c-state in DMPG a well-resolved band at 1666 cm^{-1} was observed, which can be assigned to β-sheet structure [13]. The broad shape at the high frequency edge of the β-sheet band at 1666 cm^{-1} of the Raman spectrum of M13 coat protein in the c-state (Fig. 2a) possibly indicates the presence of other secondary structures. This band could not properly be reduced by subtraction of the water- or the lipid spectrum. A most reasonable assignment for these contributions are the presence of turns. This was also taken into account by the analysis as presented by Williams [10]. The band at 1233 cm^{-1} (Fig. 3) arising from the amide III mode of the protein in the c-state, suggests anti-parallel β-sheet [14]. In the same amide III spectrum contributions from both turn and α-helix can be found at 1297 cm^{-1}.

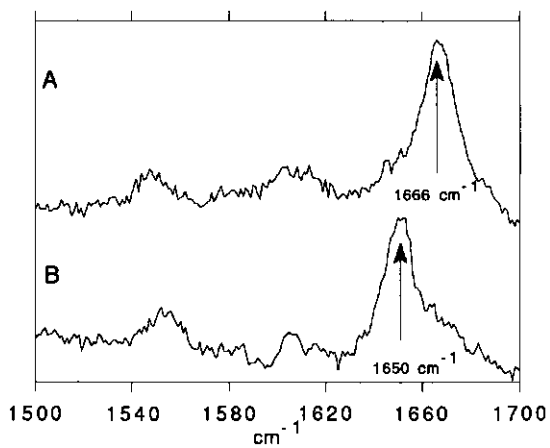

Figure 2. Raman spectra of the amide I region of M13 coat protein in the β-polymeric (A) and α-oligomeric (B) from.

In the spectra of the M13 coat protein in the b-state the amide I maximum is found to be at 1650 cm^{-1}, which denotes α-helix [13]. Apart from this band a broad band is observed at 1675 cm^{-1}. The weak band at 1276 cm^{-1} (not shown) is assigned to amide III modes, in agreement with the presence of α-helix structure as observed from the amide I region [13]. Well resolved in both cases is a band observed near 1550 cm^{-1}. This band can be assigned to the single tryptophan of the M13 coat protein [13]. The band at 1605 cm^{-1} observed in both

Raman spectra is assigned to vibrations of the thyrosines and the phenylanalines amino-acids [13].

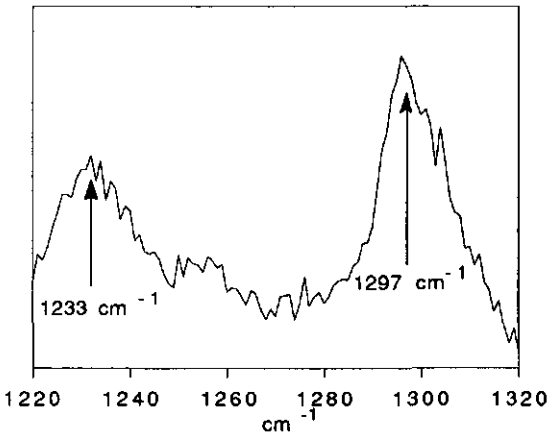

Figure 3. Raman spectrum of the amide III region of M13 coat protein in the β-polymeric form.

The results of the secondary structure analysis are presented in Table I. The ordered and disordered helix types distinguished in Williams [10] are summed in Table I. Also the parallel and anti-parallel β-sheet are taken together. The preparation of the protein spectra prior to amide I analysis gives rise to uncertainties in the percentages of secondary structure. The subtraction of the lipid spectrum in the case of DMPG is reliable due to the absence of intense lipid contributions to the spectrum in the amide I region. However in the case of DOPG a strong band arises at 1659 cm^{-1}. This band results from the C=C stretch motion in the acyl chains. Subtraction of the lipid spectrum from the complex spectrum influences the shape of the amide band at the high frequency side. An optimal subtraction was obtained by an arbitrary visual judgement. The presence of the Raman scattering of water around 1630 cm^{-1} influences most noticeably the percentage α-helix in the amide I analysis. The slope of the water spectrum at the low frequency edge however does not coincide with the amide I band and therefore allows a fairly reasonable subtraction criterium. The remaining background was fitted by a straight line drawn between minima around 1525 cm^{-1} and 1725 cm^{-1}. The cumulation of subtractions gives rise to the error indicated in the footnote in the Table I.

Infrared measurements: Infrared spectra of M13 coat protein in both conformations in DOPG bilayers in H_2O are displayed in Figs. 4 and 5. The spectra of the protein in the c-state

show an amide I absorption maximum at 1630 cm^{-1}, while the amide II band is located at 1530 cm^{-1} (Fig. 4). However the intensity of this band is much more reduced than is normally observed for proteins in H_2O. Previously, it has been noted that the intensity ratio of the two amide regions, A_{II}/A_I, was associated to changes in conformation, temperature or solvent polarity [15]. The abnormal ratio A_{II}/A_I for the M13 coat protein in the c-state could possibly be the result of the aggregation of the protein in this form, causing a very distinct amide environment. The band at 1734 cm^{-1} arises from the lipid carbonyl ester vibration.

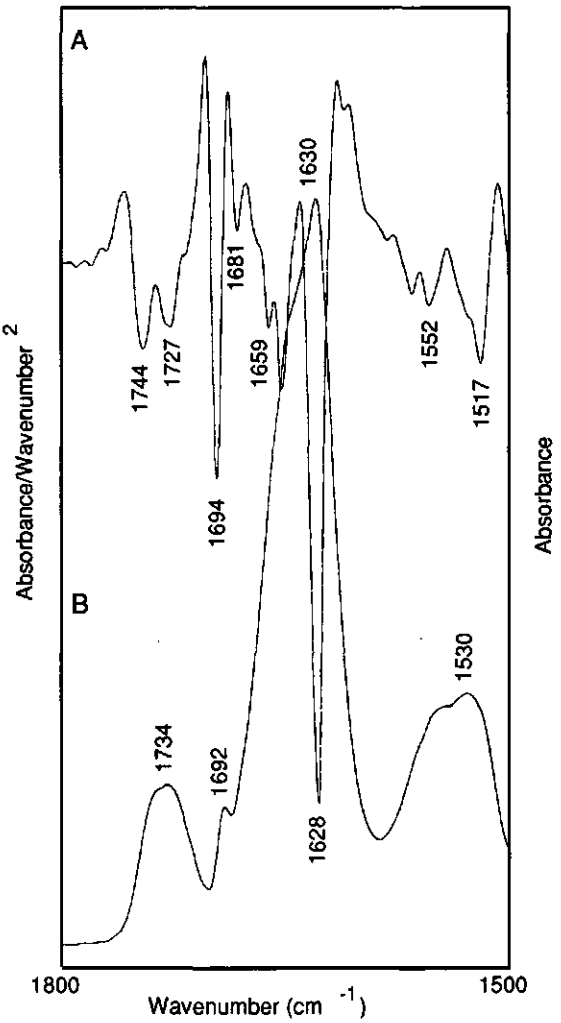

Figure 4. Infrared spectrum in H_20 (B) and the second derivative (A) of M13 coat protein in the β-polymeric form in DOPG bilayers.

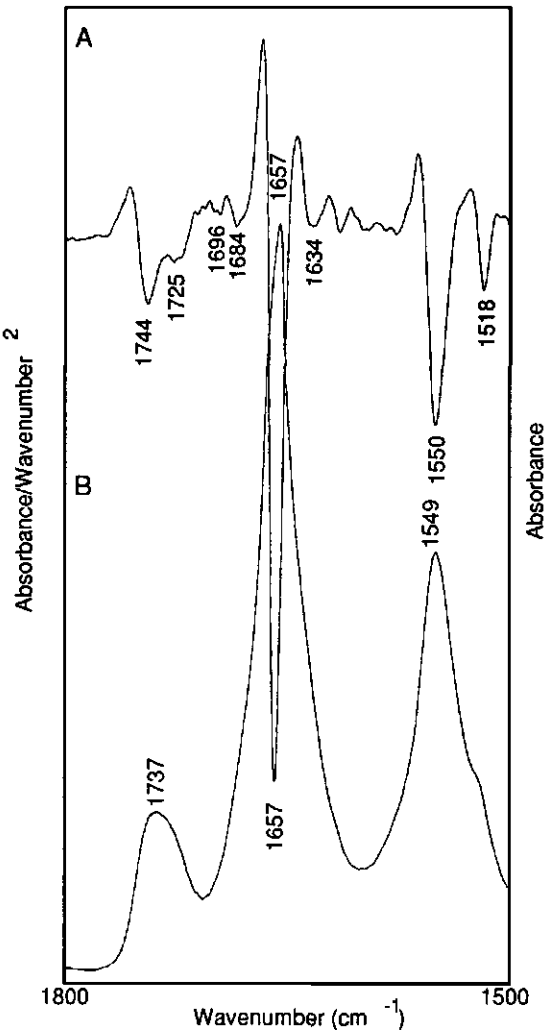

Figure 5. Infrared spectrum in H_20 (B) and the second derivative (A) of M13 coat protein in the α-oligomeric form in DOPG bilayers.

From the second derivative spectrum (Fig. 4a) it can be observed that in addition to the main band at 1628 cm^{-1}, which denoted β-sheet structure, a weaker band is observed at 1694 cm^{-1}. This component has been attributed to the high frequency component of the vibration of anti-parallel β-sheet structure [11,16]. The band at 1659 cm^{-1} most likely represents α-helical structure although overlap of absorbance from disordered structure can occur. The results obtained from a quantitative analysis performed with the program

CIRCOM are shown in Table I. Similar secondary structure contributions are observed for M13 coat protein in the c-state in DMPG bilayers (Table I).

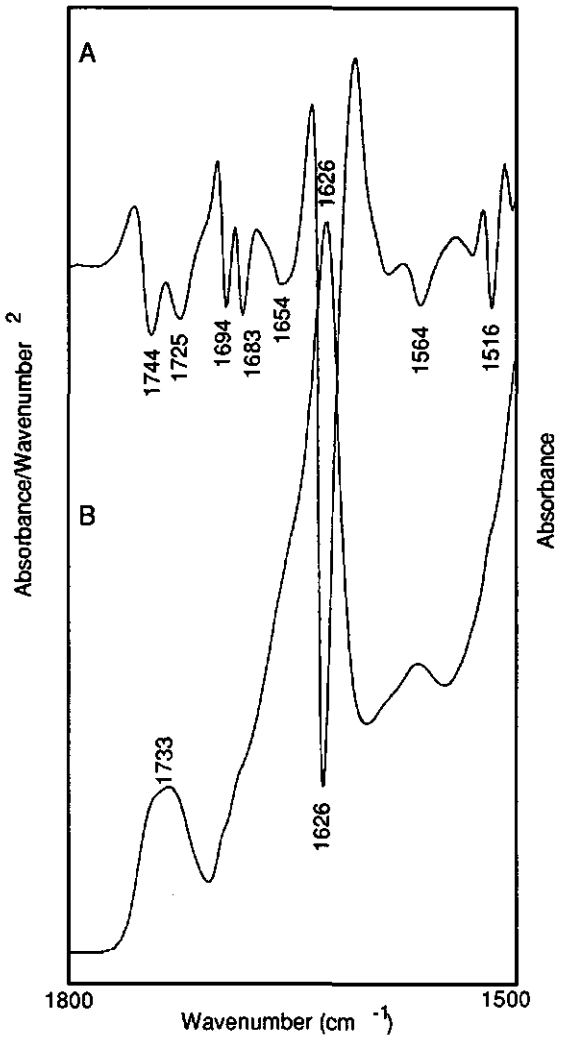

Figure 6. Infrared spectrum in D_20 (B) and the second derivative (A) of M13 coat protein in the β-polymeric form in DOPG bilayers.

The protein in the b-state show a very sharp symmetric band at 1657 cm^{-1} (Fig. 5), while the amide II band is centred at 1549 cm^{-1}, which is characteristic for α-helix

conformation [12]. The ratio A_{II}/A_{I} of 0.6 for the M13 coat protein in the b-state is in agreement with a high α-helix content [15].

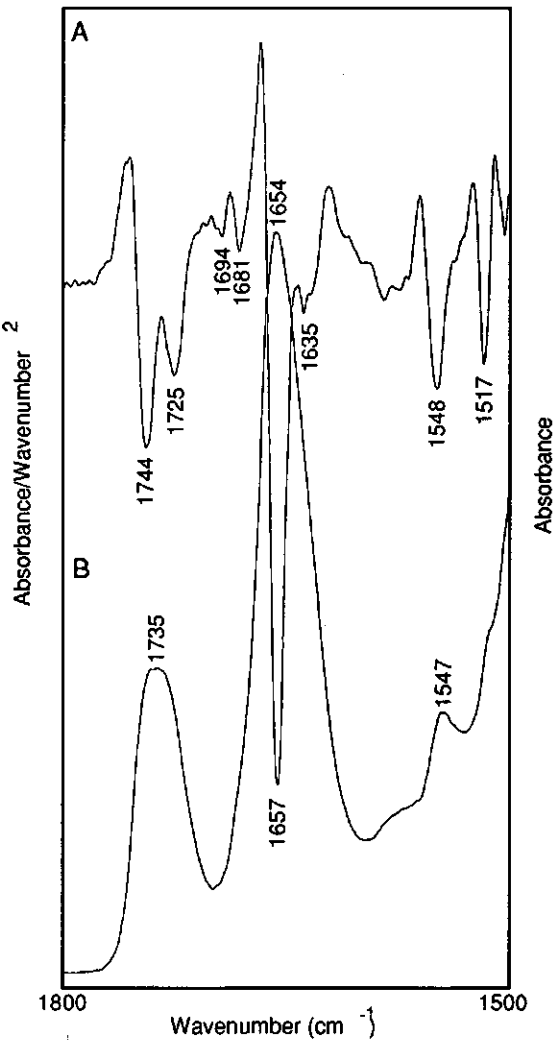

Figure 7. Infrared spectrum in D_20 (B) and the second derivative (A) of M13 coat protein in the α-oligomeric form in DOPG bilayers.

It is noteworthy that the amide I band is symmetric and very narrow. This suggests a highly homogeneous structural composition of the protein in this form. The second derivative of this spectrum shows weak bands in the amide I region at 1634 and 1696 cm^{-1} (Fig. 5a). Fitting the spectra of the M13 coat protein in the b-state with the CIRCOM program gives

values of an α-helix percentage of higher than 88% (Table I). This value is higher than the α-helical content of myoglobin, which has the highest amount of α-helix in the calibration set of proteins used in the quantitative analyses [12]. The frequency of this band is independent of the lipid type used.

Table I: Percentages of secondary arrangements of M13 coat protein in the β-polymeric and α-oligomeric form in DOPG and DMPG.

form	lipid	technique	α-helix	β-sheet	turn	remainder
β–polymeric	DOPG	CD	10	60	2	28
β–polymeric	DOPG	FTIR	20	60	10	10
β–polymeric	DMPG	CD	0	69	11	20
β–polymeric	DMPG	FTIR	25	59	3	13
β–polymeric	DMPG	Raman	6	46	38	10
α-oligomeric	DOPG	CD	95	0	2	3
α-oligomeric	DOPG	FTIR	100	0	0	0
α-oligomeric	DOPG	Raman	70	25	4	0
α-oligomeric	DMPG	CD	91	0	7	2
α-oligomeric	DMPG	FTIR	100	0	0	0

The error estimates in the analyses are for the FTIR measurements α-helix = 10 %, β-sheet = 8%, turn = 7%. For the CD measurements the error is estimated to be 5% for all secondary structure types and for the Raman measurements 10% for all secondary structure types.

The infrared spectra of the M13 coat protein of the two forms in D_2O are displayed in Figs. 6 and 7. The main amide I band in the spectra with M13 coat protein in the c-state is centred at 1626 cm^{-1} (Fig. 6) . Second derivative analysis reveals a main band at 1626 cm^{-1} with a weak component at 1694, 1683 and 1654 cm^{-1} (Fig. 6). The main band can be unambiguously attributed to β-sheet structure [12,17]. The component at 1694 cm^{-1} probably reflects the high frequency vibration of an anti-parallel β-sheet [11,16]. The bands at 1683 and 1654 cm^{-1} can be assigned to turns and α-helices, respectively [11,16].

The spectra of protein in the b-state in DOPG as well as in DMPG bilayers shows an amide I band centred at 1654 cm^{-1}, with the amide II band located at 1547 cm^{-1} (Fig. 7). The intensity of the amide II band is much reduced as a result of ^1H-D exchange. A band at 1654 cm^{-1} is fully consistent with the absorbance of α-helical structure [16,17]. Second derivative spectra reveal bands at 1657 cm^{-1} and weak features at 1635 and 1681 cm^{-1} (Fig. 7). Completely deuterium-proton exchanged M13 coat protein in lipids as indicate by the Amide II band, was obtained upon further exchange (12 hours). This causes the amide I component to shift to lower frequency (1652, 1679 and 1637 cm^{-1}).

Discussion

The major coat protein of the M13 bacteriophage reconstituted in lipid bilayers has been investigated previously using various techniques by various workers [18-25]. An interesting property of the M13 coat protein is that under different purification or reconstitution methods it adopts two different conformations, as revealed with CD. The c-state is in a strong irreversible aggregation state, whereas the coat protein in the b-state was proposed to be monomeric [7]. It was shown also that the presence of either one of these forms depends on the lipid type used [6]. Therefore, we studied M13 coat protein in both saturated and unsaturated lipids.

Most of the previous studies on the conformation of the M13 (or the closely related fd) coat protein have been performed in detergents [26,27]. No quantitative analysis has been carried out on the various structural arrangements of these forms [6]. Because the secondary structure might reflect the influence of the coat protein on lipid bilayers the aim of this investigation is to obtain a quantitative determination of the appearance of the various structural arrangements in both protein forms in lipid bilayers. This is carried out using a combination of spectroscopic techniques: CD, Raman and Fourier Transform Infrared.

The secondary structure analysis of the data obtained from CD, Raman and FTIR of the M13 coat protein in the c-state shows, in agreement with previous results [19], that this form consists predominantly of β-sheet structure. As can be noticed from Table I, a rather large percentage of turn was obtained in the analysis of the Raman spectra of the protein in the c-state. This is probably due to the high overlap of the Raman scattering of turn structure with that of β-sheet, making it difficult to discriminate between β-sheet and turn [28]. From the strong band at 1237 cm^{-1} in the Raman spectra [14] and the band at 1694 cm^{-1} in the infrared spectra, it can be concluded that the β-sheet structure is in an anti-parallel conformation. The amount of α-helix for the M13 coat protein in the c-state as obtained from infrared measurements differs from the amount of α-helix obtained from CD measurements. The low amount of α-helix as obtained with CD may be due to an

underestimation arising from absorption flattening, which is a consequence of the non-random distribution of the chromophores in these lipid samples [29,30].

M13 coat protein in the b-state consists predominantly of α-helix as can be seen from the CD, infrared and the Raman spectra. The fraction of α-helix obtained from CD is 90%, which is in good agreement with the Raman and IR results where the amount of α-helix is estimated to be 70% and 100%, respectively. A relatively large contribution of β-sheet is observed in the Raman spectra of the M13 coat protein in the b-state in DOPG bilayers (Table I). However in the case of DOPG bilayers a strong band arises at 1659 cm^{-1}, which is close to the amide I band of the α-helix. This band might be influenced by the protein giving rise to a change in shape and band position, resulting in a less optimal subtraction.

Almost similar results are found for the two protein forms independent of the lipids used. This shows that both protein forms can be obtained in saturated and unsaturated bilayers, suggesting that the presence or absence of a double bond is not the critical variable in the formation of the two different forms of the M13 coat protein, as has been suggested by Fodor et al. [6]. We have no reason to distrust either one of the techniques used. We have therefore averaged the results obtained for the two forms in the lipid bilayers. These average values are overall not, if we take in account the error estimates, in conflict with the separate values for the secondary structure of the two different protein forms, of the various techniques. The conformation of the M13 coat protein in the c-state is, based on these averages, estimated to be 57% β-sheet, 13 % α-helix, 13% turn and 16% remainder. The amount of α-helix of the protein in the b-state is estimated, based on the CD, Raman and FTIR experiments, to be 91%. It was shown using Molecular Dynamics (MD) simulation that the amount of β-sheet in the aggregated protein after 100 ps simulation was about 60%, which is in good agreement with the average values found for the c-type protein. Also the amount of α-helix in the M13 coat protein in the b-state, which was found in the MD simulations to be 80-90% (see chapter 3), agrees well with the 91% α-helix found (Table I).

Secondary structure measurements with Raman spectroscopy of the protein in micelles gave 55% α-helix, 3% β-sheet, 25% turn and 17% remainder [31] and for the M13 coat protein in lipid bilayers a high amount of β-sheet was observed [32]. These workers however, did not discriminate between the two forms (the b- and c-state) or whether they obtained a mixture, by studying the aggregation behaviour [7]. In the present study the two protein forms were studied separately.

Based on the results presented in this paper and elsewhere [33,34] the non-aggregated protein is called the α-oligomeric form. This expresses the conformation and the aggregation state of the form, namely the presence of predominantly α-helix (91%) structure and reversible aggregation as detected with HPLC. No quantitative estimation for the secondary

structure has been given previously for the aggregated protein but from the present work it follows that it consists for 57% of anti-parallel β-sheet. Therefore, this form will be called the β-polymeric protein, expressing the aggregational and conformational state of this M13 coat protein form [33,34].

As a result of the high amount of α-helix for the α-oligomeric form of the M13 coat protein the trans membrane part must be α-helical. This is in contrast with previous suggestions were the α-helix was proposed to be located in the hydrophilic part of the protein [35]. Generally it is excepted that a single transmembrane α-helix with 20 hydrophobic amino-acids will not disturb the lipid bilayers to a large extent. This is in agreement with NMR results obtained of the protein in this α-oligomeric form where only a small perturbation of the lipid headgroups and chains was observed (see chapter 4). In contrast, the anti-parallel β-sheet part of the protein in the β-polymeric protein is probably located in the membrane, giving rise to large distortions of the lipid bilayers [22,32]. Such an anti-parallel β-sheet structure would leave about 10 amino acid of the N terminus unpaired. This unpaired region in the M13 coat protein in the β-polymeric form could be either in α-helix or in a random coil conformation. On basis of the amount of α-helix in the protein in the β-polymeric form (Table I), this part is proposed to be in an α-helix conformation.

The protein in both lipid-bound forms was shown previously to be in a less α-helical state as compared to the virus-bound protein (a-state). It was therefore suggested that this protein should undergo major conformational changes upon virus formation [4,5] and several questions were asked about the energy implications of this change in conformational state. The high α-helical content as found for the α-oligomeric form of the M13 coat protein in the present work, suggests that this form of the M13 coat protein does not have to undergo such a drastic conformational change upon formation of a new phage particle. This makes it also feasible that parental M13 coat protein can be used in the formation. In contrast, the β-polymeric form has adopted a strongly changed conformation state as compared to the protein in the intact virus. Probably this conformation arises as a result from protein-protein contacts, which are formed under conditions in the preparation of the lipid-protein systems that favour these contacts.

Recently, NMR experiments on the related PF1 bacteriophage coat protein in a bilayer environment also showed a high amount of α-helix [36]. It was suggested that 30 of the 46 aminoacids (65%) were in an α-helix conformation, whereas the remaining part of the protein was proposed to be mobile. These workers showed the presence of a mobile loop, resulting in a part of the PF1 coat protein lying on the membrane surface. The higher amount of α-helix found in the present paper for the M13 coat protein in the α-oligomeric form suggests the absence of such a mobile loop. The conclusion reached for PF1 is that the membrane and virus bound form of the protein have essentially the same conformation. This

is in complete agreement with our findings that the α-oligomeric M13 coat protein is comparable with the virus bound M13 coat protein. Based on the present experiments, additional information is obtained that the α-oligomeric protein is the native form during the infection process [7].

References

1 Thomas, G. J., Prescott, B. and Day, L. J. (1983) J. Mol. Biol 165, 321-356.

2 Smilowitz, H. (1974) J. Virol. 13, 94-99.

3 Wickner, W. (1975) Proc. Natl. Acad. Sci. U.S.A. 72, 4749-4753.

4 Nozaki, Y., Chamberlain, B., Webster, R. and Tanford, C. (1976) Nature 259, 335-337.

5 Nozaki, Y., Reynolds, J. A. and Tanford, C. (1978) Biochemistry 17, 1239-1246.

6 Fodor S. P. A., Dunker, A. K., Ng, Y.C., Carsten, D. and Williams, R. W. (1981) in: Seventh. biennial Conference on Bacteriophage Assembly. pp 441-455 (Dubow, M.S., ed.) Alan R. Liss Inc., New York.

7 Spruijt, R. B., Wolfs, C. J. A. M. and Hemminga, M. A. (1989) Biochemistry 28, 9159-9165.

8 Knippers, R. and Hoffmann-Berling, H. (1966) J.Mol. biol. 21,281-292.

9 Provencher, S. W. and Glöckner, J. (1981) Biochemistry 20, 33-37.

10 Williams, R. W. (1983) J.Mol.Biol. 166, 581-603.

11 Haris, P.I., Lee, D. C. and Chapman, D., (1986) Biochim. Biophys. Acta 874, 255-265.

12 Lee, D. C., Haris, P. I., Chapman, D. and Mitchell, R. C. (1990) Biochemistry 29, 9185-9193.

13 Tu, A.T. (1982) in RAMAN spectroscopy in biology: Priciples and applications pp 65-115, John Wiley & sons, NewYork.

14 Aslanian, D., Negrerie, M. and Chambert, R. (1986) Eur. J. Biochem. 160, 395-400.

15 Nedelec, J-F., Alfsenl, A. and Lavalle, F. (1989) Biochimie 71,145-151.

16 Jackson, M., Haris, P. and Chapman, D. (1989) Biochim. Biophys. Acta 998, 75-80.

17 Susi, H. and Byler, D.M. (1987) Arch. Biochem. Biophys. 258, 465-469.

18 Datema, K. P., Wolfs, C. J. A. M., Marsh, D., Watts, A. and Hemminga, M.A. (1987) Biochemistry 26, 7571-7574.

19 Datema, K. P., Visser, A. J. W. G., van Hoek, A., Wolfs, C. J. A. M., Spruijt, R. B. and Hemminga M. A. (1987) Biochemistry 26, 6145-6152.

20 Datema, K. P., Van Boxtel, B. J. H. and Hemminga, M. A. (1988) J. Mag. Res 77, 372-376.

21 Wolfs C. J. A. M., Horvàth, L. I., Marsh, D., Watts, A. and Hemminga, M.A. (1989) Biochemistry.28, 9995-10001.

22 van Gorkom, L. C. M., Horvàth, J. I., Hemminga, M. A., Sternberg, B. and Watts, A. (1990) Biochemistry 29, 3828-3834.

23 de Jong, H., Hemminga, M. A. and Marsh, D. (1990) Biochim. Biophys. Acta 1024, 82-88.

24 Peng, K., Visser, A. J. W. G., van Hoek, A., Wolfs, C. J. A. M. and Hemminga, M. A. (1990) Eur. Biophys. J. 18, 277- 283.

25 Peng, K., Visser, A. J. W. G., van Hoek, A., Wolfs, C. J. A. M., Sanders, J. C. and Hemminga, M. A. (1990) Eur. Biophys. J. 18, 285-293.

26 Williams, R. W. and Dunker, A. K. (1977) J. Biol. Chemistry 252, 6253-6255.

27 Williams, R. W., Dunker, A. K. and Peticolas, W. L. (1980) Biophys. J. ,232-234.

28 Berjot, M., Marx, J. and Alix, A. J. P. (1987) J. Ram. Spectr. 18, 289-300.

29 Wallace, B. A. and Teeters, C. L. (1987) Biochemistry 26, 65-70.

30 Wallace, B. A. and Mao, D. (1984) Anal. Biochemistry 142, 317-328.

31 Williams, R. W., Dunker, A. K. and Peticolas, W. L. (1980) Biophys. J. 32, 232-234.

32 Dunker, A. K., Fodor, S. P. A. and Williams, R. W. (1981) Biophys. J. 37, 201-203.

33 Sanders, J. C., Poile, T. W., Spruijt, R. B., van Nuland, N. A. J., Watts, A. and Hemminga, M.A. (1991) Biochim. Biophys. Acta 1066, 102-108.

34 Spruijt, R. B. and Hemminga, M. A. (1991) Biochemistry in press.

35 Chamberlain, B., Nozaki, Y., Tanford, C., and Webster, R. (1978) Biochim. Biophys. Acta 510, 18-37.

36 Shon, K-J, Kim, Y, Colgano, L. A. and Opella, S. J. (1991) Science 252, 1303-1305.

CHAPTER 3

Conformation and aggregation of M13 coat protein studied by molecular dynamics

Johan C. Sanders, Nico A. J. van Nuland, Olle Edholm and Marcus A. Hemminga

Abstract

MD simulations are performed on M13 coat protein, a small membrane protein for which both α- and β-structures have been suggested. The simulations are started from initial conformations that are either monomers or dimers of α-helices or U-shaped β-sheets. The lipid bilayer is represented by a hydrophobic potential. The results are analyzed in terms of stability, energy and secondary structure. The U-shaped β structure changes from a planar to a twisted form with larger twist for the monomer than the dimer. The β-sheet is much more flexible than the α-helix as monitored by the rms fluctuations of the Cα atoms. A comparison of the energies after 100 ps MD simulation shows that of the monomers, the α-helix has the lowest energy. The energy difference between α- and β-structures decreases from 266 kJ/mol to 148 kJ/mol, when going from monomers to dimers. It is expected that this difference will decrease with higher aggregation numbers.

Introduction

Molecular dynamics has been shown to be a useful tool in predicting the three-dimensional structure of membrane proteins [1,2,3]. Here, MD simulations are describe of a small membrane protein, M13 coat protein, for which both α- and β-structures have been suggested [4,5,6]. The primary structure of the major coat protein of bacteriophage M13 (Reviews: [7,8,9]) is given in Fig. 1.

Three specific domains can be distinguished: an acidic N-terminus (residues 1-20) containing negatively charged glutamic and aspartic acids, which in the phage is in contact with the solvent; a basic C-terminus (residues 40-50), which contains positively charged lysines and interacts with the negatively charged DNA phosphate backbone in the intact virus; a hydrophobic core (residues 21-39), which has a possible role in the protein-protein interactions in the phage and in the hydrophobic protein-lipid interactions when the coat protein is incorporated into the membrane. Various initial conformations of monomeric and dimeric states of the M13 coat protein are created and MD simulations are performed.

These inital conformations include both α-helices and U-shaped β-sheets. The membrane core is modelled by a hydrophobic potential. The MD results are analysed in terms of stability, energies and secondary structure of the various monomer and dimer conformations.

NH_3^+-Ala-Glu-Gly-Asp-Asp-Pro-Ala-Lys-Ala-Ala-	
Phe-Asn-Ser-Leu-Gln-Ala-Ser-Ala-Thr-Glu-	Acidic domain
Tyr-Ile-Gly-Tyr-Ala-Trp-Ala-Met-Val-Val	
Val-Ile-Val-Gly-Ala-Thr-Ile-Gly-Ile-Lys-	Hydrophobic domain
Leu-Phe-Lys-Lys-Phe-Thr-Ser-Lys-Ala-Ser-COO^-	Basic domain

Figure 1. Primary amino-acid sequence of the M13 coat protein.

Methods

The initial conformations: There are two major conditions that have to be fulfilled of a reasonable structure of a membrane protein such, as the M13 coat protein: (1) The hydrophobic residues should fit into the 32 Å thick membrane core; (2) At the same time as many hydrogen bonds as possible should be satisfied in the membrane spanning part. M13 coat protein has a 20 residues long hydrophobic sequence (21-39) in the middle, while the ends are hydrophilic. This gives one obvious candidate for the structure, a membrane spanning α-helix (1.5 Å rise per residue). The hydrophilic parts outside the membrane core that stick into the aqueous phase could have a more disordered structure, because it is not necessary to form internal hydrogen bonds there. Since it is not known how to make a possibly disordered structure for the hydrophilic part, a start is made with the whole protein in an α-helical conformation.

Secondly, considering β-structures, which have a rise of about 3.4 Å per residue, it is realized that to fit 20 hydrophobic residues into a membrane core of 32 Å thickness, a reverse turn in the middle of the hydrophobic segment is necessary. This turn was put at Val-30-Val-31, giving a U-shaped structure. That the hydrophilic ends in this case do not match is not serious, since the hydrogen bonds that are not satisfied internally may be formed with water.

To study protein-protein interactions, dimers were constructed. However, there are many possibile dimer structures. For the α-helix, we took as main candidate an anti-

parallel arrangement with Lys-40 of one helix close to Glu-20 of the other one. This structure has favourable electrostatic interactions.

For a monomeric U-shaped β-structure only about half as many hydrogen bonds are satisfied as for the α-helix. The point with dimeric and polymeric structures would then be to increase the amount of hydrogen bonding. A dimer may then be constructed in six possible ways. The binding of the monomers could either be between two 1-29 strands, two 32-50 strands or between one 1-29 and one 32-50 strand. In all these three cases the strands could either be parallel or anti-parallel. Even with the basic requirement that the hydrophobic part of both monomers should stay within the membrane core, there is freedom to slide the monomers a couple of residues along each other. Two possible structures were chosen, one parallel with the 1-29 strand of one monomer binding to the 32-50 strand of the other one (residue 27 to 32, 25 to 34 and so on) and one with two monomers stacked on top of each other (no hydrogen bonding). For the other possibilities it is noted that the same strands binding parallel to one another would be unfavourable, since then the same residues would face each other and there are some with bulky side groups.

The calculations: For the EM and MD simulations the GROMOS package was used (W.F. van Gunsteren & H.J.C. Berendsen, BIOMOS B.V., Laboratory for Physical Chemistry, University of Groningen, The Netherlands). The integration of the classical equations of motion was done with a time step of 2 fs using the SHAKE algorithm to constrain the bond lengths [10]. The temperature was kept at 300 K by coupling the kinetic energy of the system to a heat bath with a relaxation time of 100 fs [11]. The potential energy function for membrane-spanning proteins is given by [2]:

$$V = V_{angle} + V_{dihedral} + V_{Hbond} + V_{Coul} + V_{LJ} + V_{hphobic} \qquad (1)$$

For the first five terms expressions and parameters were taken from Van Gunsteren and Karplus [12]. For the nonbonded interactions (Coulomb and Lennard-Jones) a cut-off at 10 Å was used and a neighbour list specifying the interacting atoms was updated every 10 steps. The fractional charges were chosen to give electroneutral residues, including Lys, Glu and Asp. Care was taken to avoid splitting of electroneutral groups by the cut-off. The long-range electrostatic interactions decay as dipole-dipole interactions. For the hydrogen bonds the cut-off was chosen to be 5 Å and the neighbour list was updated every 20 steps. Since the polypeptide atoms may form hydrogen bonds with water molecules, the hydrogen bond potential was switched off outside the membrane.

An external potential, $V_{hphobic}$, is employed to account for the lipid/water interface. This method and the parameters used, are the same as in Edholm & Jähnig [2]. According to

this definition the membrane surfaces specify the hydrophobic core of the membrane. The thickness of a fully hydrated DOPC (1,2-dioleoyl-*sn*-glycero-3-phosphocholine) bilayer is 32 Å at 300 K [13]. We thus took the thickness of the hydrophobic core equal to 32 Å and had the hydrophobic force to act over a boundary zone of 2 Å. The initial conformations were generated and positioned with their hydrophobic segments in the membrane.

The initial conformations were energy-minimized for at least 500 steps before starting the MD simulations. The MD simulations were performed on a Cray-XMP supercomputer. A 100 ps run took about 5.5 hours CPU time for the dimers. Stereo-pictures were produced on an Apollo work station.

The energies obtained from the MD simulations do not include the interaction energy with surrounding lipid and water molecules since the runs are vacuum ones. These excluded interactions are on the average attractive. They are of Lennard-Jones type and electrostatic interactions with the water dipoles. This negative contribution to the energy is proportional to the surface area of the protein. To get comparable energies, therefore, an energy is added that is proportional to the surface area. The proportionality constant is determined from a simulation including lipids, which gives a surface energy -600 kJ/mol for a helix of 23 residues (O. Edholm, unpublished data). The surface areas are calculated using a standard program [14]. Although this term will give large contributions, it should be noted that only the energy difference between the different conformations is important. Therefore, the α-helix monomer (see initial conformations) is used as a reference and the difference in surface energy is added or subtracted for the other conformations.

Results

MD simulations were performed on the M13 major coat protein. starting from various initial conditions. All runs reach a stable or at least metastable state after an equilibration period of 40-50 ps (Fig. 2).

Fig. 3 shows stereo-pictures of the M13 coat protein in the α-helix monomer configuration after 100 ps MD simulation. As can be seen, bending occurs near Gly-38. The ϕ and ψ torsion angles near this residue differ from the values of an ideal α-helix, which are -57° and -47°, respectively. Gly is known as a Chou and Fasman α-helix breaker [15]. In addition bending can only occur to the side which is marked by non bulky residues like glycines and alanines. Similar bending of an α-helix has been reported for glycophorin [2]. Therefore, it is believed that the bending at this position is occurring in a deterministic manner. In solid state NMR experiments a relative high flexibility for the termini [16] hasbeen observed.

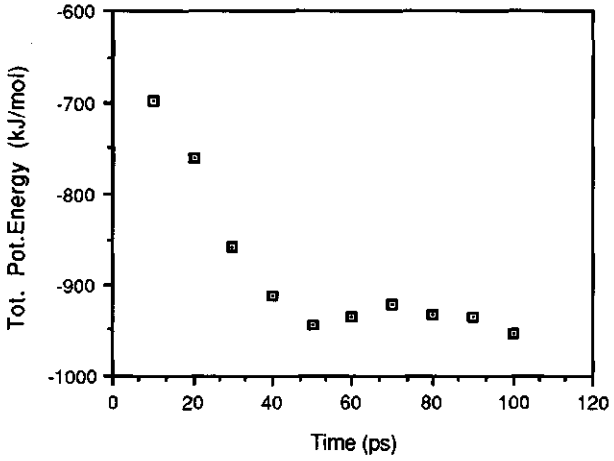

Figure 2. Temporal variation of the total potential energy averaged over successive 10 ps time intervals for the M13 coat protein in α-helical and U-shaped β-sheet monomer configuration during the 100 ps MD simulations. Membrane thickness 32 Å.

This flexibility is also found in the MD simulations, as can be seen from the rms fluctuation around the average position (Fig. 4) of the Cα atoms. These are for the α-helix monomer large in the terminal residues in contrast to the middle part, where small rms values are observed. The rms fluctuations are about 1 Å for the inner helical region, which is comparable with other MD simulations [2,17] and with experimental data on crystallized proteins [18].

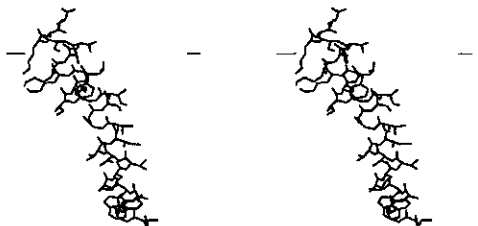

Figure 3. Stereopictures of the M13 coat protein in the α-helix conformation. The borders represent the hydrophobic membrane core. 100 ps MD structure, membrane thickness 32 Å.

The ability of the protein to form aggregates of α-helices is tested by running MD starting from a configuration with two α-helices at 10 Å distance. Fig. 5 shows stereo-pictures of the M13 coat protein α-helix dimer after a 100 ps MD. During the run the molecules become twisted around each other as a result of finding the optimum interaction between the two molecules. The α-helix content of the dimer is higher than that of the monomer (Table II). In addition the rms fluctuations of the Cα atoms in the C-terminus are smaller for the dimer than the monomer. This indicates that this part of the molecule is somewhat more rigid as a result of nonbonded interactions between the two molecules, leading to a subsequent stabilization of the α-helix structure.

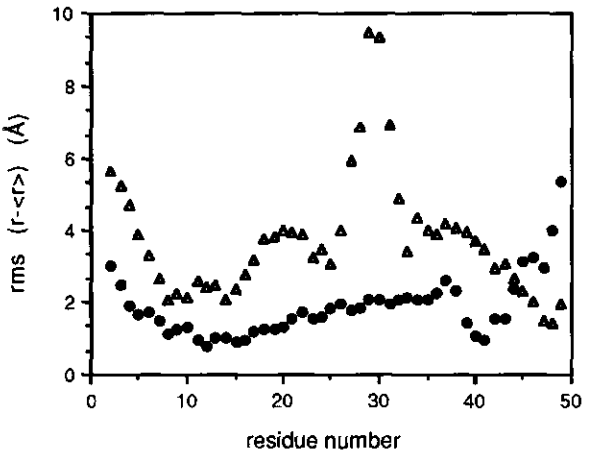

Figure 4. Variation of the rms positional fluctuations of the Cα atoms along the M13 coat protein chain during the MD simulation. Membrane thickness 32 Å.
Δ = U shaped β-sheet monomer, • = α-helix monomer.

Fig. 6 shows MD structure of the M13 coat protein in the U-shaped β-sheet conformation. Large conformational and orientational changes occur during the 100 ps MD run. While the EM structure still is an anti-parallel β-sheet, with the torsion angles ϕ and ψ equal to -139° and 135°, respectively, the chains get completely twisted during the MD run. The torsion angles become closer to the values of a twisted sheet, -90° and 105°. This agrees with results for polyalanine by Chou *et al.* [19] based on energy minimization studies. The twist is a consequence of sidechain-backbone interactions (intrachain) and interchain interactions. The twist δ per two residues is defined as the angle between the C_i-O and C_{i+2}-O vectors. The value is divided by two to get the twist per residue and assigned to residue i+1.

The average twist of the entire molecule in the U-shaped β-sheet monomer is 21° over the last 20 ps excluding the twist of residues at the end (2 and 49) and in the turn (28-31). This average twist value is within the range of observed twists of β-sheets in globular proteins, $0° < \delta < 30°$ [20]. As a result of the twisting the amount of residues within the hydrophobic membrane core is increased by six. Also the residues in the reverse turn are moved further into the hydrophobic membrane core.

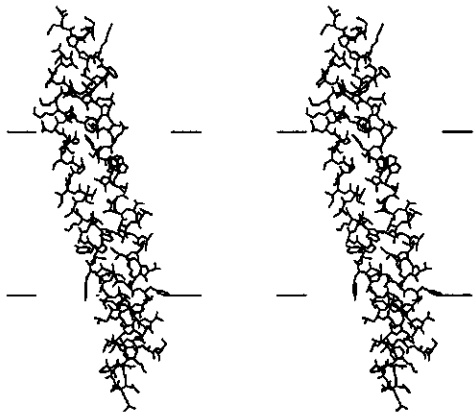

Figure 5. Stereopictures of the M13 coat protein in the α-helix conformation. The borders represent the hydrophobic membrane core of 32 Å. Dimer 100 ps MD structure.

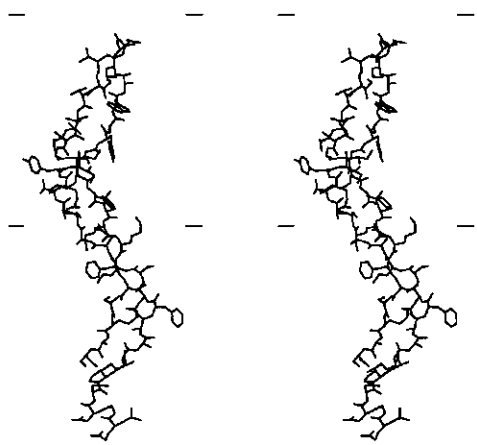

Figure 6. Stereopictures of the M13 coat protein in the U-shaped β-sheet conformation. The borders represent the hydrophobic membrane core of 32 Å. the 100 ps MD structure.

The variation of the rms fluctuations of the Cα–atoms with the position along the polypeptide chain is shown in Fig. 4. For the β–structure, there is a pronounced maximum at the reverse turn. The fluctuations are, after the structures have been given proper time to stabilize, almost a factor two larger for the β-sheet than for the α–helix. Since this means that the β-structure takes up a larger volume in phase space, it will have higher entropy that gives a negative contribution to free energy.

The U-shaped β-sheet is not the only possible β structure. An extended β-sheet, cannot be ruled out, although it has a far too long hydrophobic part to fit into an ordinarymembrane. It is favoured by the absence of the destablizing reverse turn. However, it requires a large local change of the bilayer to accommodate the hydrophobic region of the protein. Except for these effects, the results with the U-shaped β-sheet will be comparable to an extended β-sheet.

Fig. 7 shows the three-dimensional structure of the U-shaped β-sheet dimer (parallel) after 100 ps MD simulation. The average rms fluctuations of the Cα atoms are about half the size of those of the corresponding monomer (Table I) while their variation with chain position is similar (results not shown). The average twist is 10° for the dimer, which should be compared to 21° for the monomer. This agrees with the general finding that an increasing number of β-strands reduces the twist [19,20].

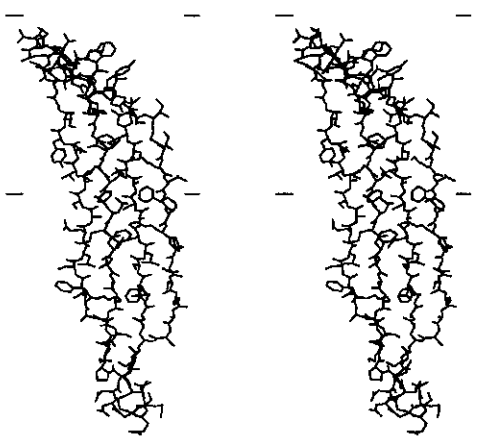

Figure 7. Stereopictures of the M13 coat protein in the U-shaped β-sheet conformation. The borders represent the hydrophobic membrane core of 32 Å. Dimer 100 ps MD structure.

Table I: The average rms positional fluctuations for five different 100 ps MD simulations of the M13 coat protein. The values represent the last 50 ps of the MD simulations.

simulation	rms (r - <r>) (Å)
α-helix	1.76
α-helix dimer	1.18
U-shape β-sheet	3.25
U-shape β-sheet paralell dimer	1.58
U-shape β-sheet stacked dimer	2.06

In Table II every residue for the conformations studied is assigned to a secondary structure type: α-helix (H), anti-parallel (A) or twisted (T) β-structure depending on the values of the torsion angles ϕ and ψ . A residue is assigned to a given structure type if its torsion angles fall within a circel of radius 30° from the ideal values of the structure type in the Ramachandran plot. For these ideal values the following values are taken H(-57°,-47°), A(-139°,135°) and T(-90°,105°).

Table II: The secondary structure of the individual residues in the different 100 ps MD simulations for the α-helix monomer and dimer and the U-shaped β-sheet monomer and dimer (parallel configuration). Membrane thickness 32 Å. H = α-helix, A = antipar. β-structure, T = twisted β-structure, R = reverse turn, - = no assigned structure and D = dubious.

Residue	α-helix	α-hel mol 1	α-hel mol 2	U-shaped β-sheet	U-s β-dim. mol. 1	U-s β-dim. mol. 2
1 Ala						
2 Glu	-	H	-	T	A	D
3 Gly	H	H	-	-	-	-
4 Asp	H	H	D	T	-	A
5 Asp	H	H	H	A	T	-
6 Pro	H	H	H	-	T	T
7 Ala	H	H	H	T	T	T
8 Lys	H	H	H	D	T	T
9 Ala	H	H	H	-	-	-
10 Ala	H	H	H	T	T	T
11 Phe	H	-	H	-	D	-
12 Asn	H	H	-	T	T	D

13 Ser	H	H	-	T	D	-
14 Leu	H	H	H	D	T	-
15 Gln	H	H	H	D	-	A
16 Ala	H	H	H	T	T	D
17 Ser	H	H	H	T	T	T
18 Ala	H	H	H	A	D	T
19 Thr	H	H	H	T	T	T
20 Glu	H	H	H	T	T	T
21 Tyr	H	H	H	T	T	T
22 Ile	H	H	H	T	A	T
23 Gly	H	H	H	T	-	T
24 Tyr	H	H	H	D	A	T
25 Ala	H	H	H	T	T	T
26 Trp	H	H	H	T	T	T
27 Ala	H	H	H	T	T	T
28 Met	H	H	H	T	T	T
29 Val	H	H	H	R	R	R
30 Val	H	H	H	R	R	R
31 Val	H	H	H	T	T	T
32 Ile	H	H	H	T	T	T
33 Val	H	H	D	T	T	T
34 Gly	H	H	-	T	T	T
35 Ala	H	H	H	T	-	T
36 Thr	H	H	H	T	A	T
37 Ile	-	H	H	D	T	T
38 Gly	-	H	H	T	T	T
39 Ile	H	H	H	T	T	T
40 Lys	H	H	H	T	T	T
41 Leu	H	H	D	A	T	-
42 Phe	H	H	H	T	T	D
43 Lys	H	H	H	T	-	T
44 Lys	H	H	H	T	T	-
45 Phe	-	H	H	A	A	-
46 Thr	-	H	H	T	T	T
47 Ser	D	H	H	T	T	D
48 Lys	D	H	H	D	T	T
49 Ala	-	H	H	-	A	T
50 Ser						

The places where the α-helices bend are easily discovered from the non-helical assignments. The fraction of α-helix is for the monomer and dimer 80% and 90%,

respectively. This shows that the helical structure is roughly stable over 100 ps. The β-structure is almost completely converted into a twisted form after 100 ps MD, as seen from Table II. The amount of β-structure, anti-parallel and twisted, is after 100 ps about 75% for both monomer and dimer.

Table III. Contribution of the individual energies in different MD simulations of the M13 coat protein. Values are expressed in kJ/mol.

	V_{ang}	V_{dihy}	V_{coul}	V_{lj}	V_{hp}	V_{hb}	V_{tot}	V_{totcpm} *
α-helix	749	520	-1022	-1103	-182	-159	-1197	-1197
α-helix dimer	1451	1009	-2301	-2730	-224	-350	-3147	-1243
U-shape β-sheet	718	532	-993	-991	-144	-76	-954	-931
U-shape β-sheet paral. dimer	1419	1025	-2283	-2549	-243	-152	-2784	-1095
U-shape β-sheet stacked dimer	1428	1045	-2188	-2446	-212	-114	-2487	-964

* Energies corrected for the lost on surface area given per subunit incase of a dimer

In Table III some different contributions to the energy from the simulations are listed. For the dimers, the non bonded energy per monomer increases substantially due to the interaction between the two units of the dimer. As seen from this table, the energies of the α-helix monomer and the α-helix dimer differ 46 kJ/mol in favour of the dimer. In the case of the U-shaped β-sheet parallel dimer the energy difference is 164 kJ/mol in favour of the dimer. From simulations, in which dimerization of the U-shaped β-sheet was due to stacked interactions, in which no hydrogen bonding takes place, a clearly smaller decrease of the energy is found (33 kJ/mol).

Discussion

In model membranes the M13 coat protein can adopt two different forms [4,5,6], the α-oligomeric and β-polymeric ones. It is of considerable interest to compare these structures, in particular in relation to their different aggregation behaviour. Recently the usefullness of MD for structure prediction of membrane spanning proteins has been investigated [3]. It was shown that one can distinguish between different packings of helices based on the energies and that the helices spontanously tilt in the correct way. This motivated

us to study the structure of M13 coat protein using MD simulations. Different initial conformations of the M13 coat protein were generated to compare α- and β-structures and to study the importance of protein/protein interactions for the stability of the various protein conformations.

Monomeric structures: The α-helix monomer has a lower energy (266 kJ/mol) than the U-shaped β-monomer (see Table III). There are several origins for this difference. First, since the β-sheet has only half as many hydrogen bonds as the α-helix, the hydrogen bonding energy favours the α-helix. However, this accounts only for about one third of the energy difference. The remaining part comes mainly from non-bonded Lennard-Jones interactions, but there are also smaller contributions of electrostatic and hydrophobic origin. It is noteworthy that bonded interactions (angles and dihedrals) are about the same (even 19 kJ/mol higher for the α-helix), so that strains in these degrees of freedom caused by the reverse turn are unimportant for the energy difference. Both monomers have almost the same surface area, so the relatively uncertain surface energy correction is of small importance.

To compare conformations, the free energy should be used instead of the energy. But to calculate the entropic contribution to the free energy of a certain structure with sufficient accuracy is not possible. The rms fluctuations (Table I) give an idea about the differences in entropy between the different structures. These are, after that the structures have been given proper time to equilibrate, almost a factor two larger for the β-sheet than for the α-helix. If we assume that the flucuations are equilibrium ones, this gives rise to an entropy difference in favour of the β-sheet that could be large enough to completely alter the free energy balance between the structures. We do, however, see that dimerization reduces the fluctuations and the difference in fluctuations between the two structures. Probably, the surrounding lipids have a similar effect. Even if the energies indicate that equilibrium is reached, the fluctuations may still need more time to reach their equilibrum value. Therefore, it can be concluded that the α-helix monomer is favourable as compared to the U-shaped β-sheet monomer. However, an entropy term will certainly reduce the energy difference so that it is not possible to give a quantitative estimate of the free energy difference.

Protein dimers: For the α-helix the energy per monomer is 46 kJ/mol lower for the dimer than the monomer after that the surface energy correction has been performed. This means that it is favourable for them to bind together. This seems reasonable, since electrostatic interactions and a few hydrogen bonds could favour protein/protein interactions

as compared to protein/lipid interactions. The conclusion is that the M13 coat protein in the α-helices has a tendency to aggregate, but a low one.

For the β-structure the corresponding energy difference is 164 kJ/mol per monomer in favour of the parallel dimer. This means that the energy difference between α- and β-structures decreases from 266 kJ/mol to 148 kJ/mol when going from monomers to dimers. It is reasonable that this difference will continue to decrease when more protein monomers in a β-sheet conformation are allowed to aggregate. This means that for highly aggregated β-structures the energy may be similar to that of α-helical monomers and the β-sheet conformation may equelly well be possible in lipid membranes as compared to the α-helix confromation. we may no longer exclude the U-shaped β-sheet conformation. For a more accurate comparison, however it will be necessary to proparly take in account the solvent effects, as well as a quantative description of the entropy differences.

References

1 Edholm, O. and Johansson, J. (1987) Eur. Biophys. J. 14, 203-209.

2 Edholm, O. and Jähnig, F. (1988) Bioph. Chem. 30, 279-292.

3 Jähnig, F. and Edholm , O. (1990) Z. Phys. B. 78, 137-143.

4 Williams, R. and Dunker, K. (1977) J. Biol. Chem. 252, 6253-6255.

5 Fodor S. P. A., Dunker, A. K., Ng, Y. C., Carsten, D. and Williams, R. W. (1981) in: Seventh. biennial Conference on Bacteriophage Assembly. pp 441-455 (Dubow, M.S., ed.) Alan R. Liss Inc., New York.

6 Spruijt, R. B., Wolfs, C. and Hemminga, M. A. (1989) Biochemistry 28, 9158-9165.

7 Pratt, D., Tzagaloff, H. and Beaudoir, J. (1969) Virology 39, 42-53.

8 Ray, D. S. (1977) in Comprehensive Virology (Fraeckel-Conrad, H., & Wagner, R.R.,

9 Rasched, I. and Oberer, E. (1986) Microbiol. Rev. 50, 401-427.

10 Rykaert, J. P., Cicotti, G. and Berendsen, H. J. C. (1977) Comp. Phys. 23, 327-341.

11 Berendesen, H. J. C., Postma, J. P. M., van Gunsteren, W. F., DiNola, A. and Haak, J. R. (1984) J. Chem. Phys. 81, 3684-3690.

12 Van Gunsteren, W. F. and Karplus, M. (1982) Macromolecules 15, 1528-1544.

13 Lis, L. J, Parsigan, V. a. and Rand R. P. (1981) Biochemistry 20, 1761-1770.

14 Lee, B. and Richards, F. M. (1971) J. Mol. Biol. 55, 379-400.

15 Levitt, M. (1978) Biochemistry 17, 4277-4285.

16 Valentine, K. G., Schneider, D. M., Leo, G. C., Colgano, L. A. and Opella, S. J. (1986) Biophys. J. 49, 36-38.

17 Elber, R. and Karplus, M. (1987) Science 235, 318-321.

18 Frauenfelder, H., Petsko, G. A. and Tsernoglou, D. (1979) Nature 280, 558-563.

19 Chou, K.-C., Nemethy, G. and Scheraga, H. A. (1983) J. Mol. Biol. 168, 389-407.
20 Richardson, J. S. (1981) Advan. Protein Chem. 34, 167-339.

CHAPTER 4

Formation of non-bilayer structures induced by M13 coat protein depends on the conformation of the protein

Johan C. Sanders, Trevor W. Poile, Cor J. A. M. Wolfs and Marcus A. Hemminga

Abstract

A comparison is made of the interaction of the coat protein of bacteriophage M13 in a predominant α-helix conformation and in a predominant β sheet conformation with lipid bilayers using ^{2}H-NMR and ^{31}P-NMR. From the ^{2}H-NMR studies on specific headgroup and chain deuterium labelled phospholipids it can be concluded that the protein in the predominant β sheet conformation causes a fraction of lipids to be trapped. By combining the results from the headgroup and acyl chains of the phospholipids, it is concluded that the trapped lipids are arranged in a non bilayer structure, probably caused by a misfitting of the hydrophobic core of the protein and the membrane bilayer. The protein in the predominant α-helix conformation perfectly fits in the lipid bilayer and has only minor influences on the surrounding lipid matrix.

Introduction

Recently it has been reported that the coat protein of bacteriophage M13 adopts two different conformations, when reconstituted into lipid systems. Also the aggregation behaviour of these two M13 coat protein conformations differs considerably. The protein in a predominant β-sheet conformation forms large irreversible aggregates [1,2,3,4,5,6,7,8]. This form of M13 coat protein will be called the β-polymeric form. M13 coat protein in a predominant α-helix conformation forms reversible small aggregates; this form will be called the α-oligomeric form [9]. The presence of either one of these M13 coat protein forms depends on the protein purification, lipid type and salt concentration [9,10,11].

Previous experiments conducted on bilayers with the M13 coat protein in the β-polymeric form showed a fraction of lipids, which could not exchange with the bulk lipids. This fraction of lipids was thought to be trapped by aggregates of the coat protein in the β-polymeric form [4,5]. In the present paper further investigations are presented to obtain information about the nature of these trapped lipids. In addition we investigate the interaction between the lipid matrix and the M13 coat protein in the α–oligomeric form.

To perform a systematic study of the interaction between the protein in its two different forms and the surrounding lipid matrix, NMR spectra of ^{2}H-nuclei of specific labelled phospholipid bilayers were measured. DOPC was specifically deuterated either in both chains at the 11-position (DOPC-d_4) or at the trimethyl moiety in the headgroup (DOPC-d_9). DMPC was deuterated at the methyl positions at the *sn-2* chain (DMPC-d_3). ^{31}P-NMR is employed to provide information about the morphological structure adopted by the reconstituted lipid protein systems. A new model is proposed to explain the presence of the trapped lipids in the lipid-protein systems.

Materials and methods

Lipids: DOPC-d_9 deuterated in the trimethyl groups of the choline moiety, was synthesized from DOPE as described by Eibl [12]. DOPC-d_4 was a kind gift from B. de Kruijff (University of Utrecht). DMPC-d_3, labelled in the terminal methyl of the sn-2 chain, was synthesised from DMPC (Sigma, St. Louis, U. S. A.) using phospholipase A2 for preparing lyso-PC with subsequent esterification with tetradecanoic-14,14,14-d_3-acid (Larodan AB, Malmö, Sweden) as described by Boss [13]. After purification, the lipids appeared as one spot on high performance silica TLC (solvent $CHCl_3$, MeOH, NH_4OH, 55:30:3, v/v/v) and were stored at -20 °C.

Sample preparation: Bacteriophage M13 was grown and purified as described previously [9]. After removing the chloroform from the desired amount of lipids with nitrogen gas, samples were lyophilized for at least 12 hours and solubulized in buffer (α-oligomeric (buffer A): 50 mM Cholate, 10 mM Tris (0.2 mM EDTA , 140 mM NaCl, pH 8.0 β-polymeric (buffer B): 8.0 M Urea, 5 mM Tris , 0.1 mM EDTA, 20 mM ammonium sulphate; 140 mM NaCl, pH 8.0). To this solution the desired amount of either the α-oligomeric protein in buffer A or the M13 coat protein in the β-polymeric form in buffer B was added followed by dialysis at room temperature against 100 fold excess buffer (10 mM Tris, 0.2 mM EDTA,140 mM NaCl, pH 8.0) for a total of 48 hours changing the buffer every 12 hours. Directly after the dialysis procedure the reconstituted lipid-protein complexes were concentrated using an Amicon stirring cell and lyophilized for at least 12 hours and resuspended in deuterium depleted water (Sigma). The aggregation state, conformation and L/P ratio of the reconstituted coat protein in lipid bilayers was checked as described previously [9].

NMR experiments: All NMR spectra were recorded on a Bruker CXP 300 spectrometer. as described in chapter 5. Oriented spectra were obtained numerically from the

experimental spectra by using an iterative depaking program [14]. The quadrupolar splittings given in the Tables are all obtained from these oriented spectra.

Results

Biochemical essays: All samples were checked for their homogeneity and for the conformation and aggregation state of M13 coat protein. Sucrose gradients of all samples showed only one band indicating that the samples were homogeneous. Previously the homogeneity of the samples was also confirmed with electron microscopy [5]. CD spectroscopy and HPLC elution profiles indicated that the α-oligomeric form of the protein was in a predominant α-helix conformation with no indication of strong protein aggregation, whereas the β-polymeric form was in a predominant β-sheet conformation and strongly aggregated. This is in agreement with previously reported results [9].

^{2}H-NMR on DOPC-d_4 bilayers: In the ^{2}H-NMR spectra of DOPC-d_4 at higher temperatures two quadrupolar splittings are observed (Table I).

Table I: Quadrupolar splittings (kHz) of DOPC-d_4 with M13 coat protein in the two conformations at different temperatures.

L/P	Temperature (°C)		
	10	20	30
∞	7.1	6.2/6.5*	5.5/5.8*
35 (α–oligomeric)	6.2	5.5	4.9
30 (β-polymeric)	7.4	5.8	5.6

*Two splittings are observed in the depaked spectra.

The most likely explanation is that the two powder patterns originate from deuterons on the two different chains. It is known that the *sn-2* chain is positioned somewhat higher in the membrane than the *sn-1* chain. This gives rise to the observed differences in quadrupolar splitting, due to the difference in the order parameter [15]. The sharp isotropic peak visible in DOPC bilayers (both chain and headgroup labelled) with and without M13 coat protein (Fig. 1), is assigned to a small fraction (< 5%) of lipids in small vesicles that have a fast rotation on the NMR time-scale.

In the spectra of bilayers of DOPC-d_4 with the α-oligomeric form of the M13 coat protein no indication of a second quadrupolar splitting can be found (Table I, Fig. 1).

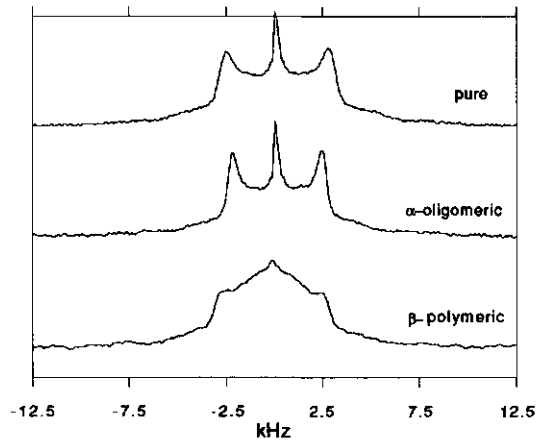

Figure 1. 46.1 MHz ^{2}H-NMR spectra of DOPC-d_4 at 30 °C of pure and protein containing samples (both forms L/P 20). Number of scans 30000.

This can either be due to the lack of resolution due to the increased linewidth, or due the fact that the protein removes the differences between the *sn-1* and *sn-2* chain. In addition the quadrupolar splitting has decreased upon addition of M13 coat protein in the α-oligomeric form (Table I), which indicates that on the ^{2}H-NMR time scale the order in the hydrophobic part of the bilayer has decreased. The T_{2e} slightly decreases with the content of the α-oligomeric form of the M13 coat protein (Table III).

Introduction of the M13 coat protein in the β-polymeric form into bilayers causes the deuterium spectra to change strongly. In addition to a component, which behaves the same as the normal bilayer component, a broad protein dependent component, which has an isotropic appearance, can be observed. In addition to these changes in the spectra the T_{2e} relaxation time decreases more considerable as compared to the changes in T_{2e} induced by the M13 coat protein in the α-oligomeric form (Table III). The T_{1z} relaxation time of DOPC-d_4 is independent of the L/P ratio for both protein conformations (Table III).

^{2}H-NMR on DOPC-d_9 bilayers: The quadrupolar splitting of bilayers of DOPC-d_9 does not change upon addition of M13 coat protein in the α-oligomeric form and is 1.0 kHz at 30 °C. The spectrum of DOPC-d9 bilayers with the M13 coat protein in the β-polymeric form shows a broad component, which has an isotropic appearance (Fig. 2). The T_{2e} relaxation time of DOPC-d_9 is slightly dependent on the L/P ratio, whereas the T_{1z} relaxation time of DOPC-d_9 is independent of the L/P ratio for both protein forms.

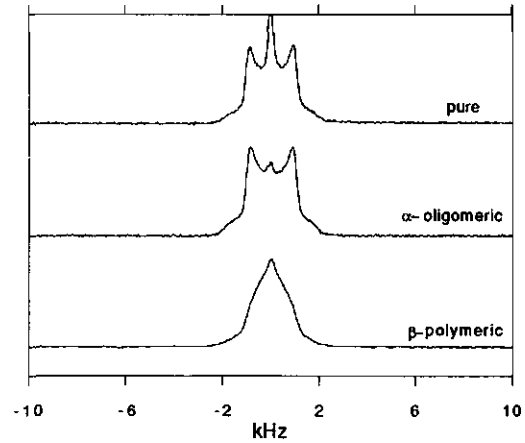

Figure 2. 46.1 MHz ^{2}H-NMR spectra of DOPC-d_9 at 30 °C of pure and protein containing samples (both forms L/P 20). Number of scans 10000.

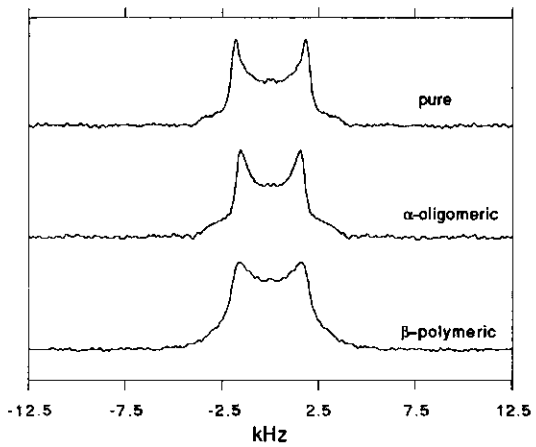

Figure 3. 46.1 MHz ^{2}H-NMR spectra DMPC-d_3 at 30 °C of pure and protein containing samples (both forms L/P 20). Number of scans 20000.

DMPC-d_3 bilayers: The effect of the M13 coat protein on the spectra of DMPC-d_3 is displayed in Fig. 3. The typical powder pattern observed for the pure lipid bilayers is not changed upon adding the α-oligomeric form of the M13 coat protein, whereas upon adding

M13 coat protein in the β-polymeric form to these bilayers an ideal powder pattern can no longer be observed. If the temperature is increased to 45 °C the shape of the spectrum of bilayers with the M13 coat protein in the β-polymeric form becomes more isotropic. This effect is fully reproducible (results not shown). As can be seen from Table II, the quadrupolar splitting decreases upon addition of the M13 coat protein independent of its forms. The T_{1z} relaxation times is hardly affected, but the T_{2e} relaxation times decrease substantially on adding the M13 coat protein (Table III). The effect on the T_{2e} is larger for bilayers with the M13 coat protein in the β-polymeric form as compared to the bilayers with the α-oligomeric form of the M13 coat protein.

Table II: Quadrupolar splittings (kHz) of DMPC-d_3 with M13 coat protein in the two conformations at 30 °C.

protein	L/P ratio		
	∞	50	20
α-oligomeric	3.9	3.8	3.3
β-polymeric	4.1	4.1	3.7

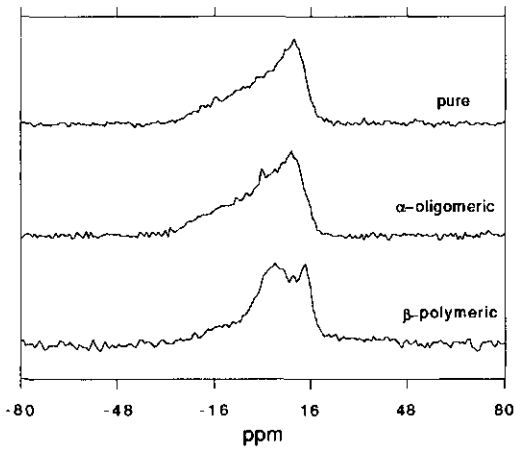

Figure 4. 121.4 MHz ^{31}P-NMR spectra of DOPC at 30 °C of pure and protein containing samples (both forms L/P 20). Number of scans 3600.

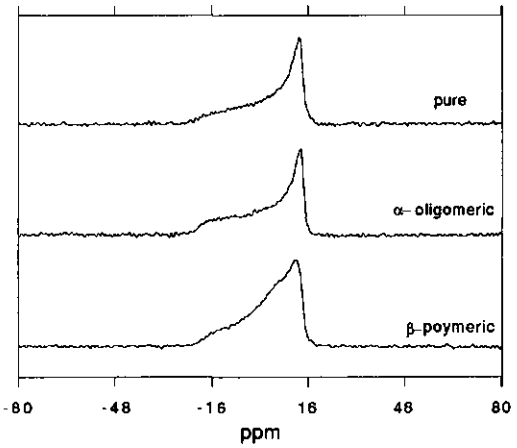

Figure 5. 121.4 MHz ^{31}P-NMR spectra of DMPC at 30 °C of pure and protein containing samples (both forms L/P 20). Number of scans 3600.

^{31}P-NMR on DOPC and DMPC bilayers: The ^{31}P-NMR spectra of the DOPC (Fig. 4) and DMPC (Fig. 5) bilayers are typical for those obtained from bilayer systems with no indication of any additional component in the case of pure bilayers and bilayers with the α-oligomeric form of the M13 coat protein. However in samples with the M13 coat protein in the β-polymeric form a distorted powder pattern can be observed (Figs. 4 and 5)

Table III: Relaxation times T_{1z} and T_{2e} for the on different positions deuterated phospholipids in the pure lipid systems and in lipid systems with the M13 coat protein in the two conformations*.

label	T_{1z} (ms)		T_{2e} (ms)	
	pure	+M13	pure	+M13
DOPC-d_4 #	11.7 ± 1.0	11.2 ± 1.0	0.66 ± 0.05	0.58 ± 0.05
DOPC-d_4 †	11.7 ± 1.0	11.1 ± 1.0	0.66 ± 0.05	0.40 ± 0.05
DMPC-d_3 #	3.0 ± 0.1	3.0 ± 0.1	1.21 ± 0.05	0.91 ± 0.05
DMPC-d_3 †	3.0 ± 0.1	3.0 ± 0.1	1.37 ± 0.05	0.71 ± 0.05

* The used temperatures are 10 °C for DOPC-d_4 and 30 °C for DMPC-d_3.

α-oligomeric protein containing sample.† β-polymeric protein containing sample.

Increasing the temperature causes the line shape to become more isotropical, subsequent cooling completely reversed this effect. Since the vesicles formed were homogeneous in L/P ratio on a sucrose gradient, the intensity of the central peak in the spectra of bilayers with the M13 coat protein in the β-polymeric form is suggested to arise from protein related lipids.

Discussion

M13 coat protein adopts two forms in model membranes, the α-oligomeric and the β-polymeric form. The M13 coat protein in the β-polymeric form is predominantly in an β-sheet conformation and strongly aggregated, whereas the α-oligomeric form of the M13 coat protein is in a predominant α-helix conformation and forms reversible small aggregates [9]. The unique opportunity provided by this viral coat protein to adopt two different conformations in membranes has enabled us to study the effect of these different secondary structures of the protein on the surrounding lipid matrix and visa versa.

The quadrupolar splitting in the ^{2}H-NMR spectra of DOPC-d_9 and the CSA in the ^{31}P-NMR spectra of DOPC bilayers do not change with increasing α-oligomeric protein content (Fig. 2), indicating that the headgroups of the phospholipids are not strongly affected by the M13 coat protein in the α-oligomeric form and that on the ^{2}H-NMR time scale the boundary and bulk lipids are in fast exchange. This is in agreement with a NMR study on various headgroup labelled phospholipids presented in chapter 5 were it is shown that the main effect of the coat protein in the α-oligomeric form is a change in the torsion angles in the headgroup as a result of the introduction of positive charges by the M13 coat protein. In bilayers of DOPC-d_4 and DMPC-d_3 a decrease of the quadrupolar splitting is observed on addition of the coat protein in the α-oligomeric conformation, which indicates that the order in the hydrophobic part of the bilayer has decreased. A small decrease in order of the hydrophobic part of the bilayers induced by various proteins has been observed previously by other workers [16].

The constant value of T_{1z} and the decreasing value of T_{2e} of lipid bilayers on addition of M13 coat protein in the α-oligomeric form show that the protein influences only slow molecular motions. Under exchange conditions the overall T_{2e} relaxation rate is the population average of the T_{2e} relaxation time of boundary (lipid molecule 2, Fig. 6A) and bulk lipids (lipid molecule 1, Fig. 6A) plus an extra term, which takes into account the exchange process [17]. The exchange contribution as well as a different T_{2e} value of the boundary lipids, could result in a decrease of the T_{2e} values. The lower T_{2e} value for the boundary lipids could be the result of motions of the protein or reorientational motions of lipids while bound to the protein [16].

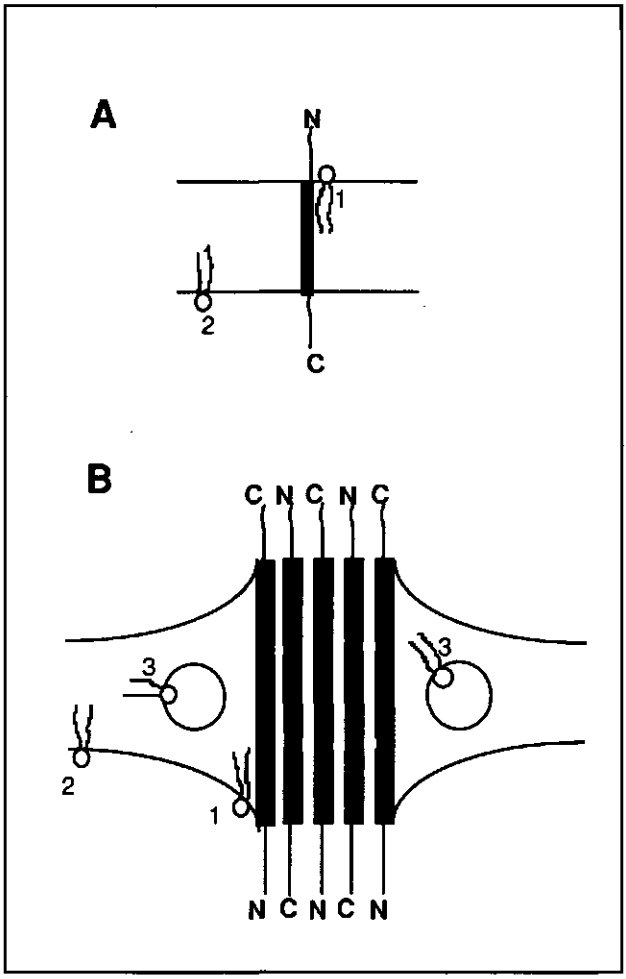

Figure 6. A schematic and speculative cartoon of the model proposed of the interaction of the M13 coat protein, in the α-oligomeric state (A) and in the β-polymeric state (B), with lipid bilayers. The protein is represented as a black bar. Bulk lipids (1) are in fast or intermediate exchange with boundary lipids (2). Lipids trapped in rodlike structures (3) are formed to match the hydrophobic part of the stretched β-polymeric protein in the lipid bilayer.

Previous experiments conducted on bilayers with various amounts of the M13 coat protein in the β-polymeric form, suggested that the protein induces a fraction of lipids trapped within protein aggregates [4,5]. These trapped lipids manifested themselves as a second spectral broad isotropic component in ^{2}H-NMR spectra of DMPC-d_9 bilayers [5] and

in a very slow exchanging boundary component in the ESR spectra obtained in various lipid bilayers [4].

For a reference, we have repeated some experiments to enable us to make a systematic comparison of the effect of the protein in the β-polymeric form on the headgroup and chains of lipids. Also in our ^{2}H-NMR and ^{31}P-NMR spectra of the headgroup labelled DOPC-d_9 with various amounts of M13 coat protein in the β-polymeric form, a second protein induced component is observed (Fig. 2), indicating the presence of trapped lipids, in agreement with results obtained by van Gorkom [5].

To investigate whether the interaction of the protein in the β-polymeric form also affects the other parts of the lipid molecule, we have studied by ^{2}H-NMR the influence of the protein in the β-polymeric form on chain labelled phospholipids (DOPC-d_4 and DMPC-d_3). In the ^{2}H-NMR spectra of DOPC-d_4 bilayers, in addition to a central broad component, of which the intensity is dependent on the amount of protein in the lipid system, a normal bilayer component can be observed, which indicates a slow exchange between a protein influenced lipid component and bulk lipids. In the spectra of DMPC-d_3 at 30 °C only one component can be observed. At 40 °C a decrease of the quadrupolar splitting is observed and a second central broad component appears. This suggests that similar effects can be observed for both lipid types, DOPC and DMPC, but at a different temperature.

The constant T_{1z} value at various amounts of M13 coat protein in this conformations indicates that M13 coat protein in this conformations causes no changes of the fast motions of the both lipid types in the membrane as detected from the constant T_{1z}. However, the slow motions are more drastically influenced by the M13 coat in the β-polymeric from as compared to the changes induced by the M13 coat protein in the α-oligomeric form, as is observed from T_{2e}. This larger decrease of the T_{2e} relaxation time suggests an additional influence on the motional behaviour of the lipids by the protein in the β-polymeric form.

It has been found experimentally that lipid bilayers adopt different morphological structures [18,19] or show membrane curvature effects [20] on adding proteins of which the hydrophobic part does not match the hydrophobic part of the membrane. Also Bloom [16] argued, that it was possible that proteins induce different lipid structures, with a distinct temperature behaviour. On basis of the fact that the whole lipid molecule is affected by β-polymeric protein (see Figs. 1 to 5), it is suggested, as a possible and tentative model to explain the NMR results presented in this paper, that the protein induces an additional lipid structure, which consists of rods of inversed lipids in the membrane close to the protein aggregates (see Fig. 6B). These lipids will show up as a central isotropic component due to the additional fast averaging that is taking place in these rodlike structures. Previously similar effects were observed on the introduction of cytochrome-c into lipid bilayers [19].

To understand why M13 coat protein in this conformation is capable of forming a different lipid structure, one has to take into account the shape of the protein. Tanford &

Reynolds [21] suggested two main possibilities for β-sheet structures in lipid membranes. Either proteins with a transmembrane β-sheet can have turns and form intra-peptide hydrogen bonds or are in an extended form with inter-peptide hydrogen bonds. If the transmembrane part of the M13 coat protein is in an extended β-sheet conformation, which has a rise of about 3.4 Å per residue, one realizes that 20 hydrophobic residues into a membrane core of 32 Å thickness cause a misfitting of the hydrophobic amino acid part of the protein with the hydrophobic part of the membrane. By forming rodlike structures in the planar bilayer the membrane will increase its thickness close to the protein resulting in an optimal hydrophobic matching. This would not be the case if M13 coat protein is considered to be in a folded β-conformation, with a turn in the hydrophobic part, forming strong intra-molecular hydrogen bonds that stabilize this structure in lipid bilayers [21]. However, it has been observed that when the protein is incorporated in a lipid bilayer, it is able to convert from the α-oligomeric form to the β-oligomeric form (R.B. Spruijt, unpublished results). A turn in the β-sheet conformation, therefore would imply the translocation of one of the hydrophilic termini through the lipid membrane upon this conversion. This is not very likely to occur. In addition from Molecular Dynamics simulations, it is found that if a β-turn is included in the β-sheet structure, a large mobility of the Cα atoms in and close to this turn is observed, suggesting that such a turn is unstable (see chapter 3). For these reasons the possibility of a folded β-conformation is rejected.

Lipids trapped in the protein induced rodlike lipid structure (lipid molecule 3, Fig. 6B) can not exchange with the bulk lipids (lipid molecule 1, Fig. 6B), because the flip-flop rates are slow. For this system it is argued that the formation of non bilayer structures is observed with lipids, which can undergo the liquid crystalline phase-hexagonal phase transition. It is known that this transition is more likely to occur for DOPC as compared to DMPC [19]. This explains that in our case in the DOPC bilayers at 30 °C this second component originating from the lipids in the rodlike structures is already clearly resolved, whereas the second component for the DMPC bilayers is only visible at 45 °C. It should be stressed that because such a component is observed with phospholipids with a phosphatidylcholine headgroup, which have a very strong tendency to form bilayers, the forces on the lipid bilayer induced by the protein to match the hydrophobic areas must be strong.

In addition to lipids in the inversed rod structures (lipid molecule 3, Fig. 6B), as proposed in the possible model, there is a fraction of lipids in contact with the protein, but not present in the inversed rod structures. This fraction of lipids will behave as boundary lipids (lipid molecule 2, Fig. 6B), which can exchange with the bulk lipids (lipid molecule 1, Fig. 6B). This exchange process explains the decrease of the quadrupolar splitting with increasing amounts of protein in the lipid bilayer (Tables I and II). Such a decrease of the quadrupolar splitting is observed also with the M13 coat protein in the α-oligomeric form

(see Tables I and II) and with various other integral membrane proteins [16]. The fact that this decrease in quadrupolar splitting is less upon the incorporation of the M13 coat protein in the β-polymeric form as compared to the α-oligomeric form (Tables I and II), can be related to the high aggregation state of the β-polymeric form of the M13 coat protein, which causes less lipids at a given lipid to protein ratio to be in a boundary state in comparison with the protein in the α-oligomeric form.

Acknowledgment

DQPC-d_4 was a kind gift from B. de Kruijff (University of Utrecht).

References

1 Datema, K. P., Wolfs, C. J. A. M., Marsh, D., Watts, A. and Hemminga, M. A. (1987) Biochemistry 26, 7571-7574.

2 Datema, K. P., Van Boxtel, B. J. H. and Hemminga, M. A. (1988) J. Magn. Reson. 77, 372-376.

3 Datema, K. P., Spruijt, R. B., Wolfs, C. J. A. M. and Hemminga, M. A. (1988) Biochim. Biophys. Acta 944, 507-515.

4 Wolfs, C. J. A. M., Horvàth, L. I., Marsh, D., Watts, A. and Hemminga, M. A. (1989) Biochemistry 28, 9995-10001.

5 van Gorkom, L. C. M., Horvath, J. L., Hemminga, M. A., Sternberg, B and Watts, A. (1990) Biochemistry 29, 3828-3834.

6 de Jong, H., Hemminga, M. A. and Marsh, D. (1990) Biochim. Biophys. Acta 1024, 82-88.

7 Peng, K., Visser, A. J. W. G., van Hoek, A., Wolfs, C. J. A. M., Sanders, J. C. and Hemminga, M. A. (1990) Eur. Biophys. J. 18, 279-285.

8 Peng, K., Visser, A. J. W. G., van Hoek, A., Wolfs, C. J. A. M. and Hemminga, M. A. (1990) Eur. Biophys. J. 18, 285-293.

9 Spruijt, R. B., Wolfs, C. J. A. M. and Hemminga, M. A. (1989) Biochemistry 28, 9159-9165.

10 Nozaki, Y., Reynolds, J. A.. and Tanford, C. (1978) Biochemistry 17, 1239-1246.

11 Fodor S. P. A., Dunker, A. K., Ng, Y. C., Carsten, D. and Williams, R. W. (1981) in: Seventh. biennial Conference on Bacteriophage Assembly. pp 441-455 (Dubow, M.S., ed.) Alan R. Liss Inc., New York.

12 Eibl, H. (1978) Proc. Natl. Acad. Sci. U.S.A. 75, 4074-4077.

13 Boss, W. F., Kelley, C. J. and Landsberger, F. R. (1975) Anal. Bioch. 64, 289-292.

14 Sternin, E., Bloom, M. and MacKay, A. (1983) J. Mag. Res. 55, 274-282.

15 Davis, J. H. (1983) Biochim. Biophys. Acta 737, 117-171.

16 Bloom, M. and Smith, I. C. P. (1985) In Progress in Lipid Protein Interaction. A. Watts, and J.J.H.H.M. De Pont editors. Elseviers Sciencew Publishers/ Holland, Amsterdam, 61-88.

17 Paddy, M. R, Dahlquist, F. F., Davis, J. H. and Bloom, M. (1981) Biochemistry 20, 3152-3162.

18 De Kruijff, B., Cullis, P. R. and Verkleij, A. J. (1980) Trends Biochem. Sci. 5, 79-81.

19 De Kruijff, B., Cullis, P. R., Verkleij, A. J., Van Echteld, C. J. A., Taraschi, T. F., Van Hoogevest, P., Killian, J. A., Rietveld, A. and Van der Steen, A. T. M. (1985) In Progress in Lipid Protein Interaction. A. Watts, and J. J. H. H. M. De Pont editors. Elseviers Sciencew Publishers/ Holland, Amsterdam, 89-142.

20 Israelachvili, J. N. (1977) Biochim. Biophys. Acta 469, 221-225.

21 Tanford, C. and Reynolds, J. A. (1976) Biochim. Biophys. Acta 457, 133-170.

CHAPTER 5

A NMR investigation on the interactions of the α-oligomeric form of the M13 coat protein with lipids, which mimic the Escherichia coli inner membrane

Johan C. Sanders, Trevor W. Poile, Ruud B. Spruijt, Nico A. J. Van Nuland, Anthony Watts and Marcus A. Hemminga

Abstract

The interaction of the M13 bacteriophage major coat protein in the α-oligomeric form with specifically deuterated phospholipid headgroups which mimic the *E. Coli* inner membrane, has been studied using NMR methods. As can be seen from the deuterium NMR spectra obtained with headgroup trimethyl deuterated DOPC, the coat protein in the α-oligomeric form does not give rise to trapped lipids as observed with M13 coat protein in the β-polymeric form (van Gorkom *et. al., Biochemistry 29,* 1990, 3828-3834 [1]). The quadrupolar splittings of the α head-group methylene deuterons of deuterated phosphatidylcholine and phosphatidylethanolamine decrease, whereas the quadrupolar splittings of the β head-group methylene deuterons of the two lipids increase with increasing protein content. All deuterated segments in the phosphatidylglycerol headgroup show the same relative decrease of the NMR quadrupolar splittings. These results are interpreted in terms of a change in torsion angles of the methylene groups, induced by positive charges, probably lysine residues of the protein at the membrane surface. For all lipid bilayer compositions studied the head-group perturbations are similar. It is concluded that there is no strong specific interaction between one of the lipid types examined and the M13 coat protein. From the spin-spin (T_{2e}) relaxation time and spin-lattice (T_{1z}) relaxation time of all deuterated lipids it is concluded that at the bilayer surface only slow motions are affected by the M13 coat protein.

Introduction

It has been shown that in model membranes M13 coat protein (MW: 5240; Reviews: [2,3]) can adopt two different conformations, which depend critically on the headgroup type and the degree of unsaturation of the acyl chains [4,5,6]. The two forms of the M13 coat protein differ in their α-helix content and also show differences in the aggregation state of the protein. The protein in the α-oligomeric form has been shown to be in a less aggregated

state than the protein in the β-polymeric form [6]. The protein in the α-oligomeric form has oligomers of less than 25 subunits [6] and can be obtained directly from the phage particle or when folded from a random coil conformation [4,7].

A)

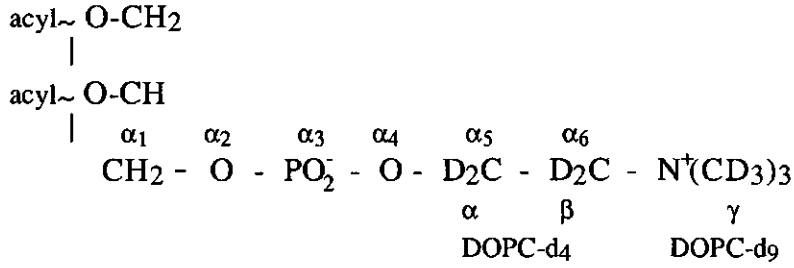

B)

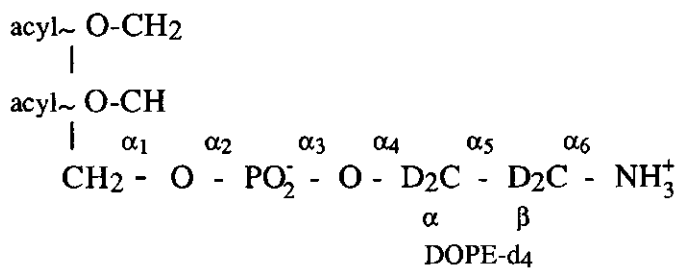

C)

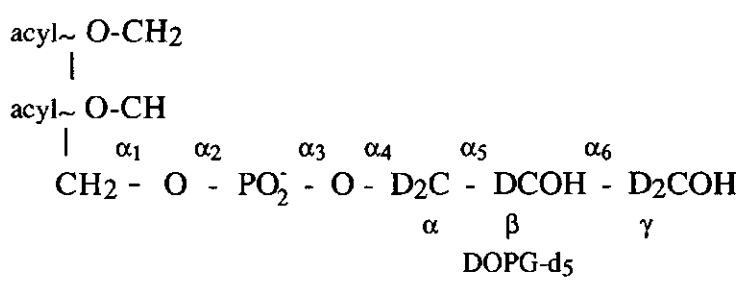

Figure 1. Chemical formula of A) DOPC labelled at various positions in the headgroup region (DOPC-d_4 and DOPC-d_9); B) DOPE labelled in the headgroup (DOPE-d_4); C) DOPG labelled in the headgroup (DOPG-d_5). Acyl is a dioleoyl fatty acid.

In this investigation we have studied M13 coat protein in the α-oligomeric form and its interaction with lipid bilayers which mimic the *E. coli* inner membrane. The composition of the inner membrane of *E. coli*, which is normally 74% PE, 19% PG and 4% CL, is changed during infection when the relative level of PE decreases in preference to an increase in the relative concentration of the lipids PG and CL [8]. This NMR investigation was performed to

investigate how M13 coat protein interacts with one of the lipid bilayer components of the *E.Coli* inner membrane. To mimic the *E. coli* inner membrane mixtures of the phospholipids DOPC, DOPE, DOPG and CL were used.

DOPC was specifically deuterated either in the headgroup at both the α and β methylene segments (DOPC-d_4) or at the trimethyl moiety (DOPC-d_9, Fig. 1A). DOPE was deuterated at both the α and β methylene segments of the choline headgroup (Fig. 1B) and DOPG-d_5 was labelled at the α, β and γ segments (Fig. 1C). In addition a comparison will be made with the results previously obtained with the protein in the β-polymeric form [1,9,10,11,12,12,13,14,15].

Materials and methods

Lipid synthesis: DOPC-d_9 deuterated in the trimethyl groups of the choline moiety, was synthesized from DOPE as described by Eibl [16]. The synthesis of 1,2-dioleoyl-*sn*-glycero-3-phospho-*rac*-glycerol, perdeuterated in the glycerol headgroup, 1,2-dioleoyl-*sn*-glycero-ethanolamine and 1,2-dioleoyl-*sn*-glycero-phosphatidylcholine, both deuterated in the α and β methelene segments has been described before [17]. After purification, the lipids appeared as one spot on high performance silica TLC (solvent $CHCl_3$, MeOH, NH_4OH, 55:30:3, v/v/v) and were stored at -20 °C. DOPE, DOPC, DOPG and CL were obtained from Sigma (St. Louis, U. S. A.) and used without any further purification.

Protein purification and reconstitution: Bacteriophage M13 was grown and purified as described previously [6]. The desired amounts of lipids (40 mg for DOPC-d_9, 75 mg for DOPC-d_4,75 mg for DOPE-d_4 and 75 mg for DOPG-d_5) were mixed with the desired amount of unlabelled lipids in chloroform. After removing the chloroform with nitrogen gas, samples were lyophilized for at least 12 hours and solubulized in buffer (50 mM Cholate (Sigma), 10 mM Tris (Sigma), 0.2 mM EDTA (Sigma), 140 mM NaCl, pH 8.0) by sonication (Branson B15, duty cycle 50%, 40W). To this solution the desired amount of protein in the same buffer was added followed by dialysis at room temperature against 100 fold excess buffer (10 mM Tris, 0.2 mM EDTA,140 mM NaCl, pH 8.0) for a total of 48 hours changing the buffer every 12 hours. The reconstituted lipid-protein complex was concentrated using an Amicon stirring cell to 500 µl and lyophilized for at least 12 hours and resuspended in 500 µl of deuterium depleted water (Sigma). The L/P ratio of each sample was determined by a phosphate assay with AMP as a standard [18] and a modified Lowry procedure to determine the protein content, using BSA as a standard [19]. To check sample homogeneity, aliquots were layered on a linear 0-40% w/w sucrose gradient and centrifuged at 100,000 g for 16 hr at 5 °C. The homogeneity was checked visually. For CD measurements, samples were diluted to a protein concentration of 0.1 mg/ml and an average

of at least five scans were recorded at room temperature on a Jovin-Ivon Dichograph Mark V in the wavelength range 200-250 nm, using a 0.1 cm path length. The spectra were analyzed using reference spectra of Greenfeld and Fasman (1969). The aggregation state of M13 coat protein was checked by HPLC as described previously [6].

NMR measurements: All NMR spectra were recorded on a Bruker CXP 300 spectrometer. The 46.1 MHz ^{2}H-NMR spectra and T_{2e} relaxation times were recorded using a quadrupolar echo pulse sequence, using quadrature detection (90°_x-τ-90°_y-τ-acq.) with full phase cycling [21]. The T_{2e} relaxation times were determined by plotting the intensity of the echo peak as a function of 2τ, where τ is the separation between the two pulses. The T_{1z} relaxation times were recorded using an inversion recovery method in combination with the quadrupolar echo sequence (180°_x-τ_2-90°_x-τ_1-90°_y-τ_1-acq.) and the relaxation times were determined as a function of the echo intensity versus τ_2. Typical instrumental parameters were: spectral width of 100 kHz, 90° pulse width of 5 µs and relaxation delay of 250 ms. 121.4 MHz ^{31}P-NMR spectra and T_2 relaxation times were recorded with broadband decoupling and a Hahn-echo sequence (90°_x-τ-180°_y-τ-acq.) using full phase cycling [22] Typical instrumental parameters for ^{31}P-NMR were spectral width 100 kHz, 90° pulse width of 5 µs and relaxation delay of 2.5 s. The temperature was controlled with a nitrogen gas flow unit and measured with an accuracy of ±1 °C. Oriented spectra were obtained numerically from the experimental spectra by using an iterative depaking program [23]. The quadrupolar splittings given in the Tables are all obtained from these oriented spectra.

Results

All the samples were checked for their homogeneity and for the conformation and aggregation state of the protein. Sucrose gradients of all samples showed only one band indicating that the samples were homogeneous. CD spectroscopy and HPLC elution profiles indicated that the protein was in the α-oligomeric form, with a predominant α-helix conformation and no indication of strong protein aggregation [6]. All the spectra containing DOPE were recorded at 5 °C. No indication was found for the presence of phospholipids in a hexagonal phase by ^{31}P-NMR spectra.

The quadrupolar splitting of the γ head-group segment of DOPC-d_9 is independent of the L/P ratio. A typical example of the spectra obtained from DOPC-d_9 is shown in Fig. 2. The T_{2e} relaxation time of DOPC-d_9 decreases with increasing protein concentration whereas the T_{1z} relaxation time is independent of the L/P ratio (Table I).

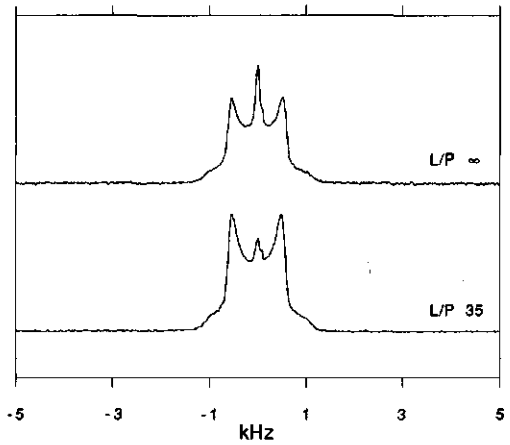

Figure 2. 46 MHz ^{2}H-NMR spectra of DOPC-d_9 at 25 °C L/P ∞ and L/P 35. Experimental parameters as described in the text.

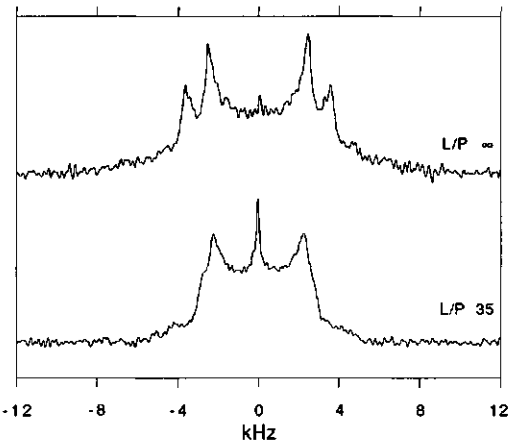

Figure 3A. 46 MHz ^{2}H-NMR spectra of DOPC-d_4 with and without M13 coat protein at 25 °C.

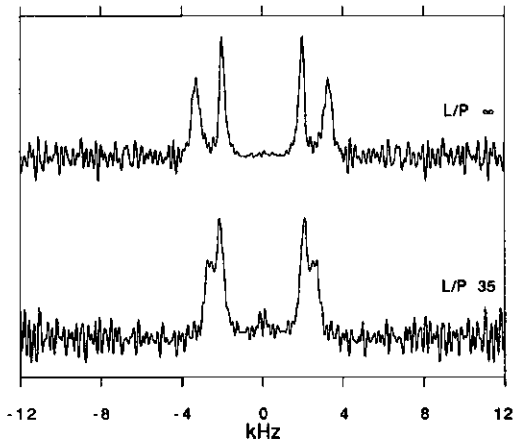

Figure 3B: oriented ^{2}H-NMR spectra of DOPC-d_4 with and without M13 coat protein at 25 °C.

Table I: Relaxation times T_{1z} and T_{2e} for the on different positions deuterated phospholipids with and without the M13 coat protein[a].

	T_{1z} (ms)		T_{2e} (ms)	
	pure	+M13	pure	+M13
DOPC-d_9	52 ± 1.0	55 ± 1.0	2.6 ± 0.1	2.1 ± 0.1
DOPC-d_4	8.9 ± 1.0	8.4 ± 1.0	0.60 ± 0.05	0.40 ± 0.05
DOPE-d_4/DOPC	5.9 ± 0.1	7.0 ± 0.1	0.97 ± 0.05	0.55 ± 0.05
DOPE-d_4/DOPG	6.9 ± 0.1	7.0 ± 0.1	0.86 ± 0.05	0.78 ± 0.05
DOPE-d_4/DOPG/CL	6.1 ± 0.1	5.4 ± 0.1	1.07 ± 0.05	0.66 ± 0.05
DOPG-d_5/DOPE	7.6 ± 0.1	7.1 ± 0.1	1.45 ± 0.05	1.32 ± 0.05
DOPG-d_5/DOPC	6.8 ± 0.1	7.1 ± 0.1	1.11 ± 0.05	0.94 ± 0.05

[a] The used temperatures are 25 °C for DOPC-d_4 and 40 °C for DOPC-d_9. The L/P ratios are 35 for DOPC-d_4 and 40 for DOPC-d_9. The various DOPE systems with.(L/P 38 ± 4) and without M13 coat protein were prepared in lipid mixtures with the ratios; DOPE-d_4/PG and DOPE-d_4/PC (3/1, w/w) and DOPE-d_4/DOPG/CL (15/3/2, w/w/w) and measured at at 5 °C. DOPG-d_5 with (L/P 38 ± 4) and without M13 coat protein in the mixtures with DOPC and DOPE(3/1, w/w) were measured at 5 °C. Samples were prepared and measured as described under materials and methods.

The ^{2}H-NMR spectra of DOPC-d_4 bilayers with L/P ratios of ∞ and 35 are shown in Fig. 3A. The spectra are a superposition of two powder patterns from the α head-group and β head-group deuterons. The outer splitting is attributed to the α head-group deuterons and the inner component is attributed to the β head-group deuterons [24]. The equivalent oriented spectra obtained by depaking clearly show changes in α and β segment splittings in the presence of protein. The splitting of the β segment increases with decreasing L/P ratio, in addition a corresponding decrease of the splitting of the α segment is observed (Fig. 3B).

In Table II the values of the quadrupolar splittings of DOPC-d_4 are given for various L/P ratios. The T_{2e} relaxation time, which can be described by a single exponential decay for all the systems measured, decreases with increasing protein content (Table I). For all samples the T_{1Z} relaxation times of DOPC-d_4 are analyzed as a single exponential decay and are independent of the L/P ratio (Table I).

Table II: Quadrupolar Splittings ($\Delta\nu_Q$ in kHz ± 0.05 kHz) of DOPC-d_4 with different M13 coat protein contents at 25 °C.

L/P	α	β
∞	6.70	4.10
55	6.00	4.30
35	5.60	4.40

Deuterium NMR spectra of bilayers consisting of the lipid mixtures DOPE-d_4/DOPC (3/1, w/w), DOPE-d_4/DOPG (3/1, w/w) or DOPE-d_4/DOPG/CL (15/3/2, w/w/w) are a superposition of the powder patterns from the α and β deuterons in the DOPE-d_4 head-group (Fig. 1). The outer quadrupolar splitting is attributed to the α head-group segment, the inner to the β head-group segment, according to Seelig and Gally [25].

Deuterium NMR spectra of the lipid mixture DOPE-d_4/DOPG/CL with and without M13 coat protein are shown in Fig. 4, which demonstrate the decrease of the α quadrupolar splitting and the slight increase in the β splitting with increasing M13 coat protein content. This is a general feature for all the DOPE-d_4 systems as shown in Table III. In the lipid mixture DOPE-d_4/DOPC it is possible to distinguish both α deuterons, whereas this is not possible in bilayers of the lipid mixtures DOPE-d_4/DOPG and DOPE-d_4/DOPG/CL. The observation that the α-CD_2 of DOPE-d_4 gives rise to two quadrupolar splittings (Table III) has been shown previously in other systems [24,26,27]. In Table I the spin lattice

relaxation times T_{1z} and the spin-spin relaxation times T_{2e} of DOPE-d_4 with different M13 coat protein content are given. There are no substantial changes in the T_{1z} relaxation times induced on adding M13 coat protein. In all lipid systems there is a significant decrease (up to 40%) of T_{2e} on adding M13 coat protein.

Table III: Quadrupolar splitting ($\Delta\nu_Q$ in kHz ± 0.1 kHz (α) or ± 0.05 (β) kHz) of DOPE-d_4 with (L/P 38 ±4) and without M13 coat protein in DOPE-d_4/X (3/1, w/w) and DOPE-d_4/X/Y (15/3/2, w/w/w) systems at 5 °C.

	DOPC		DOPG		DOPG, CL	
	-M13	+M13	-M13	+M13	-M13	+M13
α	12.8/12.2*	11.1/10.5*	13.8	12.8	13.5	12.7
β	3.70	3.90	3.90	4.30	4.00	4.10

*Two splittings are observed in the depaked spectra.

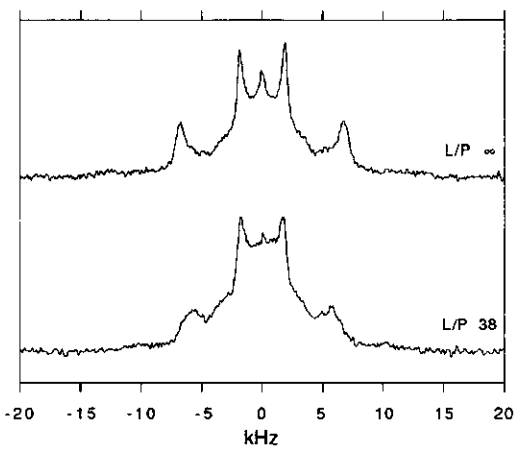

Figure 4. 46 MHz ^{2}H-NMR spectra of DOPE-d_4/DOPG/CL (15/3/2, w/w) with and without M13 coat protein (L/P 38) at a temperature of 5 °C.

^{2}H-NMR spectra of the lipid mixture DOPE/DOPG-d_5 (3/1, w/w) bilayers with and without M13 coat protein shown in Fig. 5, are a superposition of the powder patterns from the α, β and γ head-group deuterons. The outer quadrupolar splitting is attributed to the α head-group segment, the next to the β head-group segment and the inner quadrupolar splitting to the γ head-group segment, according to Sixl and Watts [28]. Fig. 5 demonstrates the decrease in α, β and γ quadrupolar splittings induced by the incorporation of M13 coat protein. As is shown in Table IV, the effect of incorporation of M13 coat protein on the quadrupolar splittings of DOPG-d_5 is the same for both lipid mixtures DOPE/DOPG-d_5 and DOPC/DOPG-d_5 (3/1, w/w). The fact that more than one component is observed for the α and γ head-group quadrupolar splittings in some cases is probably due the motional inequivalance, which could arise from the fact that DOPG-d_5 is in the headgroup racemic as a result of the synthetic procedure used for labelling [28,29].

Table IV: Quadrupolar splitting ($\Delta\nu_Q$ in kHz ± 0.1 kHz (α) or ± 0.05 (β,γ)kHz) of DOPG-d_5 with (L/P 38 ± 4) and without M13 coat protein in X/DOPG-d_5 systems (3/1, w/w) at 5 °C.

	DOPG		DOPC	
	-M13	+M13	-M13	+M13
α	12.0	10.5	11.9/11.4*	10.6
β	5.00	4.30	6.90	6.10
γ	1.10	0.90	1.90/1.40*	1.60/1.20*

*Two splittings are observed in the depaked spectra.

In Table I the spin lattice relaxation times T_{1z} and the spin spin relaxation times T_{2e} of DOPG-d_5 with different M13 coat protein content are given. There is no substantial change in the T_{1z} relaxation times on adding M13 coat protein. The T_{2e} relaxation time decreases slightly (10-15%) in both systems on adding M13 coat protein.

The ^{31}P-NMR spectra (not shown) are typical for those obtained from bilayer systems with no indication of any second component. The chemical shift anisotropy (-36 ppm) of the spectra and the T_2 relaxation time (0.6 ± 0.1 ms, 17 °C) of the ^{31}P nucleus of the DOPC bilayers are independent of the L/P ratio, within experimental error. Both in the pure lipid and samples containing protein there is an isotropic component observable in the ^{2}H- and ^{31}P-NMR spectra. This component is always less than 3% of the total intensity and is

independent of the L/P ratio. This component is assigned to lipids in smaller vesicles, which rotate fast on the NMR time scale.

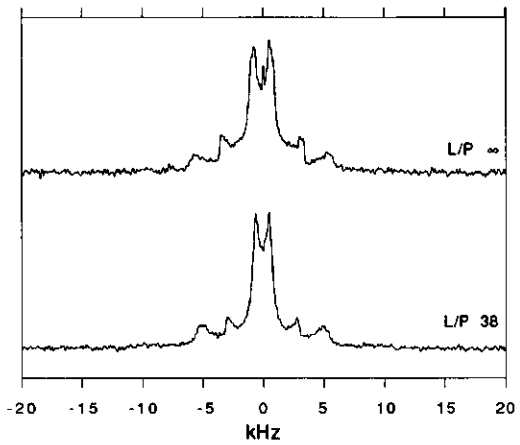

Figure 5. 46 MHz ^{2}H-NMR spectra of DOPC/DOPG-d_5 (3/1, w/w) bilayers with and without M13 coat protein (L/P 38) at a temperature of 5 °C.

Discussion

The β-polymeric form of M13 coat protein has been investigated previously [1,9,10,11,13,14,15]. With NMR and ESR methods it has been shown that the protein in the β-polymeric form gives rise to a fraction of lipids trapped by the protein aggregates [1,12]. To test if this is also the case for the α-oligomeric form of the M13 coat protein we have performed ^{2}H-NMR measurements on DOPC-d_9. To study in more detail the interaction of the α-oligomeric form of M13 coat protein with the surrounding lipid matrix we have studied mixtures of the deuterated phospholipids DOPC-d_4, DOPE-d_4 and DOPG-d_5, which mimic the *E. coli* membrane.

In ^{2}H-NMR spectra of DMPC-d_9 with M13 coat protein in the β-polymeric form two components were observed that were attributed to bulk and trapped lipids. Trapping lipids by lipid-protein complexes is possible, since the protein in the β-polymeric form is known to form large aggregates [1]. In contrast to the protein in the β-polymeric form, for the α-oligomeric form of M13 coat protein no trapped lipids are observed in the DOPC-d_9 ^{2}H-NMR spectra (Fig. 2). This is in agreement with the information obtained from HPLC, which show less strong aggregation for this form of the M13 coat protein. This means that in the case of the protein in the α-oligomeric form the spectrum is determined by a fast exchange of

boundary lipids and lipids, which are not in contact with the protein. However, due to the fast exchange, it is not possible to obtain the amount of boundary lipids per protein subunit, because the quadrupolar splitting of the boundary lipids is unknown.

To study in more detail the interactions between M13 coat protein and phospholipids we have studied various lipid mixtures. Differences in the quadrupolar splitting of headgroup labelled PC and PE for various mixtures of lipids have been reported previously [30]. The effect of M13 coat protein in the α-oligomeric form on both DOPC-d_4 as well as DOPE-d_4 is a decrease of the quadrupolar splitting associated with the α methylene (CD_2) deuterons, whereas the quadrupolar splittings of the β methylene (CD_2) deuterons show a corresponding increase (Table III). It has been shown with many other positively charged membrane substitutes that the effect observed with DOPC-d_4 can be explained by a change in torsion angles within the headgroup as a result of the introduction of positive charges at the membrane surface [31,32]). Spectroscopic and crystallographic data suggest that the headgroup conformations for PC and PE are similar [33]. In addition the charge distribution of the PE and PC headgroups are alike. This explains the similar effect of M13 coat protein on the PE headgroup as compared to the effects on the PC headgroup.

Table IV demonstrates the decrease of the quadrupolar splittings of the glycerol headgroup, when M13 coat protein is introduced to the bilayers. In mixtures of DOPG/DOPE and DOPC/DOPE the same relative decrease for all splittings upon incorporation of M13 coat protein is observed. This suggests that a change in order induced by the protein is an effect of the whole glycerol moiety. The T_{1z} relaxation times of the deuterons in PG-headgroup and the phosphorus spectra are not influenced, therefore a change in the torsion angles α_3 and α_4 (Fig 1C) can probably explain the changes of the quadrupolar splittings in the glycerol headgroup on addition of M13 coat protein. A decrease of all the quadrupolar splittings induced by adding a positively charged protein has also been observed previously on the introduction of myelin basic protein [34].

The differences between the observed changes in the quadrupolar splittings of headgroup deuterated PE and PC, as compared to the changes of the quadrupolar splittings of headgroup deuterated PG induced by the positive charges of the M13 coat protein, are probably due to the differences in hydrogen bonding capabilities and differences in charge distribution of the headgroups used. PE and PC have a net dipole, in contrast to PG, which has one negative charge. These differences result in a different conformation of the PE and PC headgroup as compared to the PG headgroup on introduction of positive charges at the membrane surface.

It can be concluded that in this system the changes induced by the M13 coat protein on the lipid headgroups may be due to a charge induced effect. However, the changes in quadrupolar splittings are small as compared to previous reported results upon introduction of positive amphiphiles in a lipid membrane [32]. This suggests a larger distance between

the charges and the headgroup or a different a distribution of charges at the surface of the lipid bilayer in the case of the M13 coat protein as compared to the charges induced by the amphiphiles. Since the charge effect is small, only weak electrostatic interaction with the lipids occurs. Similar effects of positively charged M13 coat protein on DOPE-d_4 are observed in all the mixtures used, indeed showing no detectable specificity for the negatively charged lipids PG or CL.

The positive charges introduced by the protein at the membrane surface, causing the observed effects in the ^{2}H-NMR spectra, can be assigned to its positively charged lysine residues. It should be noted that lysine 40 is situated at the end of the hydrophobic part of the protein, therefore probably lying close to the membrane bilayer surface. Also lysine residues 43 and 44 are in the vicinity of the bilayer surface. Due to the dialysis procedure in preparing the lipid protein systems, the protein is probably randomly inserted in the membrane giving a completely symmetric bilayer with a net positive charge at both membrane surfaces.

The T_{2e} relaxation times of the α and β head-group labelled lipids DOPE-d_4 and DOPC-d_4 can be analysed as a single exponential decay. This indicates that both labelled head-group segments of the phospholipid undergo similar motions. This is clearly not the case for the γ labels in comparison to the α and β labels of the lipids DOPG-d_5 and DOPC-d_4. This can also be observed in the spectra of DOPG-d_5 at different inter pulse delays (τ). After long delay times all the intensity of the signals originating from the α and β head-group labels has disappeared, whereas the the quadrupolar splitting of the γ head-group segment is still visible (results not shown). This means that the given relaxation time for DOPG-d_5 is a weighted average of the relaxation times of all labelled segments. The T_{2e} relaxation time of the γ segment deuterons of DOPG-d_5 can be estimated and is close to the relaxation times obtained for DOPC-d_9, whereas the relaxation time of the α and β segment deuterons is close to the relaxation times obtained from the other lipids labelled at identical positions. This suggest that similar segments in the heagroups of different lipids undergo similar motions in lipid bilayers.

The value of T_{2e} decreases upon incorporation of M13 coat protein. This decrease of T_{2e} and the constant value of T_{1z} relaxation times of all systems investigated indicates that only slow motions are affected by M13 coat protein. A possibility to explain a decrease in the T_{2e} relaxation time upon incorporation of membrane proteins in lipid bilayers is that under intermediate exchange conditions the overall T_{2e} relaxation rate is the population average of boundary and bulk lipids plus an extra term, which takes into account the exchange process [35]. If it is assumed that the T_{2e} relaxation time for the lipid fractions influenced by the protein is identical to the relaxation time of the bulk lipids and the number of lipids in the boundary shell is at least four, this being the number of boundary lipids found in an aggregated system [1], then exchange rates are obtained, which would in the NMR spectra

give rise to slow exchange. Since this is not the case, this would mean that the boundary lipids are undergoing a restricted motion as compared to the bulk lipids. This is in agreement with results obtained from ESR and time resolved fluorescence spectroscopy of M13 coat protein incorporated in lipid bilayers (chapter 6).

Acknowledgment

We thank Leon van Gorkom for preparing DOPC-d_4 and DOPC-d_9.

References

1 van Gorkom, L. C. M., Horváth, J. I., Hemminga, M. A., Sternberg, B. and Watts, A. (1990) Biochemistry 29, 3828-3834.

2 Pratt, D., Tzagoloff, H. and Beadoin, J. (1969) Virology 39, 42-53.

3 Rashed, I. and Oberer, E. (1986) Microbiol. Rev. 50, 401-42.

4 Nozaki, Y., Reynolds, J. A.. and Tanford, C. (1978) Biochemistry 17, 1239-1246.

5 Fodor S. P. A., Dunker, A. K., Ng, Y. C., Carsten, D. and Williams, R. W. (1981) in: Seventh. biennial Conference on Bacteriophage Assembly. pp 441-455 (Dubow, M.S., ed.) Alan R. Liss Inc., New York.

6 Spruijt, R., Wolfs, C. J. A. M. and Hemminga, M. A. (1989) Biochemistry 28, 9159-9165.

7 Makino, S., Woolford, J., Tanford, C. and Webster, R. (1975) J. Biol. Chem. 250, 4327-4332.

8 Chamberlain, B. K. and Webster, R. E. (1976) J. Biol. Chem. 24, 7739-7745.

9 Datema, K. P., Wolfs, C. J. A. M., Marsh, D., Watts, A. and Hemminga, M. A. (1987) Biochemistry 26, 7571-7574.

10 Datema, K. P., Visser, A. J. W. G., van Hoek, A., Wolfs, C. J. A. M., Spruijt, R. B. and Hemminga M. A. (1987) Biochemistry 26, 6145-6152.

11 Datema, K. P., Van Boxtel, B. J. H. and Hemminga, M. A. (1988) J. Mag. Res 77, 372-376.

12 Wolfs, C. J. A. M., Horvàth, L. I., Marsh, D., Watts, A. and Hemminga, M. A. (1989) Biochemistry 28, 9995-10001.

13 de Jong, H., Hemminga, M. A. and Marsh, D. (1990) Biochim. Biophys. Acta 1024, 82-88.

14 Peng, K., Visser, A. J. W. G., van Hoek, A., Wolfs, C. J. A. M. and Hemminga, M. A. (1990) Eur. Biophys. J. 18, 277- 283.

15 Peng, K., Visser, A. J. W. G., van Hoek, A., Wolfs, C. J. A. M., Sanders, J.C. and Hemminga, M. A. (1990) Eur. Biophys. J. 18, 285-293.

16 Eibl, H. (1980) Proc.Natl. Acad. Sci. U.S.A. 75, 4074-4077.
17 Sixl, F. and Watts, A. (1982) Biochemistry 21, 6446-6452.
18 Bartlett, G. R. (1959) J. Biol. Chem 234, 466-468.
19 Peterson, G. (1977) Anal. Biochem. 83, 346-356.
20 Greenfeld N. and Fasman G. D. (1969) Biochemistry 18, 4108-4116.
21 Griffin, R. G. (1981) Meth. Enzymol. 72, 108-173.
22 Rance, M. and Byrd, R. A. (1983) J. Magn. Reson. 52, 221-240.
23 Sternin, E., Bloom, M. and MacKay, A. (1983) J. Mag. Res. 55, 274-282.
24 Gally, H-U., Niederberger, W. and Seelig, J. (1975) Biochemistry 14, 3647-3652.
25 Seelig, J. and Gally, H-U (1976) Biochemistry 15, 5199-5204.
26 Brown, M. F. and Seelig, J. (1978) Biochemistry 17, 381-384.
27 Akutsu, H. and Seelig, J. (1981) Biochemistry 20, 7366-7373.
28 Sixl, F. and Watts, A. (1985) Biochemistry 24, 7906-7910.
29 Wohlgemuth, R., Waespe-Sarcevic, N. and Seelig, J. (1980) Biochemistry 19, 3315-3321.
30 Sixl, F. and Watts, A. (1983) Proc. Natl. Acad. Sci.U.S.A. 80, 1613-1615.
31 Browning J. L. and Akutsu, H. (1982) Biochim. Biophys. Acta 684, 172-178.
32 Scherer P. G. and Seelig J. (1989) Biochemistry 28, 7720-7728.
33 Büldt, G. and Seelig, J. (1980) Biochemistry 16, 6170-6175.
34 Sixl, F., Brophy, P.J. and Watts, A. (1984) Biochemistry 23, 2032-2039.
35 Paddy, M.R., Dahlquist, F.F., Davis, J.H. and Bloom, M. (1981) Biochemistry 20, 3152-3162.

CHAPTER 6

A small protein in model membranes: a time-resolved fluorescence and ESR study on the interaction of M13 coat protein with lipid bilayers

Johan C. Sanders, M. Francesca Ottaviani, Arie van Hoek, Antonie J. W. G. Visser and Marcus A. Hemminga

Abstract

Model membranes with unsaturated lipid chains containing various amounts of M13 coat protein in the α-oligomeric form were studied using time-resolved fluorescence and ESR spectroscopy. The L/P ratios used were >12 to avoid protein-protein contacts and possible irreversible aggregation. In the ESR spectra of the 12-SASL probe in dioleoyl-phosphatidylcholine bilayers no second protein induced component can be observed upon incorporation of M13 coat protein. However, strong effects on the ESR lineshapes upon changing the protein concentration were observed. Using lineshape simulations, it was shown that increasing the protein concentration from L/P ∞ to LP 15 results in a decrease of the rotational diffusion of $3.4 * 10^7$ to $1.9 * 10^7$ s^{-1}. Using time-resolved fluorescence, with as probe DPH-propionic acid, one observes that increasing the M13 coat protein concentration causes an increase of both lifetimes. In addition, the value of the order parameter $\langle P_2 \rangle$ and the $\langle P_4 \rangle$ increases from 0.34 to 0.55 and from 0.59 to 0.77, respectively upon adding M13 coat protein (L/P 35) to DOPC bilayers. The rotational diffusion coefficient decreases upon incorporating M13 coat protein as obtained from the time resolved fluorescence experiments, which is in agreement with the results obtained from ESR. It is argued based on the ESR and time-resolved fluorescence results that M13 coat protein in the α-oligomeric does not immobilize lipids but restricts the motion and increases the order of the lipids, due to its cylindrical form and geometric proportions.

Introduction

The infection of *Escherichia coli* with the bacteriophage M13 starts with the entry of the phage via a sex pilus and the subsequent release of the viral DNA into the cytoplasm and storage of the major coat protein as an integral membrane protein in the cytoplasmic membrane of the host [1,2]. The newly synthesized coat protein is inserted into the membrane as a preprotein and is converted to mature protein (MW = 5240) by cleavage with a leader peptidase. This newly synthesized protein and probably also the stored parental

protein are used for the membrane-bound assembly of new bacteriophage particles [3]. The secondary structure of the coat protein in the bacteriophage, as determined by neutron scattering data and Raman experiments, is 100% α–helical [4]. It has been shown that in model membranes the M13 coat protein can adopt two different forms, the α-oligomeric and the β-polymeric form. The presence of either one of these forms critically depends on the headgroup type and the degree of saturation of the acyl chains of the lipids used [5-7].

The β-polymeric form is an aggregated β-sheet protein complex [8,9], whereas the protein in the α-oligomeric form has about 90% α-helix structure and forms only small aggregates, perhaps monomers [5,10]. This form was recently studied with ^{2}H-NMR (see chapter 5). Here, we study the effects of the M13 coat protein in the α-oligomeric form on bilayers consisting of DOPC with time-resolved fluorescence and ESR spectroscopy. These techniques are suitable to investigate changes in order and dynamics of the lipid chains upon incorporation of the M13 coat protein. The results obtained from both techniques can directly be compared, since they are both sensitive for motions on the nanosecond time scale. The L/P ratios studied are taken to be >12, because for an ideal single trans-membrane α-helix it is expected that 12 lipids will surround the protein. In this L/P region, protein-protein contacts that may result in protein aggregation and a change in conformation [5] are avoided

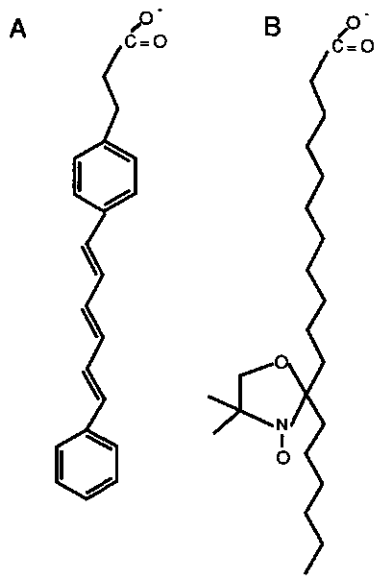

Figure 1. Chemical formulas of A) DPH-prop and B) 12-SASL.

Materials and methods

Chemicals: DOPC is obtained from SIGMA (St. Louis, U. S. A.) and used without further purification. The fluorescent label DPH-prop 2-(3(1,6-diphenylhexatrienyl)propanic acid (Fig. 1A) is obtained from Molecular Probes Inc and spin labelled fatty acid (12-SASL; Fig. 1B) from SIGMA. The probes are used without further purification.

Protein purification and reconstitution: Bacteriophage M13 is grown and purified as described previously [5]. After removing the chloroform with nitrogen gas the desired amounts of lipids are lyophilized for at least 12 hours. If desired, DPH-prop and 12-SASL was added to the chloroform solution in a molar ratio of 1:500 and 1:1, respectively. The lyophilized samples are solubilized in buffer (50 mM cholate, 10 mM Tris, 0.2 mM EDTA, pH 8.0). To the buffer solution the desired amount of protein, purified as described previously [5], in the same buffer is added before removing the cholate by dialysis at 25 °C against a 100 fold excess buffer (10 mM Tris, 0.2 mM EDTA, pH 8.0) for a total of 48 hours changing the buffer for every 12 hours. The samples used for optical experiments were diluted to an OD of 0.1. The corresponding background samples without protein were prepared and diluted in the same way as the corresponding protein containing samples. The ESR samples were lyophilized, resolubilized and concentrated using an Amicon Stirring cell. The L/P ratio of the samples is determined with a phosphate and protein determination. The conformation of M13 coat protein is checked with CD spectroscopy. An average of at least five scans is recorded at room temperature on a Jovin-Ivon Dichograph Mark V in the wavelength range 200-240 nm, using a 0.1 cm path length. The aggregation state is checked with HPLC as described by Spruijt *et al.* [5].

ESR studies: ESR spectra were recorded on a Bruker ER 200 spectrometer with nitrogen gas flow temperature regulation (± 1 °C). ESR settings were: 5 mW microwave power, 0.1 mT modulation amplitude, 200 ms time constant, 200 s scan time, 10 mT scan width and 339 mT centre field. Up to 12 spectra were accumulated to improve the signal to noise ratio. The ESR simulations were performed with a computer program developed by Schneider and Freed [11]. The parameters used for the simulation are as follows: components of the hyperfine coupling tensor A (in mT) 0.62, 0.56, 3.25; components of the g-tensor 2.0088, 2.0061, 2.0027. The values used for the g-tensor are the same as used by other workers for the same type of radical [12,13].

Time-resolved fluorescence studies: The experimental set-up for the polarized fluorescence decay measurements has been described previously [14]. The excitation wavelength is 340 nm and the emission wavelength (437 nm) is selected by a filter (Balzer

437). The fluorescence decay is detected by time-correlated single photon counting [15]. The analysis is performed using a global analysis program, which uses a non-linear fitting least square procedure [16]. The quality of the fit is determined by the weighted residues and the chi-square.

After correction for the background fluorescence, the fluorescence decay ($I_f(t)$) of DPH-prop in DOPC bilayers with various amounts of M13 coat protein is, after correction for the background fluorescence, analyzed in a sum of exponentials:

$$I_f(t) = \sum_{i=1}^{2} \alpha_i \, e^{-t/\tau_i} \qquad (1)$$

in which τ_i is the fluorescence lifetime and α_i a pre-exponential factor. Typically, two exponential components were sufficient to analyze the fluorescence decay.

After correction for background fluorescence, the time-resolved fluorescence anisotropy decay of DPH-prop in DOPC bilayers with various amounts of M13 coat protein is analyzed in a sum of exponentials, which are expressed in terms of four variables, $\langle P_2 \rangle$, $\langle P_4 \rangle$, $D_\perp$ and r(0) [16,17]. $\langle P_2 \rangle$ and $\langle P_4 \rangle$ are the orientational order parameters expressed in Legendre polynomials of the second and fourth rank. In view of the geometrical form of the molecule, its rotational diffusion in the membrane is assumed to be cylindrically symmetric. Because, the ratio the motion about the molecular symmetry axis ($D_\parallel$) and the motion of the molecular symmetry axis ($D_\perp$) is large, for the fluorescence experiments only the rotational diffusion parameter $D_\perp$ is taken into account. The initial anisotropy, r(0), gives information about the angle between the absorption and emission moments. This parameter is fixed to a value of 0.39 as has been obtained by other authors [17,18].

Results

Protein studies: M13 coat protein is able to adopt two conformations, an α-helix or a β-sheet, depending on its lipid environment and history of preparation [5]. Since the purpose of this study was to investigate the α-helix structure, care was taken to avoid protein-protein contacts and protein aggregation that may result in the formation of a β-sheet, by using L/P ratios >12. We checked the conformation and aggregation state of the protein in the various lipid bilayers. The CD spectra of M13 coat protein show that the α-helix content of the protein is approximately 90%, whereas HPLC demonstrated the absence of large aggregates in the measured samples. After the experiments the conformational and aggregation state of M13 coat protein was checked again. No changes could be detected, showing that state of the protein in these bilayers is stable at all L/P ratios used.

ESR studies: ESR spectra of 12-SASL in DOPC bilayers at 10 °C, which have a liquid crystalline transition temperature of -16 °C [19], with various amounts of M13 coat protein are given in Fig. 2. At low L/P ratios no distinct bound component can be observed, as has been reported previously for the β-polymeric form of the M13 coat protein in similar bilayers, but strong effects on the lineshape are observed (Fig. 2). Similar, but somewhat less pronounced effects were observed for 14-SASL (results not shown). To describe the spectral changes observed upon incorporation of M13 coat protein in terms of changes in order parameters and rotational diffusion coefficients, ESR spectra with and without protein were simulated using the program of Schneider and Freed (solid lines in Fig. 2).

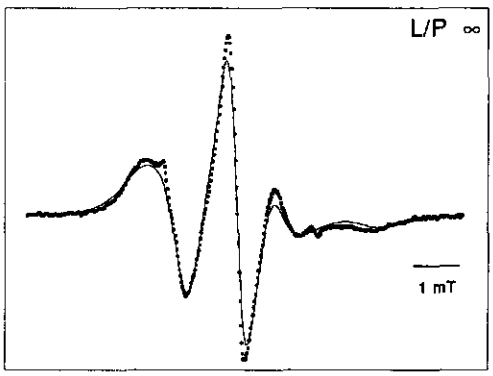

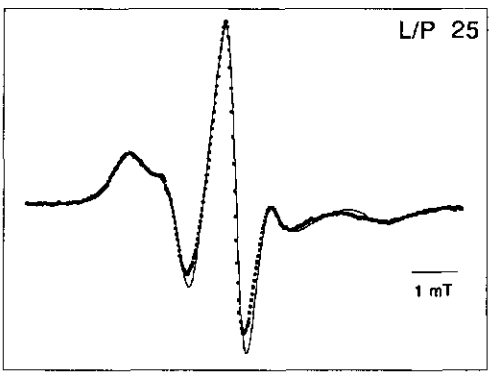

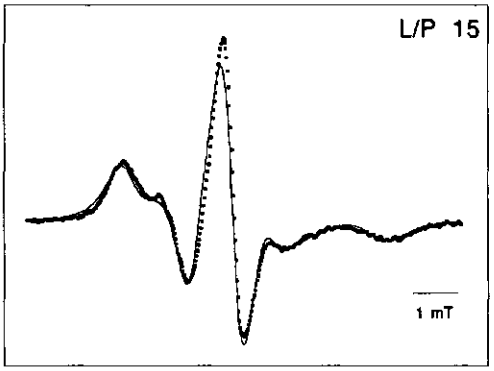

Figure 2. ESR spectra of 12-SASL in DOPC bilayers at 10 °C with various L/P (mole/mole) ratios of M13 coat protein. The dotted lines are the experimental data and the straight lines represent the simulations. For the simulations the values for the A and g tensor were used as described in the Material and methods. The values for $D_{\perp}$ are 3.4 $*10^{-7}$ s^{-1} for L/P ∞, 2.4 $*10^{-7}$ s^{-1} for L/P 25 and 1.9 $*10^{-7}$ s^{-1} for L/P 15. The order parameter was taken to be zero in all spectra.

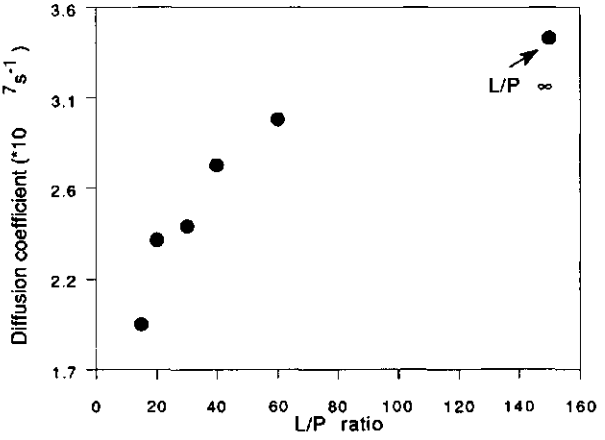

Figure 3. The diffusion coefficient, $D_{\perp}$, obtained from the analysis of the ESR spectra of spin labels in DOPC bilayers at 10 °C with various amounts of M13 coat protein.

The motional behaviour of the probe is found to be well described by an anisotropic brownian diffusion. The choice of other motional models (free or jump diffusion) gave less good fitting. Axial diffusion is assumed with a fixed ratio between the parallel ($D_{\parallel}$) and perpendicular ($D_{\perp}$) diffusion coefficients ($D_{\parallel}/D_{\perp} = 4$), in agreement with simulations performed by Schneider and Freed [11]. All simulations were carried out for an order parameter equals zero. The introduction of a non-zero order parameter was also tried, but did not result in an improved fitting of the experimental ESR spectra. The simulations resulted in a consistent set of data, in which the spectra at the various L/P ratios were considered as single component spectra characterized by different values of $D_{\perp}$. The resulting values of $D_{\perp}$ at various L/P ratios are given in Fig. 3.

Important is also the observation that the same ESR spectra were found for lower L/P ratios at higher temperatures as compared to spectra observed at higher L/P ratios. This indicates that increasing the temperature compensates the effect of the protein on the ESR lineshape. For example, a temperature increase of 15 °C is compensated by increasing the protein concentration with a factor of two.

Table I: Fluorescence lifetimes (τ_i), the relative contribution (α_i) and the values for $\langle P_2 \rangle$, $\langle P_4 \rangle$ and $D_{\perp}$ of DPH-prop in DOPC membranes with various amounts of M13 coat protein. The error in the values is estimated to be less than 5% for all parameters (10% for $D_{\perp}$).

L/P	T (° C)	α_1	τ_1 (ns)	α_2	τ_2 (ns)	$\langle P_2 \rangle$	$\langle P_4 \rangle$	$D_{\perp}$ ($*10^9$ s^{-1})
∞	5	0.47	2.94	0.53	6.00	0.34	0.59	0.10
55	5	0.43	3.10	0.57	6.21	0.39	0.62	0.09
35	5	0.45	3.28	0.55	6.42	0.55	0.77	0.08
∞	20	0.38	1.97	0.62	5.40	0.32	0.57	0.18
55	20	0.37	2.29	0.63	5.78	0.36	0.59	0.14
35	20	0.40	2.73	0.60	6.08	0.50	0.68	0.14

Time-resolved fluorescence: The fluorescence decay behaviour of DPH-prop in bilayers of DOPC with various amounts of M13 coat protein is shown in Table I. Two fluorescence

lifetime components are needed to analyse the fluorescence decays, in agreement with previous reports [20]. The origin of this multi-exponential behaviour is still unknown because the photophysics of DPH-prop has not yet been studied in detail. However, this will not affect our analysis of the anisotropy decay, especially since the two lifetimes behave similarly under the various experimental conditions (Table I). For example, both lifetimes decrease with increasing L/P ratios, and increasing the temperature from 5 to 20 °C causes both lifetimes to decrease (Table I).

The parameters $\langle P_2 \rangle$, $\langle P_4 \rangle$ and $D_\perp$ obtained from the analysis of the anisotropy decay of DPH-prop as a function of protein concentration and temperature are shown in Table I. As can be seen from Table I, a decrease of temperature and an increase of protein concentration causes the order parameters $\langle P_2 \rangle$ and $\langle P_4 \rangle$ to decrease. The effect of an increase of the temperature from 5 to 20 °C leads to an increase of the $D_\perp$ by nearly a factor of two. The $D_\perp$ decreases only slightly upon increasing the protein concentration in the bilayers (Table I).

Discussion

During the infection process of *E. coli* by the M13 bacteriophage high amounts of old and newly synthesized M13 coat protein are stored in the cytoplasmatic membrane of the host. In this paper, membranes with unsaturated lipid chains with various amounts of the M13 coat protein in the α-oligomeric form are studied with ESR and time-resolved fluorescence spectroscopy to probe the effect of this form of the M13 coat protein on lipid bilayers. Care was taken to avoid reversible and irreversible protein-protein (aggregation) contacts, because it is expected that protein-protein contacts will give rise to a fraction of lipids, which is trapped by protein molecules [21]. Therefore, protein-protein contacts were avoided by using L/P ratios >12 and using the reconstitution conditions described by Spruijt *el al.* [5]. The absence of irreversible protein-protein aggregation is clearly demonstrated with HPLC and the conformation of the M13 coat protein is mainly α-helix (90%) [5].

Diffusion coefficient: The changes in the ESR spectra of the 12-SASL spin probe upon introduction of M13 coat protein can be analyzed by a computer simulation in terms of a decrease in the rotational diffusion coefficient $D_\perp$. $D_\perp$ is directly coupled to $D_\parallel$ by the relation $D_\parallel = 4^*D_\perp$ (see results) and $D_\perp$ shows a non-linear dependence on the protein concentration (Fig. 3): a strong decrease is observed, especially at higher protein concentrations. This effect may be expected, since going to very low L/P ratios finally totally immobilized lipid would result by trapping of the lipids between the protein molecules.

The DPH-prop probe also senses a decrease of the diffusion coefficient, $D_\perp$, upon incorporating M13 coat protein. However, the effect of M13 coat protein on the diffusion

coefficient is in this case less as compared to the changes observed from ESR. Also the rate of the motion of the DPH-prop probe is 2.5 times faster as the rate of the 12-SASL probe. This might be due to differences in size and molecular properties of the probes (Fig. 1). These differences will also affect the order parameters obtained from the two probes and will be discussed below.

Order parameters: The molecular structure of the 12-SASL probe gives rise to a high flexibility, which arises from the trans-gauche isomerisation of the acyl chain to which the nitroxide moiety is attached. Therefore, the order parameter found with the 12-SASL probe is less than 0.1 as has been found in our simulations (results not shown). This is in agreement with other studies [22]. As a result of this low order, changes in order parameter induced by the protein are not possible to determine by computer simulations. Therefore, the order parameter was taken to be zero.

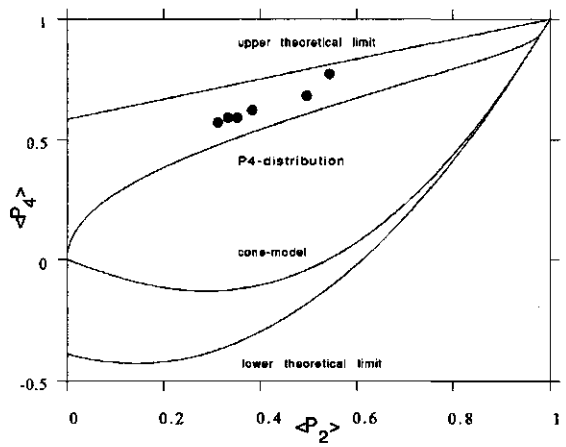

Figure 4. A $<P_2>$-$<P_4>$ plot, using the data of Table I. The upper and lower theoretical boundaries for $<P_2>$-$<P_4>$ are shown. In addition, the dependencies are shown for the $<P_4>$-distribution and the cone model.

Because the DPH-prop probe is a rigid molecule, as a result of the presence of the conjugated bonds (Fig. 1) it senses the "average" order at different depths in the membrane. In Table I it can be observed that increasing the protein concentration causes an increase in both order parameters, $<P_2>$ and $<P_4>$, of DPH-prop in DOPC bilayers. This indicates that the order of the lipid bilayers as sensed by the DPH-prop probe has increased upon incorporation of the M13 coat protein. The increase in order correlates with the observed

increase of both lifetimes on adding protein to the bilayers. It has been shown previously that lifetimes of DPH analogues show a remarkable correlation with order [23]. This increase of the lifetimes was interpreted as arising from a reduced water penetrability into the lipid bilayer as a result of reduced lipid flexibility [23,24].

The value of $\langle P_4 \rangle$ is larger than the value of $\langle P_2 \rangle$ and shows the same tendency with protein concentration as $\langle P_2 \rangle$. The increase of $\langle P_4 \rangle$ with increasing protein concentrations can be related to a decrease of the width of the angular distribution of the lipid probe in the membrane. If $\langle P_2 \rangle$ is plotted versus $\langle P_4 \rangle$ at various temperatures and at various protein concentrations an almost linear relation is observed (Fig. 4). This suggests that changing the temperature is comparable to adding protein to lipid bilayers. This is in agreement with the finding from the ESR experiments, that increasing the protein concentration results in a change in diffusion coefficient, which can be compensated by increasing the temperature. From Fig. 3 it can also be observed that in agreement with the findings of Best *et al.* [24], the relation between $\langle P_2 \rangle$ and $\langle P_4 \rangle$ can not be considered as as being described by the cone model. The relation between $\langle P_2 \rangle$ and $\langle P_4 \rangle$ is best described by a P_4-distribution model, indicating that the interaction energy of the DPH-prop probe is proportional to $P_4(\cos\beta)$, where β is the angle represents the angle between the probe molecule and the normal on the bilayer. This is in agreement with results obtained by Pottel *et al.* [18] for DPH molecules in DMPC and DPPC.

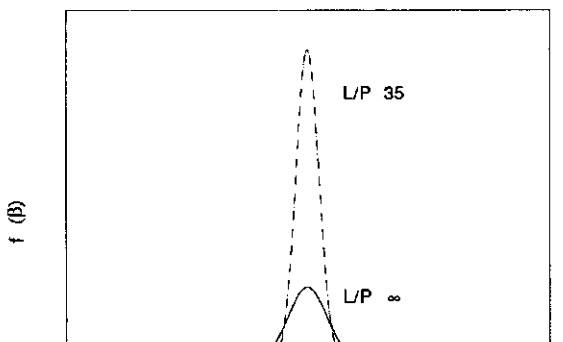

Figure 5. The angular distribution function, $f(\beta)$ [17], constructed from the experimental values of $\langle P_2 \rangle$ and $\langle P_4 \rangle$ using the information theory of the DPH-prop in DOPC bilayers with and without M13 coat protein.

In Fig. 5 the angular distribution function, calculated using the information theory, is given for a sample with and without protein [17]. From Fig. 5, it can be observed from the maximum at $\beta = 0°$, that the protein orders the lipids along the normal of the bilayer. Also a small maximum at $\beta = 90°$ is observed in Fig. 5. This maximum probably arises from an artifact as a result of not taking in account a higher expansion in order parameters of the distribution function and will be disregarded [24].

General conclusions: As observed from the ESR experiments in this paper, M13 coat protein in the non-aggregated α-oligomeric state at high L/P ratios (L/P > 12), is not able to induce a long living lipid boundary shell and consequently an immobilization of the lipids. This is in contrast with ESR studies performed by Peelen *et al.* [25] on M13 coat protein in the α-oligomeric state at low L/P ratios (L/P <12), where an immobilized component was observed of which the intensity depended on the M13 coat protein concentration [25]. For this system, it was estimated that about four lipids bind per protein monomer [25]. This low number of boundary lipids indicates that at these low L/P ratios protein-protein contacts take place [8] and that lipid sites are shared by two or more protein monomers. This effect results in an immobilized ESR spectral component, as has also been observed in studies with the β-polymeric M13 coat protein [8,9].

M13 coat protein in the α-helical conformation has a rigid trans-membrane α-helix that provides the hydrophobic surface to interact with the lipid chains. In general, it has been assumed that immobilization of lipids by proteins originates from the rigidity of the protein backbone of the membrane bound domain of the protein [26-28]. Based on our experiments, it is clear that not only the rigidity of the trans-membrane part of the protein is important, but also the size of the hydrophobic surface of the protein region, since a single M13 coat protein molecule is not able to cause any immobilization, in contrast to an aggregated complex of protein molecules with an α-helix conformation.

However, when small trans-membrane α-helical M13 coat protein monomers are incorporated in lipid systems, an overall effect on the lipids is induced, resulting in a reduction of in the dynamics and an increase in order of the lipids, as observed by ESR and time-resolved fluorescence measurements. This overall effect of the protein on the lipid bilayer can be countereffected by increasing the temperature. In this respect the effect of the M13 coat protein resembles that observed upon introducing rigid amphipathic molecules, such as cholesterol, in lipid bilayers [25]. A long range perturbation of the M13 coat protein in the α-oligomeric form at low L/P ratios has been observed by Peelen *et al.* [25]. In this study a fluid component, which was characteristic of a lower temperature than at which the corresponding spectra of the lipid protein systems was recorded, had to be used in the spectral simulations. This indicates that also in the case that protein-protein contacts

take place, M13 coat protein induces an overall lipid effect, similar as is found for the monomeric form.

These results suggests that mainly the geometric properties of the protein in the hydrophic membrane interior determine its effect on the lipid environment. This conclusion is in agreement with the observation that the hydrophobic region of M13 coat protein perfectly matches the lipid bilayer, resulting in a minimal distortion of the bilayer structure of the lipid system (chapter 4).

References

1 Pratt, D., Tzagoloff, H. and Beadoin, J. (1969) Virology 39, 42-53.

2 Rashed, I. and Oberer, E. (1986) Microbiol. Rev. 50, 401-42.

3 Model, P., McGill, C., Mazur, B. and Fulford, W. D. (1982) Cell 29, 329-35.

4 Day, L. A. (1969) J. Mol. Biol. 39, 265-297.

5 Spruijt, R., Wolfs, C. J. A. M. and Hemminga, M. A. (1989) Biochemistry 28, 9159-9165.

6 Nozaki, Y., Reynolds, J. A. and Tanford, C. (1978) Biochemistry 17, 1239-1246.

7 Fodor S. P. A., Dunker, A. K., Ng, Y. C., Carsten, D. and Williams, R. W. (1981) in: Seventh. biennial Conference on Bacteriophage Assembly. pp 441-455 (Dubow, M.S., ed.) Alan R. Liss Inc., New York.

8 Wolfs, C. J. A. M., Horvàth, L. I., Marsh, D., Watts, A. and Hemminga, M. A. (1989) Biochemistry 28, 9995-10001.

9 Datema, K. P., Wolfs, C. J. A. M., Marsh, D., Watts, A. and Hemminga, M. A. (1987) Biochemistry 26, 7571-7574.

10 Spruijt, R. B. and Hemminga, M. A. (1991) accepted for Biochemistry

11 Schneider, D. J. and Freed, J. H. (1989) in Biological Magnetic Resonance, volume 8: Spin labelling (Berliner, J., L. and Reuben, J., Eds) 7, pp 1-76, Plenum Press, New York.

12 Meirovitch, E., Nayeem, A. and Freed, J. H. (1984) J. Phys. Chem 88, 3453-3465

13 Moser, M., Marsh, D., Meier, P., Wassmer K-H. and Kothe, G. (1989) Biophys. J. 55, 111-123.

14 Visser, A. J. W. G., Ykema, T. and van Hoek, A., O'Kane, D. J. and Lee, J. (1985) Biochemistry 24, 1489-1496.

15 O'Connor, D.V. and Phillips, D. (1984) Time correlated single photon counting 19, 7-49.

16 Beechem, J. M. and Graton, E. (1989) SPIE 909, 70-81.

17 Ameloot, M., Hendrickx, H., Herreman, W., Pottel, H., van Cauwelaert, F. and van der Meer, W (1984) Biophys. J. 46, 525-539.

18 Pottel, H., van der Meer, B. W., Herreman, W. and Depauw, H. (1986) Chem. Phys. J. 102, 37-44.

19 Dijck, van P. W. M., De Kruijff, B., Deenen van, L. L. M. and De Gier, J. (1976) Biochem. Biophys. Acta 455, 576-587.

20 Stubbs, C. D., Kinosita, K., Munkonge, F., Quinn, P. J. and Ikegami, A. (1984) Biochem. Biophys. Acta 775, 374-380.

21 van Gorkom, L. C. M., Horváth, J. I., Hemminga, M. A., Sternberg, B. and Watts, A. (1990) Biochemistry 29, 3828-3834.

22 Wassall, S. R., Yang, R. C., Wang, L., Phelps, T. M., Ehringer, W. and Stillwell, W. (1990) Bull. Magn. Reson. 12, 60-64.

23 Straume, M. and Litman, B. J. (1980) Biochemistry 27, 7723-7733.

24 Best, L., John, E. and Jähnig, F. (1987) Eur. Biophys. J. 15, 87-102.

25 Peelen, S. J. C. J., Sanders, J. C., Hemminga, M. A. and Marsh, D (1992) Biochemistry in press.

26 Jost, P. C., Griffith, O. H., Capaldi, R. A. and Vanderkooi, G. A. (1973) Proc. Natl. Acad. Sci. USA 70, 480-484.

27 Marsh, D. (1981) in Membrane spectroscopy (E. Grell. Ed) pp. 51-142, Springer Verlag, New York.

28 Devaux, F. (1983) Biol. Magn. Reson. 5, 183-299.

CHAPTER 7

Summarizing discussion

In this thesis a small part of the reproductive cycle of the M13 bacteriophage is studied in more detail, namely the interaction of the major coat protein (MW 5240) with lipid bilayers. During the infection process is the major coat protein of M13 bacteriophage stored in the cytoplasm membrane of the *E. coli* cell, while DNA replication takes place in the cytoplasm. The M13 coat protein in model lipid bilayers is present in two forms, which were previously called the α-oligomeric (b-state) and the β-polymeric (c-state) form. The secondary structure of the strongly aggregated M13 coat protein in the β-polymeric form is dominated by a high percentage of β-sheet conformation whereas the non-aggregated M13 coat protein in the α-oligomeric form was previously estimated to consist of 50% α-helix.

A more precise knowledge of the secondary structure of the M13 coat protein in both forms helps to understand how protein-lipid interactions take place. Therefore, Circular Dichroism, Raman and Fourier Transform Infrared spectroscopy has been applied on lipid M13 coat protein systems reconstitutes. Care was taken to study either the aggregated or non aggregated form of the M13 coat protein. The β-polymeric form of M13 coat protein has a secondary structure of 13% α-helix, 57% β-sheet, 13% turn and 16% remainder and the α-oligomeric M13 coat protein is in a 91% α-helix, 5% β-sheet, 3% turn and 1% remainder conformation. The overall conformation of the M13 coat protein in the α-oligomeric form corresponds well with the conformation of virion bound coat protein.

In a more theoretical study it was tried to relate the conformation and aggregation state of the M13 coat protein. MD simulations were performed on M13 coat protein in the β-polymeric and the α-oligomeric form. The simulations were started from initial conformations of M13 coat protein as monomers or dimers of α-helices or U-shaped β-sheets. The M13 coat protein in the U-shaped β structure changes from a planar to a twisted form with larger twist for the M13 coat protein as monomer than as a dimer. The M13 coat protein in the β-sheet conformation (β-polymeric) is much more flexible than the M13 coat protein in an α-helix conformation (α-oligomeric) as monitored by the rms fluctuations of the Cα atoms. A comparison of the energies after 100 ps MD simulation shows that of the monomers, M13 coat protein in an α-helix has the lowest energy. The energy difference between α- and β-structures decreases from 266 kJ/mol to 148 kJ/mol, when going from monomers to dimers. It is expected that this difference will decrease with higher aggregation numbers, suggesting that the M13 coat protein in the β-sheet conformation must be aggregated, in agreement with observations performed with HPLC.

Using ^{2}H-NMR and ^{31}P-NMR the interaction of the M13 coat protein in both forms with specific headgroup and chain deuterium labelled phospholipids is studied. It can be

concluded from the spectra that the protein in the predominant β sheet conformation causes a fraction of lipids to be trapped. Together with the information obtained from the structure and aggregation state of this form (chapters 2 and 3) it is suggested that the trapped lipids are arranged in a non bilayer structure, probably induced by a misfitting of the hydrophobic core of the protein and the membrane bilayer. The protein in the predominant α-helix conformation perfectly fits in the lipid bilayer and has only minor influences on the surrounding lipid matrix.

However, because in the inner membrane only α-helical proteins are found, the correspondence with the conformation of the virion bound protein and the fact that the aggregation of the β-polymeric protein is irreversible it is suggested that the α-oligomeric protein is the more likely form of the M13 coat protein to be found in the *E. coli*. Therefore, a more detailed study was performed on the interaction of this form of the M13 coat protein with lipid bilayers. The ^{2}H-NMR quadrupolar splittings of the α head-group methylene deuterons of deuterated phosphatidylcholine and phosphatidylethanolamine decrease, whereas the quadrupolar splittings of the β head-group methylene deuterons of the two lipids increase with increasing protein content. All deuterated segments in the phosphatidylglycerol headgroup show the same relative decrease of the NMR quadrupolar splittings. These results are interpreted in terms of a change in torsion angles of the methylene groups, induced by positive charges, probably lysine residues of the protein at the membrane surface. For all lipid bilayer compositions studied the head-group perturbations are similar. It is concluded that there is no strong specific interaction between one of the lipid types examined and the M13 coat protein.

In the ESR spectra of spin labels in lipid bilayers no second protein induced component can be observed upon incorporation of M13 coat protein in the α-oligomeric form. It is argued on the bases of ESR and time resolved fluorescence results that M13 coat protein in the α-oligomeric does not immobilize lipids but restricts the order and motion of the lipids, due to its cylindrical form, proportions and non specific interaction with lipids in the bilayer.

Finally, from this work it can be concluded that the influences of the M13 coat protein in its probably natural form, the α-oligomeric form, on the lipid membranes are small. Positive charges are introduced at the bilayer surface and the hydrophobic area is less fluid in the presence of the M13 coat protein. This let us to understand that higher amounts of cardiolipin are produced when M13 is infecting *E. coli*. M13 coat protein changes the charge density at the membrane surface which is counteraffected by cardiolipin. In addition the machinery of *E. coli* is also capable in retaining the fluidity of its membranes simply by

changing the lipid tail composition. This let us understand that even high concentrations of M13 coat protein are not lethal for its host, *E. coli*.

Samenvatting

In dit proefschrift wordt een gedeelte uit de levenscylus van de M13 bacteriofaag in meer detail onderzocht namelijk de interactie van het belangrijkste manteleiwit van de M13 bacteriofaag met lipide bilagen. Tijdens het infectieproces is het belangrijkste manteleiwit opgeslagen in het cytoplasmatisch membraan van de *E. coli* cel, terwijl in het cytoplasma DNA replicatie plaatsvindt. In model membranen zijn twee verschillende vormen van het M13 manteleiwit aangetoond, die de alfa-oligomere (b-staat) en de beta-polymere (c-staat) vorm genoemd worden. De secundaire structuur van het sterk geaggregeerde manteleiwit in de beta-polymere vorm is voornamelijk in een beta-plaat conformatie terwijl het niet geaggregeerde manteleiwit in de alfa-oligomere vorm voornamelijk uit alfa-helix structuur bestaat.

Een meer gedetailleerde kennis van de structuur van beide vormen van het M13 manteleiwit is noodzakelijk voor een beter begrip op het gebied van lipide eiwit interacties. Met behulp van Circulair Dichroisme, Raman en FTIR is de structuur van M13 manteleiwit in de twee verschillende vormen onderzocht. De beta-polymere vorm heeft een secundaire structuur die bestaat uit 3% alfa-helix, 57% beta-plaat, 13% turn en 16% overig. De alfa-oligomere vorm van het M13 manteleiwit bestaat uit 91% alfa-helix, 5% beta-plaat, 3% turn en 1% overig. De secundaire structuur van het manteleiwit in de alfa-oligomere vorm lijkt veel op de secundaire structuur van het virus gebonden manteleiwit.

In een meer theoretische studie is een poging gedaan om met Moleculaire Dynamica het conformatie en het aggregatie gedrag van het manteleiwit in de twee vormen te bestuderen. Als uitgangsstructuren zijn M13 manteleiwit monomeren en dimeren in een pure alfa-helicis en U vormige beta-sheet conformaties gebruikt. M13 manteleiwit in een U vormige beta-structuur verandert van een platte in een gedraaide structuur. De draaiing is groter voor het monomeer dan voor het dimeer. Uit de rms fluctuaties van de C-alfa atomen blijkt dat het M13 manteleiwit in een beta-plaat conformatie flexibeler is dan M13 manteleiwit in een alfa-helix. Als na een berekening van 100 ps de energie van de monomere structuren vergeleken worden dan is de energie van het M13 manteleiwit in de alfa-helix conformatie de laagste. Het energie verschil tussen het M13 manteleiwit in een alfa-helix of beta-plaat structuur neemt van 266 kJ/mol af tot 148 kJ/mol als we van monomeren naar dimeren gaan. Het verschil zal waarschijnlijk nog verder afnemen als de aggregatie toeneemt. Dit duidt erop dat, overeenkomstig met de HPLC resultaten, het M13 manteleiwit in beta-plaat conformatie geaggregeerd is.

Met behulp van deuterium en fosfor NMR is de interactie van het M13 manteleiwit in beide vormen met selectief gelabelde lipiden bestudeerd. Uit de NMR spectra blijkt dat de beta-polymeren een fractie ingevangen lipiden induceert. Uit de structuur, de aggregatie toestand van deze vorm en de NMR spectra kan geconcludeerd worden dat de ingevangen

lipiden door het niet passen van het hydrofobe gedeelte van het eiwit in het membraan, deel uitmaken van een niet-bilaag structuur. Het manteleiwit in een alfa-helix conformatie past echter precies in het hydrofobe gedeelte en heeft daarom slechts geringe invloed op de lipide omgeving.

De interactie van de alfa-oligomere vorm van het M13 manteleiwit met lipide bilagen in meer detail bestudeerd, omdat 1) in het cytoplasmatisch membraan alleen transmembraan alfa-helices gevonden worden, 2) de secundaire structuur van de alfa-oligomere vorm op het virus gebonden eiwit lijkt en 3) het manteleiwit in alfa-oligomere vorm niet irreversibel geaggregeerd is en dus de alfa-oligomere vorm de vorm lijkt te zijn die in *E. coli* voorkomt.

De alfa-kopgroep-methyleen deuterium NMR splitsingen van gedeutereerd fosfatidylcholine en fosfatidylethanolamine nemen af terwijl de splitsingen van de beta-kopgroep-methyleen kernen toenemen met toenemende M13 manteleiwit concentraties. De kwadrupool splitsingen van alle gedeutereerde segmenten van fosfatidylglycerol nemen relatief gelijk af. Deze waarnemingen kunnen verklaard worden door een verandering in de torsie hoeken in de kopgroep als gevolg van de introductie van positieve ladingen op het membraan oppervlak. Deze positieve ladingen zijn waarschijnlijk afkomstig van de lysines van het eiwit. Omdat voor alle soorten lipiden en membraansamenstellingen gelijke resultaten gevonden worden moet de specificiteit voor een bepaald lipiden gering zijn.

Het M13 manteleiwit in de alfa-oligomere vorm induceert geen tweede immobiele lipide component in de ESR spectra van gespinlabelde lipiden. De afwezigheid van een immobiele component is waarschijnlijk het gevolg van de cilindrische vorm, de grote van het eiwit en de niet specifieke interacties van het M13 manteleiwit met lipiden in de bilagen. Uit ESR en tijdopgeloste fluorescentie resultaten blijkt dat het M13 manteleiwit niet de lipiden immobilseert maar wel hun beweging en orde beinvloed.

Uit dit proefschrift kan geleerd worden dat de invloed van het natuurlijk voorkomende M13 manteleiwit, de alfa-oligomere vorm, op lipide membranen klein is. Positieve ladingen op het membraan oppervlak en een vermindering van de vloeibaarheid zijn de belangrijkste invloeden. De positieve ladingen worden gecompenseerd door de extra productie door *E. coli* van het negatief geladen cardiolipine. *E. coli* heeft ook voldoende mogelijkheden om veranderingen in de vloeibaarheid op te vangen door middel van veranderingen in de compositie van lipide staarten. Dit laat ons begrijpen dat zelfs hoge concentraties van het M13 manteleiwit niet leiden tot de dood van de gastheer.

ABBREVIATIONS

α_i	Normalized contribution of fluorescence component i.
β_i	Normalized contribution of anisotropy component i.
β_n	Nuclear magneton.
CSA	Chemical shift anisotropy.
CD	Circular dichroism.
CL	Cardiolipin.
Coli CL	Eschericia coli-phosphatidylcardiolipin.
Coli PG	Eschericia coli-phosphatidylglycerol.
$D_\perp$	Perpendicular rotational diffusion coefficient.
$D_\parallel$	Parallel rotational diffusion coefficient.
DOPC	Dioleoylphosphatidylcholine.
DOPE	Dioleoylphosphatidylethanolamine.
DOPG	Dioleoylphosphatidylglycerol.
DMPC	Dimyristoylphosphatidylcholine.
DPH-prop	Diphenylhexatrienyl-propanic acid.
EDTA	Ethylenediaminetetraacetic acid.
EM	Energy minimization.
ESR	Electron spin resonance.
θ_i	Correlation time of component i.
FTIR	Fourier transform infrared.
$H_{(..)}$	(Terms in a) Hamiltonian.
H_0	Magnetic field.
HPLC	High Performance Liquid Chromatography.
J(..)	Spectral density.
g	g-factor.
h	Planck constant.
h_i	Hydrophobicity of atom i.
L/P	Lipid to protein molar ratio.
MD	Molecular dynamics.
MW	Molecular weight.
NMR	Nuclear magnetic resonance.
^{2}H-NMR	Deuterium nuclear magnetic resonance.
^{31}P-NMR	Phosphorus nuclear magnetic resonance.
rms	Rooth mean square.
$\langle P_2 \rangle$, $\langle P_4 \rangle$	Order parameters.
PC	Phosphatidylcholine.

PE	Phosphatidylethanolamine.
PG	Phosphatidylglycerol.
ppm	Parts per million.
Q	Nuclear quadrupole moment.
r (0)	Initial anisotropy.
SDS	Sodium dodecyl sulphate
σ_i	Chemical shif anisotropy tensor element i.
τ_i	Fluorescence lifetime of component i.
T_{1z}	Spin lattice relaxation time.
T_{2e}	Deuterium quadrupolar echo spin-spin relaxation time.
T_2	Spin-spin relaxation time.
Tris	Tris(hydroxymethyl)aminomethane hydrochloride.
UV	Ultra violet.
ν	Frequency.
$V_{(...)}$	Potential Energy Term.
$V^{(2,0)}$	Irreducible quadrupole tensor components.
Z_0	Half the distance between the membrane surfaces.

CURRICULUM VITAE

Johannes Cornelis Sanders werd geboren op 1 februari 1966 in Eindhoven. In 1984 werd het examen atheneum-b afgelegd en werd met de studie Moleculaire Wetenschappen aan de Landbouwuniversiteit te Wageningen begonnen. Afstudeervakken werden gevolgd bij de vakgroepen Wiskunde, Biochemie en Moleculaire Fysica. In 1988 werd het ingenieursexamen cum laude behaald.

Vanaf october 1988 tot en met december 1991 verichtte hij, in dienst van de stichting van Biofysica (NWO) het onderzoek dat leidde tot dit proefschrift. Vanaf januari 1992 werkt hij als onderzoeker bij het Unilever Research laboratorium te Vlaardingen.